TITLE:

Kinetic Studies on Living Radical Polymerizations with Particular Reference to Activation Processes(Dissertation_全文)

AUTHOR(S):

Goto, Atsushi

CITATION:

Goto, Atsushi. Kinetic Studies on Living Radical Polymerizations with Particular Reference to Activation Processes. 京都大学, 2001, 博士(工学)

ISSUE DATE:

2001-03-23

URL:

https://doi.org/10.11501/3183462

RIGHT:

京都大学学術情報リポジトリ
KURENAI 紅
Kyoto University Research Information Repository

新制
工
1208

Kinetic Studies on Living Radical Polymerizations with Particular Reference to Activation Processes

Atsushi Goto

2001

Kinetic Studies on Living Radical Polymerizations with Particular Reference to Activation Processes

Atsushi Goto

2001

Table of Contents

Part II

Nitroxide-Mediated Living Radical Polymerizations (LRP)

Chapter 1

General Introduction

1.1. Introduction

Free radical polymerization is most widely used to synthesize polymers in both industrial and laboratory scales. In contrast to ionic polymerizations, it does not require stringent experimental conditions (e.g., the rigorous exclusion of water and the use of ultrapure reagents) and can polymerize a whole host of vinyl monomers. However, the properties of the products such as chain length and its distribution have been difficult to control due to the inherent bimolecular termination of the highly reactive radical intermediates. This drawback, however, has recently been overcome by the realization of living radical polymerization (LRP).[1-4] LRP retains the advantages of the conventional radical polymerization, i.e., simplicity, robustness, and versatility, and yet allows fine control of polymer structures owing to the living mechanism. Polymers with complicated topologies[5] such as block, graft, star, and comb-shaped structures can also be tailored by LRP. With these attractive features, LRP is expected to create new advanced materials that have not been achieved by either conventional radical polymerization or other living polymerizations. Novel gels,[6] surfactants,[7] and elastomers,[8] and high-density polymer brushes on solid surfaces,[9] for example, have in fact been realized via LRP until now. Further elaboration will furnish a wider range of unique materials by this promising polymerization.

1.2. General Kinetic Features of LRP – A Brief Survey

Despite its synthetic utility, little is known about the mechanism and kinetics of LRP. Even the very fundamental questions as to why low-polydispersity polymers are attainable by LRP and what factors determine the polymerization rates, for example, remain open. In this section, the author will answer these questions by illustrating general kinetic features of LRP.

Mechanistically, LRP is distinguished from other living polymerizations such as living anionic polymerization.[10] In the latter system, the propagating (carbanionic) species is

stabilized by itself and stays alive for a long time; the system is essentially free from chain-breaking reactions such as termination and transfer. On the other hand, LRP is based on the reversible activation-deactivation process (Scheme 1.1) where the propagating species is a free radical. This means that LRP unavoidably includes chain-breaking reactions such as bimolecular termination, and accordingly, it is characterized by both the reversible activation and chain-breaking reactions. This provides LRP with unique kinetic features that are different from both of those of conventional radical polymerization and those of ionic living polymerizations.

1.2.1. Reversible Activation Processes

The basic mechanism common to all the variants of LRP is the alternating activation-deactivation process (Scheme 1.1), in which P-X is supposed to be activated to $P^{\bullet}$ by thermal, photochemical, and/or chemical stimuli. In the presence of monomer M, $P^{\bullet}$ will undergo propagation until it is deactivated back to P-X. This cycle is supposed to be repeated enough times to give every "living" chain a virtually equal chance to grow, which results in the formation of low-polydispersity polymers. In this thesis, the author defines a "living" chain as either an active or a dormant chain with the quotation specifying the presence of the two states. In a practically useful system, it usually holds that $[P^{\bullet}]/[P\text{-}X] \leq 10^{-5}$, which means that a "living" chain spends most of its polymerization time in the dormant state. In this circumstance, termination does occur, but the number of dead chains accumulated in the course of polymerization is small compared with that of "living" chains, and consequently the contribution of termination becomes minor.

There are three main mechanisms of reversible activation, which are (a) dissociation-combination, (b) degenerative (exchanging) chain transfer and (c) atom transfer (Scheme 1.1). Reversible addition-fragmentation chain transfer (RAFT: Scheme 1.2) is a branch of degenerative chain transfer. Each LRP system includes one (or more) of these activation mechanisms. Although tentative mechanisms are proposed in each system, none of these proposals have been verified experimentally. The activation rate constant for each mechanism will take the form

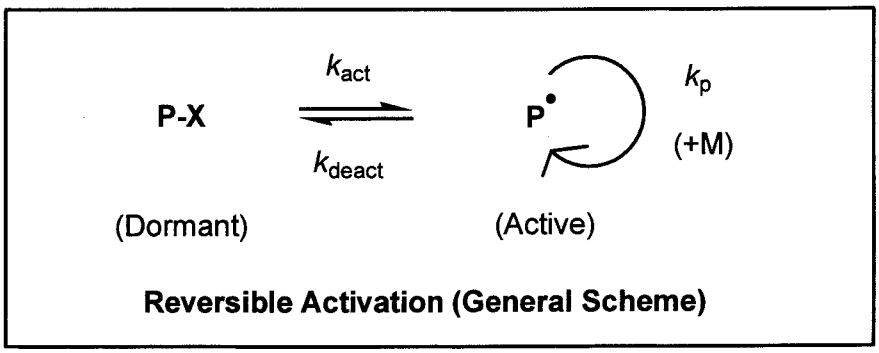

(a) Dissociation-Combination

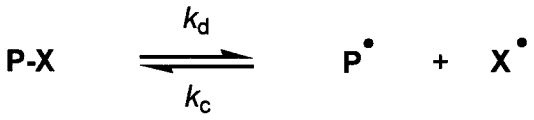

(b) Degenerative Chain Transfer

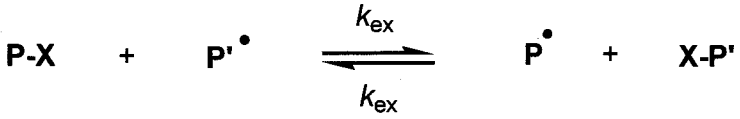

(c) Atom Transfer

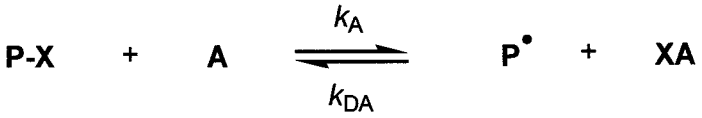

Scheme 1.1. A general scheme and the three main mechanisms (a, b, and c) of reversible activation.

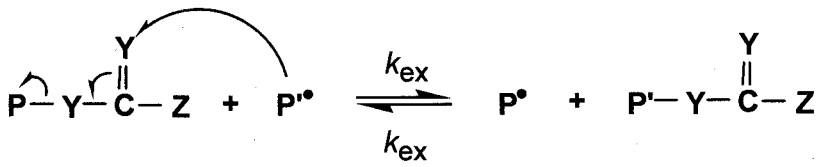

a: Y = S, Z = CH_3 or Ph

b: Y = C, Z = $COOCH_3$

Scheme 1.2. Reversible addition-fragmentation chain transfer (RAFT).

$$k_{act} = k_d \quad \text{(dissociation-combination)} \quad (1.1)$$

$$k_{act} = k_{ex}[P^\bullet] = C_{ex}R_p/[M] \quad \text{(degenerative chain transfer; } C_{ex} = k_{ex}/k_p) \quad (1.2)$$

$$k_{act} = k_A[A] \quad \text{(atom transfer)} \quad (1.3)$$

where the rate constants k_d, k_{ex}, and k_A are defined in Scheme 1.1, $C_{ex} = k_{ex}/k_p$, R_p is the polymerization rate, and A is an activator like a transition metal complex. Thus measurements of k_{act} as a function of [P•], [A] or R_p help us understand mechanistic details of activation processes. Such attempts will be seen in the following chapters.

Examples of blocking agents X include sulfur compounds (Scheme 1.3**a**[1,11] and 1.3**e**[12]), stable nitroxides (1.3**b**),[2,3,13-24] transition metal complexes (1.3**c**),[25-27] iodine (1.3**d**),[28-30] halogens with transition metal catalysts (1.3**f**),[31-36] and others.[37-42] Systems **e** and **f** are often classified as RAFT-based LRP[12] and atom transfer radical polymerization (ATRP),[32] respectively, which are named after their tentative activation mechanisms.

1.2.2. Polydispersities

In actual LRPs, there are at least five elementary reactions (Scheme 1.4) besides reversible activation (Scheme 1.1). However, it is instructive to consider "ideal LRP" in which reactions other than activation, deactivation, and propagation are absent and the P• concentration is constant. The polydispersity index Y (= $M_w/M_n - 1$) of this system is given by[43]

$$Y = w_A^2 Y_A + w_B^2 Y_B \quad (1.4)$$

$$Y_B = F(C)y_n^{-1} + x_{n,B}^{-1} \quad (1.5)$$

where Y_A is the Y value of the initiating adduct P_0-X, and Y_B, $x_{n,B}$, and w_B are the Y value, the number-average degree of polymerization, and the weight fraction of the propagated portion of the chains, respectively, ($w_A + w_B = 1$). $F(C) = 2$ when the monomer concentration is constant, and $F(C) = (1–2C^{-1})\ln(1–C)$ for a batch system (C = monomer conversion).[44] y_n is

(a) "Iniferter" polymerization (Otsu et al., 1982[1])

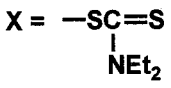

(b) Nitroxide (Solomon et al., 1985[2]; Georges et al., 1993[3])

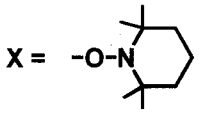

(TEMPO)

(c) Cobalt/Porphyrin Complexes (Wayland et al., 1994[25])

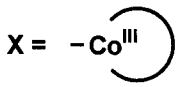

(d) "Iodine Transfer" (Tatemoto et al., 1991[28]; Sawamoto et al., 1994[29], Matyjaszewski et al., 1995[30])

X = −I

(e) "RAFT" (Moad et al., 1995[38] & 1998[12])

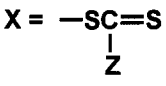

(Z = CH_3 or Ph)

(f) "ATRP" (Sawamoto et al., 1995[31]; Matyjaszewski et al., 1995[32])

X = −Br or Cl + Metal (e.g., Cu(I)Br/2L)

Scheme 1.3. Examples of blocking agents X.

the average number of activation-deactivation cycles that a chain experiences during polymerization time t, and is related to the activation rate constant by

$$y_n = k_{act} t \tag{1.6}$$

In the limit of $y_n^{-1} = 0$, equation 1.5 reduces to that of the Poisson distribution. The derivation of equation 1.5 is shown in Appendix.

(a) Initiation

$$R_i = k_i[M]^3 + k_i'[I]$$

(b) Propagation

$$P^\bullet + M \xrightarrow{k_p} P^\bullet$$

(c) Termination

$$P^\bullet + P^\bullet \xrightarrow{k_t} \text{dead polym.}$$

(d) Chain transfer

$$P^\bullet + RH \xrightarrow{k_{tr}} PH + R^\bullet$$

(e) Decomposition of P-X

$$P\text{-}X \xrightarrow{k_{dec}} \text{dead polym.} + XH$$

Scheme 1.4. Possible elementary reactions other than reversible activation.

This discussion indicates that k_{act} is the most fundamental parameter that characterizes the performance of a given LRP system; if k_{act} is large enough, the system potentially produces low-polydispersity polymers, while low-polydispersity polymers cannot be expected from a system with a very small k_{act}. Any deviations from equation 1.5 are ascribed to the non-stationarity of [P•] and/or side reactions. Side reactions such as termination, conventional initiation, irreversible chain transfer, and the degradation of the active chain end[15,45] (Scheme 1.4), deactivate P• irreversibly, and necessarily make the polydispersity higher than the ideal value (equation 1.5), usually in a predictable fashion. (Here *conventional initiation* refers to the initiation induced thermally or by the decomposition of a conventional initiator like benzoyl peroxide, and should not be confused with the activation of an initiating dormant species P_0-X.) The relative importance of side reactions depends on the rate of the individual reactions and experimental conditions such as concentrations, temperature, and reaction time.

Matyjaszewski has recently noted that equation 1.5 provides a poorer prediction of M_w/M_n rather than the following equation only of C;[46]

$$M_w/M_n = 1 + [\text{P-X}]\,(k_p/k_{deact})\,(2C^{-1} - 1) \tag{1.7}$$

where k_{deact} is $k_c[\text{X}^\bullet]$, $k_{ex}[\text{P-X}]$, and $k_{DA}[\text{XA}]$ for the system of dissociation-combination type (Scheme 1.1a), degenerative chain transfer type (Scheme 1.1b), and atom transfer type (Scheme 1.1c), respectively. However, this is a misunderstanding. With the function $F(C)$ given above for a batch polymerization, equations 1.5 and 1.7 are equivalent (for $M_n^{-1} = 0$). Experimentally, equation 1.5 is usually more easily accessible than equation 1.7.

1.2.3. Polymerization Rates

Knowledge about polymerization rate R_p is useful to design experimental conditions. Such knowledge is also important to predict the properties of dead polymers, since side reactions such as termination are directly related to the $\text{P}^\bullet$ concentration hence R_p.

Firstly discussed is the R_p of the system of dissociation-combination type (Scheme 1.1a), where $\text{X}^\bullet$ is a stable free radical. This is the case with the nitroxide system, for example. (Experimental establishment of the activation mechanism in the nitroxide system is presented in Chapter 3.) Of the seven reactions in Schemes 1.1a and 1.4, dissociation, combination, *conventional* initiation, and termination are relevant to changes in the radical concentrations, and thus $[\text{P}^\bullet]$ and $[\text{X}^\bullet]$ will follow the differential equations

$$d[\text{P}^\bullet]/dt = k_d[\text{P-X}] - k_c[\text{P}^\bullet][\text{X}^\bullet] + R_i - k_t[\text{P}^\bullet]^2 \tag{1.8}$$

$$d[\text{X}^\bullet]/dt = k_d[\text{P-X}] - k_c[\text{P}^\bullet][\text{X}^\bullet] \tag{1.9}$$

where R_i is the rate of conventional initiation and k_t is the rate constant of termination. The author is particularly interested in the case where dead chains are very small in number compared to "living" chains, i.e., the equality $[\text{P-X}] = A_0$ holds approximately, where A_0 is the concentration of the initiating dormant species ($A_0 = [\text{P}_0\text{-X}] = [\text{P-X}]_0$). Also it usually holds

that [X•] » [P•] or d[X•]/dt » d[P•]/dt. Under these conditions, equations 1.8 and 1.9 can be approximately solved for [X•] for the time range in which the quasi-equilibrium

$$[P^{\bullet}][X^{\bullet}] = K[P\text{-}X]\ (= KA_0) \qquad (K = k_d/k_c) \tag{1.10}$$

holds. Fischer has shown this to be the case excepting the very initial stage of polymerization (t < 100 ms) and noted the importance of the time range where the quasi-equilibrium holds.[47] He has also pointed out that the quasi-equilibrium exists only if K is below $A_0k_c/4k_t$ ($\approx 10^{-2}$ M).[48] This condition is usually met in the actual LRPs ($K < 10^{-8}$ M). By taking the difference between equations 1.8 and 1.9, and adopting d[X•]/dt » d[P•]/dt, one has

$$d[X^{\bullet}]/dt = k_t[P^{\bullet}]^2 - R_i \tag{1.11}$$

Insertion of equation 1.10 into equation 1.11 and the subsequent integration yield the solution, which can be cast into the form

$$\ln\{[(1+x)/(1-x)]\bullet[(1-x_0)/(1+x_0)]\} - 2(x-x_0) = at \tag{1.12}$$

$$x = (R_i/k_tK^2A_0^2)^{1/2}[X^{\bullet}] \tag{1.13}$$

$$a = 2R_i^{3/2}/(k_tK^2A_0^2)^{1/2} \tag{1.14}$$

where x_0 is the value of x at t = 0 (R_i is assumed to be constant.). The P• concentration and hence $R_p = k_p[P^{\bullet}][M]$ follow from equations 1.12-1.14 with $[P^{\bullet}] = KA_0/[X^{\bullet}]$ (equation 1.10).

Two special cases have been studied experimentally by the author's and other groups.[43,47,49] One is the case in which $R_i > 0$, $[X^{\bullet}]_0 = 0$, and t is sufficiently large (at » 1). In this limit, equation 1.12 simply reduces to x = 1 (the "stationary state") or equivalently

$$[X^{\bullet}] = (KA_0)/(R_i/k_t)^{1/2} \qquad \text{(stationary state)} \tag{1.15}$$

or

$$[P^{\bullet}] = (R_i/k_t)^{1/2} \qquad \text{(stationary state)} \qquad (1.16)$$

Thus R_p is independent of the reversible activation reaction and identical with the stationary-state rate of polymerization of the $X^{\bullet}$ free system.

To test equation 1.16, we examined the time-conversion relation in the nitroxide-mediated LRP.[49] Figure 1.1 compares the $\ln([M]_0/[M])$ vs. t plots for the styrene polymerizations with and without BS-TEMPO (**14**; Figure 2.1 in Chapter 2) or PS-TEMPO (**27**; n ≈ 21, Figure 2.3 in Chapter 2), where BS is 2-benzoyloxy-1-phenylethyl, TEMPO is 2,2,6,6-tetramethylpiperidinyl-1-oxy, and PS is polystyrene,. In all cases, no extra nitroxide was added (i.e., $[X^{\bullet}]_0 = 0$). Clearly, the R_ps of the nitroxide systems are the same with each other, and when the conversion is small (< 30 %), they are equal to that of the nitroxide-free (thermal) system. Equation 1.16 was thus confirmed by this experiment. The deviations at higher conversions are due to changes in k_t arising from differences in chain length and viscosity. In fact, the dotted curve, which was calculated with a $[M]^3$-dependent R_i (Scheme 1.4a)[50] and a constant k_t, gives the smallest R_p at high conversions, since a constant k_t

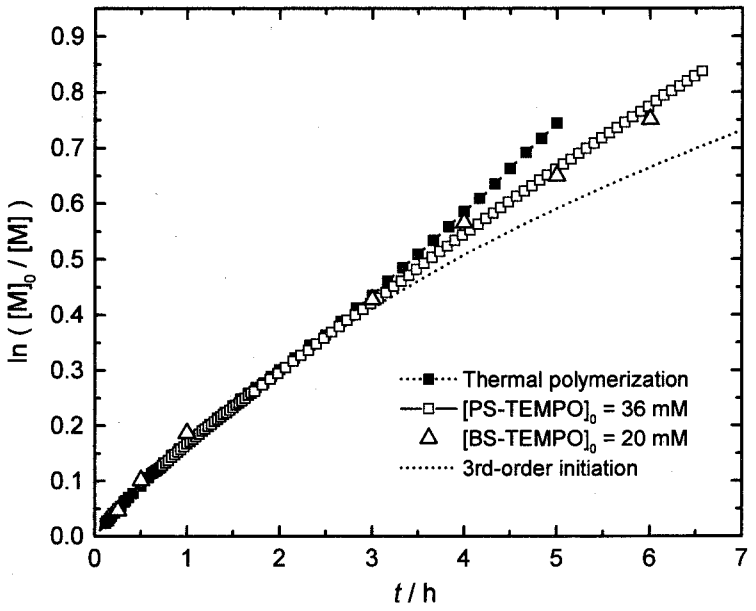

Figure 1.1. Plot of $\ln([M]_0/[M])$ vs. t for the styrene polymerization at 125 °C: $[PS\text{-}TEMPO]_0$ = 36 mM (□); $[BS\text{-}TEMPO]_0$ = 20 mM (△); no nitroxide (■); the dotted line shows the $[M]^3$-dependent initiation with constant k_t (no nitroxide), (ref. 49).

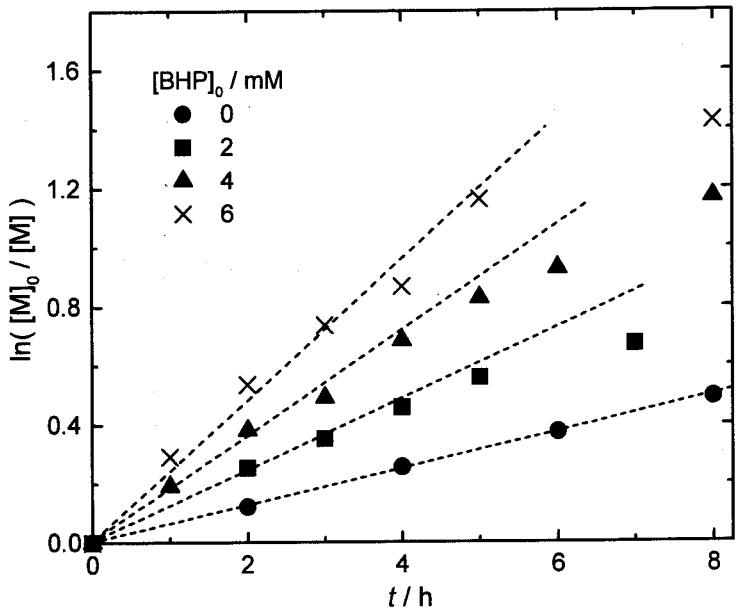

Figure 1.2. Plot of $\ln([M]_0/[M])$ vs. t for the styrene polymerization at 114 °C with PS-TEMPO (P_0-X) and BHP: $[P_0\text{-X}]_0 = 48$ mM and $[BHP]_0 = 0$ (●), 2 (■), 4 (▲), and 6 (×) mM, (ref. 43).

overestimates the actual k_t. In an alternative way to test equation 1.16, we added the conventional radical initiator *t*-butylhydroperoxide (BHP) to a PS-TEMPO/styrene system.[43] Figure 1.2 shows the plot of $\ln([M]_0/[M])$ vs. t. It can be observed that the R_p increases with increasing [BHP], as in a conventional (nitroxide-free) system. In addition, while the addition of 4 mM of BHP, for example, enhanced R_p by a factor as large as 3, the chain length and its distribution were well controlled at least in this range of R_p. This result importantly indicates that a conventional initiator has a possibility to "awake" the systems in which the reversible activation of P-X does occur but a thermal initiation does not, and for this reason, controlled polymerization does not proceed with a desirable rate. *tert*-Butyl acrylate (tBA) is one of such monomers. In Chapter 5, the author discusses these details. Regarding the roles of conventional initiation[51,52] and initiators[53] in a nitroxide system, Greszta and Matyjaszewski have drawn nearly the same conclusions independently. The independence of R_p from [P-X] has also been observed by Catala et al., although they differently interpreted their results.[16]

This stationary-state kinetics is expected to hold also for degenerative transfer-type

systems (Scheme 1.1b), since the radical concentration is basically unchanged by a transfer reaction unless it is a retarding or degradative one. Iodide-mediated and RAFT-based LRPs, which involve degenerative transfer as an activation process, should follow this stationary-state kinetics. In Chapters 6 and 7, these details are experimentally examined for both systems.

The other case that has been discussed is the one with $R_i = 0$ ($a = 0$), where equation 1.12 simplifies to

$$[X^\bullet]^3 - [X^\bullet]_0^3 = 3k_t(KA_0)^2t \tag{1.17}$$

Equation 1.17 with $[X^\bullet]_0 = 0$ is the case discussed firstly by Fischer[47] and subsequently by the author's group.[54] Fischer has obtained the equation without *ad hoc* assumption of the equilibrium in equation 1.10. In this sense, the accordance of the two results (by Fischer and the author's group) is noteworthy. Equations 1.10 and 1.17 with $[X^\bullet]_0 = 0$ give the characteristic power-law behavior of the conversion index $\ln([M]_0/[M])$:

$$\ln([M]_0/[M]) = (3/2)k_p(KA_0/3k_t)^{1/3}t^{2/3} \tag{1.18}$$

The validity of equation 1.17 has been confirmed by Fischer et al.[21,48] by following the concentration of the nitroxide radicals produced by the homolysis of a model alkoxyamine. Equation 1.18 has also been examined by the author's group[54] in the study of the alkoxyamine-initiated polymerization of a styrene derivative in which spontaneous thermal initiation is almost absent. The results showed that the conversion index in this system obeys the power lows in equation 1.18 with respect to both t and $[P\text{-}X]_0$.

Equation 1.12 is applicable to more general cases in which, for example, R_i is nonzero but so small that the stationary state is reached only after a long time or never reached at all in the duration of a typical experiment. It also describes the case in which, for example, R_i is nonzero, *and* $[X^\bullet]_0$ is considerably larger than the stationary concentration given by equation 1.15. What happens in this case would be that the polymer radicals produced by the

conventional initiation combine with the extra X• radicals to produce extra adducts P-X until [X•] decreases down to the stationary concentration (equation 1.15 with A_0 so modified as to include the extra adducts produced from the extra X•.). Correspondingly, the R_p in such a system would be small or virtually zero when t is small because of the extra X•, and gradually increase up to the stationary value given by equation 1.16. Such intermediate behaviors are clearly different from those for the two special (limiting) cases discussed above. The behavior that one would experimentally observe depends basically on the magnitudes of the two parameters x_0 and a, as equation 1.12 shows.

The above equations for dissociation-combination systems are basically applicable to the atom transfer system (ATRP: Scheme 1.1c) by the reinterpretations of X• = AX, k_d = k_A[A], and k_c = k_{DA} (K = k_A[A]/k_{DA}). The stationary kinetics would be expected also for ATRP system with conventional initiation. However, since K is usually very large (~10^{-9} M) in ATRP[55] (cf. K ~10^{-11} M in the styrene/TEMPO at 125 °C[49]), the stationary state (at » 1) will come only after a long, sometimes impractically long time. In the practically useful time range, at remains virtually zero, and thus equation 1.17 would better describe the rates in ATRP. However, for the ATRP of styrene at 110°C, Matyjaszewski et al. have experimentally observed a first-order dependence of the conversion index ln([M]$_0$/[M]) on all t, [P-X]$_0$, and [A]$_0$, where P-X and A were an alkyl halide initiator and the Cu(I)X complex with a bipyridine derivative (X = Br or Cl), respectively.[55] This discrepancy has been rationalized by the same group in terms of the chain length dependence of k_t (see below).[56]

There are several causes that can introduce deviations from equation 1.12. One may be the inadequacy of the assumptions on which equation 1.12 is based, in particular, the approximation of [P-X] = A_0 (= constant). When R_i = 0, [X•] increases and [P-X] necessarily decreases with time because of termination (cf. equation 1.17). The magnitude of error introduced by this cause would be on the same order as that involved in the approximation [P-X] = A_0. For example, if [P-X] is smaller than A_0 by 10 % at time t, the [X•] (hence R_p) estimated from equation 1.17 would be in error by about 10 %. The second cause may be side reactions other than initiation and termination. For example, alkoxyamines are known to undergo thermal degradation.[15,45] Also notably, the conventional initiation can be

accelerated by the presence of a nitroxide.[57] The third possible cause of deviations may be the dependence of the kinetic parameters on chain length and/or polymer concentration. In a living polymerization, chain length and conversion or polymer concentration are directly related to each other. Since k_t is particularly sensitive to these factors, the change of k_t often causes serious deviations, as observed in the ATRP system.

It should be noted that all the rate equations given here include the k_t term. This means that bimolecular termination, which usually gives minor effects on the polymer properties, plays an important role in determining the polymerization rate. This is characteristic of LRP and uncommon to other living polymerizations such as the anionic counterpart.

1.3. Outline of This Thesis

1.3.1. Purpose of This Thesis

The purpose of this thesis is to elucidate the mechanism and kinetics of LRPs on the theoretical and the experimental basis. The knowledge on the kinetic aspect should be helpful to describe the systems, to predict the product properties, and to optimize the experimental conditions for the highest possible achievement.

The theoretical discussion in the last section noted the particular importance of the reversible activation as a key process of LRP. However, the details of this process have never been disclosed in any variant of LRP. The main subject of this thesis is to examine the activation processes in individual systems by determining k_{act}. Such attempts allow us to evaluate the fundamental ability of each system and establish the activation mechanism. Some k_{act} values have so far been determined for low-mass adducts (initiators for LRP). However, there have been no k_{act} values available for polymer adducts, which are particularly important to determine polydispersities (cf. equation 1.5). This is due to the lack of the corresponding methods. (Methods useful for determining k_{act} of low-mass adducts are in many cases difficult to apply to polymer adducts.) In this thesis, the author devises two GPC methods that are applicable to polymer adducts. These methods can substantially be adopted to all the variants of LRPs and thus can be general tools to examine the activation processes in

LRP. These methods also permit to determine k_{act} in the presence of monomer, which is of prime importance because it directly corresponds to the actual polymerization system.

Another important subject of this thesis is to examine the validity of the theoretical rate equations 1.12-1.18 for individual systems. Most of the rate equations derived in the last section remain to be compared with experiments.

Good understanding of the activation processes and the polymerization rates also allows us to improve existing systems and moreover develop new and better systems. With the knowledge on the polymerization rates, the author achieves an application of the nitroxide-mediated LRP to an acrylate in this thesis (Chapter 5), where major difficulty, slow R_p, is circumvented by the addition of a conventional radical initiator (see above). Another attempt made in this thesis for developing new systems is to establish the principle for designing high-performance nitroxides. Determination of k_{act} for various polymer-nitroxide adducts gives such principle, which should be helpful to develop new effective nitroxides. Similar attempts are also made in this thesis for RAFT and ATRP systems.

1.3.2. Introduction to Individual Chapters

This thesis consists of four parts. **Part I** (Chapter 2) describes the general methods for determining k_{act} which are used in the studies in Parts II-IV. Adoption of these methods is shown for nitroxide-mediated LRPs in **Part II** (Chapters 3-5), iodide-mediated and RAFT-based LRPs in **Part III** (Chapters 6 and 7), and ATRP in **Part IV** (Chapters 8 and 9). Studies on R_p are also presented in Parts II-IV.

Chapter 2

Two GPC methods for determining k_{act} of polymer adducts, the direct and indirect methods, are described. They are used in the studies in Chapters 3-8. The direct method includes the peak-resolution of the GPC charts, while the indirect method is based on the analysis of the polydispersity according to equations 1.4 and 1.5. A method for determining k_{act} of initiator adducts for ATRP, the nitroxide capping method along with the use of ^{1}H NMR, is also illustrated. This method is used in Chapter 9.

Chapter 3

In order to establish the activation mechanism in the nitroxide-mediated LRP, the k_{act} of PS-TEMPO is determined as a function of the P$^{\bullet}$ concentration. This system is supposed to involve thermal dissociation and/or degenerative transfer as activation processes. The contribution of each process is quantitatively discussed. The temperature dependence of k_{act} in this system is also examined.

Chapter 4

The k_{act} values of PS-DBN (di-*tert*-butyl nitroxide), and -DEPN (*N*-*tert*-butyl-1-diethylphosphono-2,2-dimethylpropyl nitroxide) adducts are determined as a function of temperature and compared with that of PS-TEMPO obtained in Chapter 3 to clarify the relation between k_{act} and the nitroxide structure. Since the open-type nitroxide such as DBN have large steric hindrance compared with the ring-type nitroxides such as TEMPO, the comparison of the k_{act} values of PS-DBN and PS-TEMPO can make clear the importance of steric effects on k_{act}. The study on PS-DEPN will provide useful information about the polar as well as steric effects on k_{act}, due to the contained electron-withdrawing group.

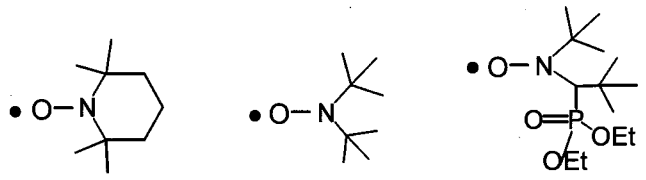

Figure 1.3. Structures of nitroxides.

Chapter 5

The nitroxide-mediated LRP of tBA is kinetically studied for two purposes. One is to manipulate the polymerization rates by adding a conventional radical initiator, dicumyl peroxide (DCP) (see equation 1.16). This may overcome the major drawback of this polymerization, i.e., slow polymerization resulting from the absence of spontaneous initiation. The other purpose is to make clear the factors affecting the chain length distributions in this

system that do not narrow as in a styrene-nitroxide system. The possible cause is discussed in terms of the magnitude of k_{act} and the contribution of side reactions.

Chapter 6

The polymerization of styrene in the presence of polystyryl iodide (PS-I) as a mediator and benzoyl peroxide (BPO) as a radical initiator are studied with respect to the polymerization rate and the activation process. The expected stationary-state kinetics (equation 1.16) is examined by following the time-conversion relation. The iodide-mediated system is supposed to involve degenerative transfer as an activation process. This assumption is examined by determining k_{act} as a function of the P$^{\bullet}$ concentration. Taking the observed small k_{act} into account, the possibility and limitation of this polymerization are also discussed.

Chapter 7

Kinetic studies are made on the polymerizations of styrene and MMA containing polymer-dithiocarbonate adducts and BPO. The polymerization rates in both styrene and MMA systems are compared with theoretical equation 1.16. The propriety of the proposed activation process, RAFT, is discussed on the basis of k_{act} values. The k_{act} values are determined for various adducts with different dithiocarbonate groups and polymers to show the differences in k_{act} among adducts. The key for successful synthesis of block copolymers in this polymerization is also discussed.

Chapter 8

The k_{act} of a polystyryl bromide (PS-Br) is determined in the presence of Cu(I)Br/2L (L = 4,4'-*n*-heptyl-2,2'-bipyridine). The result explains why the ATRP system provides the polymers with M_w/M_n as low as 1.04-1.05 even from an early stage of polymerization. The mechanism of the activation process in this system is concurrently examined.

Chapter 9

The k_{act} values of low-mass alkyl halide initiators for ATRP are determined by the nitroxide

capping method along with the use of ^{1}H NMR. Sufficiently fast activation of initiators is one of the requisites for obtaining low-polydispersity polymers. Dependence of k_{act} on the kinds of halogen and the steric factors of the alkyl group are systematically examined to explore effective initiators.

References

(1) Otsu, T.; Yoshida, M. *Makromol. Chem. Rapid Commun.* **1982**, *3*, 127.

(2) Solomon, D. H.; Rizzardo, E.; Cacioli, P. *Eur. Pat. Appl. EP135280* (Chem. Abstr. **1985**, *102*, 221335q).

(3) Georges, M. K.; Veregin, R. P. N.; Kazmaier, P. M.; Hamer, G. K. *Macromolecules* **1993**, *26*, 2987.

(4) For recent reviews, see: (a) *Controlled Radical Polymerization*; Matyjaszewski, K., Ed.; ACS Symposium Series 685; American Chemical Society: Washington, DC, **1998**. (b) Malmström, E. E.; Hawker, C. J. *Macromol. Chem. Phys.* **1998**, *199*, 923. (c) Matyjaszewski, K. *Chem. Eur. J.* **1999**, *5*, 3095. (d) Sawamoto, M.; Kamigaito, M. *CHEMTECH* **1999**, *29*(6), 30. (e) Fukuda, T.; Goto, A.; Ohno, K. *Macromol. Rapid Commun.* **2000**, *21*, 151. (f) *Controlled/Living Radical Polymerization*; Matyjaszewski, K., Ed.; ACS Symposium Series 768; American Chemical Society: Washington, DC, **2000**.

(5) (a) Hawker, C. J. *Acc. Chem. Res.* **1997**, *30*, 373. (b) Matyjaszewski, K.; Miller, P. J.; Fossum, E.; Nakagawa, Y. *Appl. Org. Chem.* **1998**, *12*, 667. (c) Ueda, J.; Kamigaito, M.; Sawamoto, M. *Macromolecules* **1998**, *31*, 6762. (d) Rizzardo, E.; Chiefari, J.; Chong, B. Y. K.; Ercole, F.; Krstina, J.; Jeffery, J.; Le, T. P. T.; Mayadunne, R. T. A.; Meijs, G. F.; Moad, C. L.; Moad, G.; Thang, S. H. *Macromol. Symp.* **1999**, *143*, 291. (e) Haddleton, D. M.; Waterson, C. *Macromolecules* **1999**, *32*, 8732. (f) Heise, A.; Nguyen, C.; Malek, R.; Hedrick, J. L.; Frank, C. W.; Miller, R. D. *Macromolecules* **2000**, *33*, 2346. (g) Angot, S.; Taton, D.; Gnanou, Y. *Macromolecules* **2000**, *33*, 5418.

(6) Ide, N.; Fukuda, T. *Macromolecules* **1999**, *32*, 95.

(7) (a) Wendler, U.; Bohrisch, J.; Jaeger, W.; Rother, G.; Dautzenberg, H. *Macromol. Rapid Commun.* **1998**, *19*, 185. (b) Bouix, M.; Gouzi, J.; Charleux, B.; Vairon, J.-P.; Guinot, P. *Macromol. Rapid Commun.* **1998**, *19*, 209. (c) Huang, H.; Remsen, E. E.; Wooley, K. L. *Chem. Commun.* **1998**, 1415.

(8) (a) Moineau, C.; Teyssié, M. P.; Jérôme, R. *Macromolecules* **1999**, *32*, 8277. (b) Cassebras, M.; Pascual, S.; Polton, A.; Tardi, M.; Vairon, J.-P. *Macromol. Rapid Commun.* **1998**, *19*, 261.

(9) (a) Ejaz, M.; Yamamoto, S.; Ohno, K.; Tsujii, Y.; Fukuda, T. *Macromolecules* **1998**, *31*, 5934. (b) Husseman, M.; Malmström, E. E.; McNamara, M.; Mate, M.; Mecerreyes, D.; Benoit, D. G.; Hedrick, J. L.; Mansky, P.; Huang, E.; Russell, T. P.; Hawker, C. J. *Macromolecules* **1999**, *32*, 1424. (c) Huang, X.; Wirth, M. J. *Macromolecules* **1999**, *32*, 1694. (d) Zhao, B.; Brittain, W. J. *J. Am. Chem. Soc.* **1999**, *121*, 3557. (e) won Werne, T.; Patten, T. E. *J. Am. Chem. Soc.* **1999**, *121*, 7409. (f) Matyjaszewski, K.; Miller, P. J.; Shukla, N.; Immaraporn, B.; Gelman, A.; Luokala, B. B.; Garoff, S.; Siclovan, T.; Kickelbick, G.; Vallant, T.; Hoffmann, H.; Pakula, T. *Macromolecules* **1999**, *32*, 8716.

(10) Szwarc, M. *Nature* **1956**, *178*, 1169.

(11) Ajayaghosh, A.; Francis, R. *Macromolecules* **1998**, *31*, 1436.

(12) Le, T. P. T.; Moad, G.; Rizzardo, E.; Thang, S. H. *International Pat. Appl. PCT/US97/12540, WO9801478* (Chem. Abstr. **1998**, *128*, 115390).

(13) Greszta, D.; Matyjaszewski, K. *Macromolecules* **1994**, *27*, 638.

(14) Hawker, C. J. *J. Am. Chem. Soc.* **1994**, *116*, 11185.

(15) Li, I.; Howell, B. A.; Matyjaszewski, K.; Shigemoto, T.; Smith, P. B.; Priddy, D. B. *Macromolecules* **1995**, *28*, 6692.

(16) Catala, J. -M.; Bubel, F.; Hammouch, S. O. *Macromolecules* **1995**, *28*, 8441.

(17) Fukuda, T.; Terauchi, T.; Goto, A.; Tsujii, Y.; Miyamoto, T.; Shimizu, Y. *Macromolecules* **1996**, *29*, 3050.

(18) Puts, R. D.; Sogah, D. Y. *Macromolecules* **1996**, *29*, 3323.

(19) Baldoví, M. V.; Mohtat, N.; Scaiano, J. C. *Macromolecules* **1996**, *29*, 5497.

(20) Bon, S. A. F.; Bosveld, M.; Klumperman, B.; German, A. L. *Macromolecules* **1997**, *30*, 324.

(21) Kothe, T.; Marque, S.; Martschke, R.; Popov, M.; Fischer, H. *J. Chem. Soc., Perkin Trans.* **1998**, *2*, 1553.

(22) Grimaldi, S.; Lemoigne, F.; Finet, J. P.; Tordo, P.; Nicol, P.; Plechot, M. WO 96/24620.

(23) Benoit, D.; Chaplinski, V.; Braslau, R.; Hawker, C. J. *J. Am. Chem. Soc.* **1999**, *121*, 3904.

(24) Benoit, D.; Grimaldi, S.; Robin, S.; Finet, J. P.; Tordo, P.; Gnanou, Y. *J. Am. Chem. Soc.* **2000**, *122*, 5929.

(25) Wayland, B. B.; Poszmik, G.; Mukerjee, S. L.; Fryd, M. J. *J. Am. Chem. Soc.* **1994**, *116*, 7943.

(26) Mardare, D.; Matyjaszewski, K. *Macromolecules* **1994**, *27*, 645.

(27) Arvanitopoulos, L. D.; Grenel, M. P.; Harwood, H. J. *Polym. Prepr. (Am. Chem. Soc., Div. Polym. Chem.)* **1994**, *35(2)*, 549.

(28) Yutani, Y.; Tatemoto, M. *Eur. Pat. Appl.* **1991**, *048937OA1*.

(29) Kato, M.; Kamigaito, M.; Sawamoto, M.; Higashimura, T. *Polym. Prepr., Jpn.* **1994**, *43*, 225.

(30) Matyjaszewski, K.; Gaynor, S.; Wang, J.-S. *Macromolecules* **1995**, *28*, 2093.

(31) Kato, M.; Kamigaito, M.; Sawamoto, M.; Higashimura, T. *Macromolecules* **1995**, *28*, 1721.

(32) Wang, J.-S.; Matyjaszewski, K. *J. Am. Chem. Soc.* **1995**, *117*, 5614.

(33) Percec, V.; Barboiu, B. *Macromolecules* **1995**, *28*, 7970.

(34) Granel, C.; Dubois, Ph.; Jérôme, R.; Teyssié, Ph. *Macromolecules* **1996**, *29*, 8576.

(35) Haddleton, D. M.; Jasieczek, C. B.; Hannon, M. J.; Scooter, A. J. *Macromolecules* **1997**, *30*, 2190.

(36) Leduc, M. R.; Hayes, W.; Fréchet, J. M. J. *J. Polym. Sci. Part A.: Polym. Chem.* **1998**, *36*, 1.

(37) Druliner, J. D. *Macromolecules* **1991**, *24*, 6079.

(38) Krstina, J.; Moad, G.; Rizzardo, E.; Winzor, C. L. *Macromolecules* **1995**, *28*, 5381.

(39) Yang, W.; Ranby, B. *Macromolecules* **1996**, *29*, 3308.

(40) Chung, T. C.; Janvikul, W.; Lu, H. L. *J. Am. Chem. Soc.* **1996**, *118*, 705.

(41) Colombani, D.; Steenbock, M.; Klapper, M.; Müllen, K. *Macromol. Rapid Commun.* **1997**, *18*, 243.

(42) Detrembleur, C.; Lecomte, Ph.; Caille, J.-R.; Creutz, S.; Dubois, Ph.; Teyssié, Ph.; Jérôme, R. *Macromolecules* **1998**, *31*, 7115.

(43) Goto, A.; Fukuda, T. *Macromolecules* **1997**, *30*, 4272.

(44) Müller, A. H. E.; Zhuang, R.; Yan, D.; Litvinenko, G. *Macromolecules* **1995**, *28*, 4326.

(45) Ohno, K.; Tsujii, Y.; Fukuda, T. *Macromolecules* **1997**, *30*, 2503.

(46) Matyjaszewski, K. In *Controlled/Living Radical Polymerization*; Matyjaszewski, K., Ed.; ACS Symposium Series 768; American Chemical Society: Washington, DC, 2000; Chapter 1.

(47) Fischer, H. *Macromolecules* **1997**, *30*, 5666.

(48) Fischer, H. *J. Polym. Sci. Part A.: Polym. Chem.* **1999**, *37*, 1885.

(49) Fukuda, T.; Terauchi, T.; Goto, A.; Ohno, K.; Tsujii, Y.; Miyamoto, T.; Kobatake, S.; Yamada, B. *Macromolecules* **1996**, *29*, 6393.

(50) Hui, A. W.; Hamielec, A. E. *J. Appl. Polym. Sci.* **1972**, *16*, 749.

(51) Greszta, D.; Matyjaszewski, K. *Macromolecules* **1996**, *29*, 5239.

(52) Greszta, D.; Matyjaszewski, K. *Macromolecules* **1996**, *29*, 7661.

(53) Greszta, D.; Matyjaszewski, K. *J. Polym. Sci. Part A.: Polym. Chem.* **1997**, *35*, 1857.

(54) Ohno, K.; Tsujii, Y.; Miyamoto, T.; Fukuda, T.; Goto, M.; Kobayashi, K.; Akaike, T. *Macromolecules* **1998**, *31*, 1064.

(55) Matyjaszewski, K.; Patten, T. E.; Xia, J. *J. Am. Chem. Soc.* **1997**, *119*, 674.

(56) Shipp, D. A.; Matyjaszewski, K. *Macromolecules* **1999**, *32*, 2948.

(57) Moad, G.; Rizzardo, E.; Solomon, D. *Polym. Bull.* **1982**, *6*, 589.

Part I

Methods for Determining Activation Rate Constants

Chapter 2

Three Novel Methods for Determining Activation Rate Constants

Abstract

Two gel permeation chromatographic (GPC) methods for determining the pseudo-first-order activation rate constants k_{act} of polymer adducts, the direct and indirect methods, were proposed. The direct method includes the peak-resolution of the GPC curves, while the indirect one is based on the analysis of the polydispersity. They are applicable to all the variants of LRP and thus can be general tools to examine the activation processes in LRP. The measurements in both methods are carried out in the monomer used in the actual LRP system, which is also the great advantage of these methods. As a method for determining k_{act} of initiator adducts for atom transfer radical polymerization (ATRP), the nitroxide capping method along with the use of proton magnetic resonance (^{1}H NMR) was also proposed.

2.1. Introduction

As discussed in Chapter 1, reversible activation (Scheme 1.1) is the key process of living radical polymerization (LRP), and the frequency of the activation-deactivation cycles, which, in an equilibrium system, is equal to the activation rate constant k_{act} of the *polymer* adduct, is the most fundamental parameter to characterize the performance of LRP (see equation 1.5). In the nitroxide-mediated LRP, some k_{act} values have been determined for *low-mass* adducts.[1-10] Low-mass alkyl-nitroxide (alkoxyamine), -halogen, and -dithioester adducts such as those given in Figures 2.1 and 2.2 are often used as initiators of LRP, whose sufficiently fast activation is one of the requisites for obtaining low-polydispersity polymers. Moreover, such low-mass adducts may provide useful information as models for polymer adducts. However, there have been no k_{act} values directly determined for polymer adducts. The k_{act} value of a polymer adduct may or may not be very different from that of a low-mass model adduct with similar structure. This should be established experimentally. Methods useful for determining k_{act} of low-mass adducts are in many cases difficult to apply to polymer adducts. In this chapter, the author proposes two gel permeation chromatographic (GPC) methods that are applicable to polymer adducts. These methods, adaptable to all the variants of LRP, can be general tools to examine the activation processes in LRP. They are used in the studies in Chapters 3-8, in which the polymer adducts **27-35** given in Figure 2.3 are examined. Regarding low-mass adducts, some k_{act} values were reported in the nitroxide system, as mentioned above, while there was only one k_{act} (or k_A) value[11] reported in atom transfer radical polymerization (ATRP), in which k_A is the rate constant of atom transfer (Scheme 1.1c). In Chapter 9, the author determines the k_A for various alkyl halide/copper complex systems to explore effective initiating systems. A novel method designed for this purpose is also presented in this chapter.

2.2. Literature Methods and Data for Low-Mass Alkoxyamines

Prior to describing the author's methods, the literature methods used for low-mass alkoxyamines are briefly summarized in this section. The corresponding k_{act} values are also listed in Tables 2.1 and 2.2, which would give some important information to be contrasted to

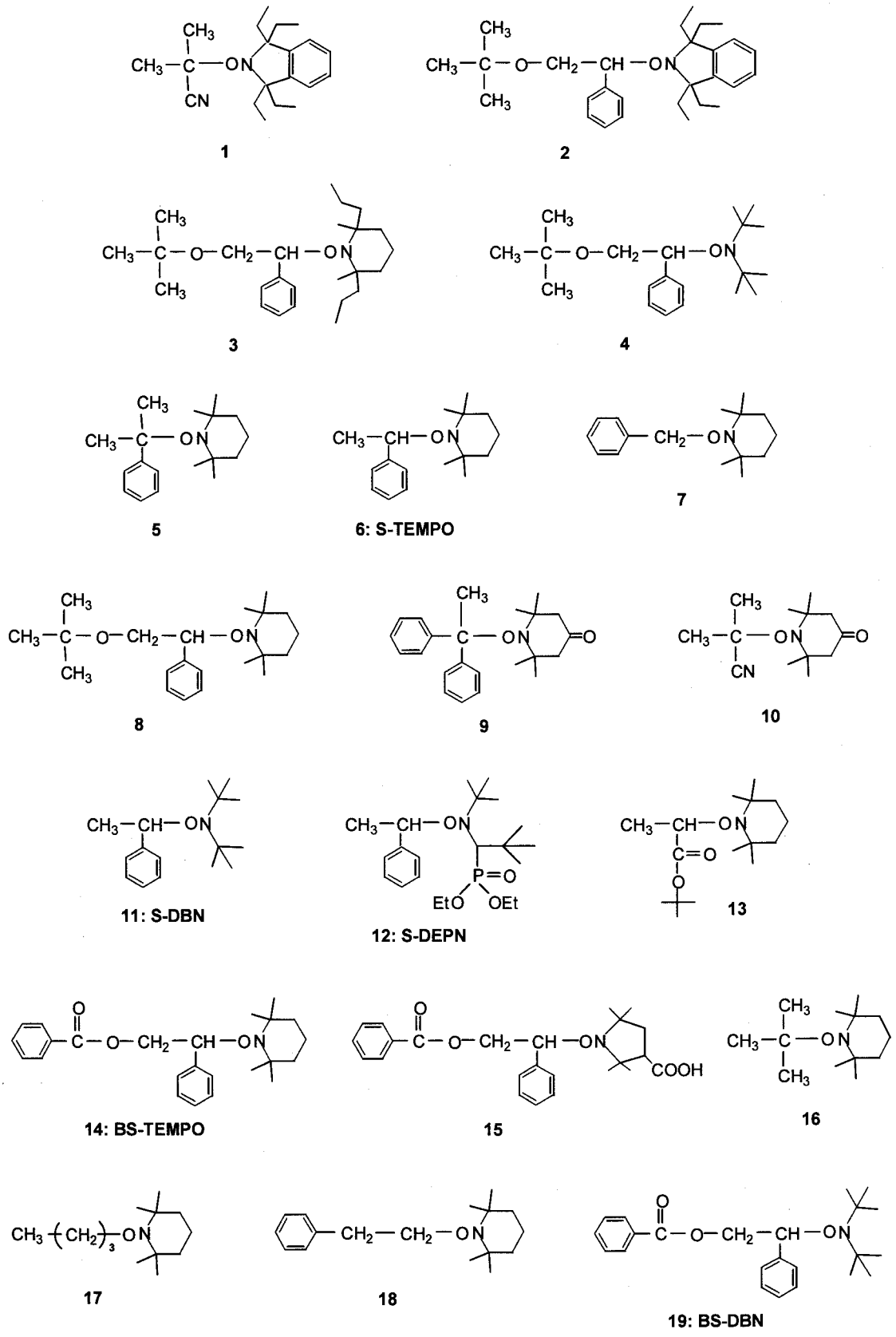

Figure 2.1. Examples of low-mass alkoxyamines.

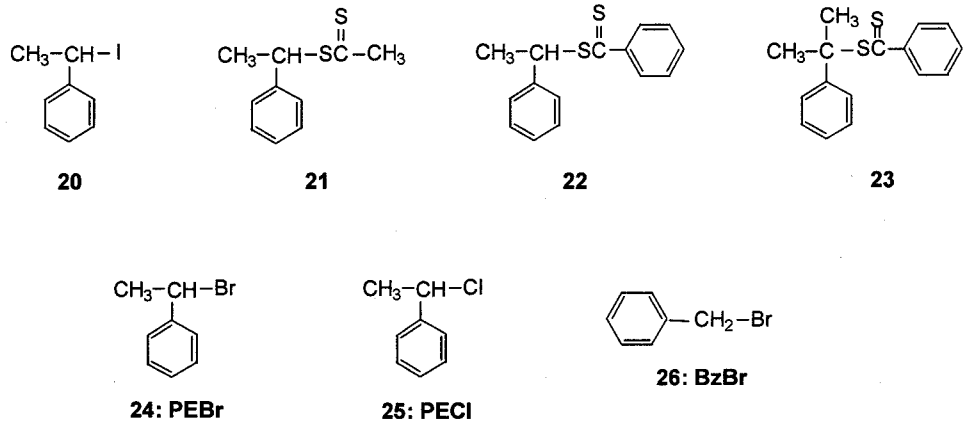

Figure 2.2. Examples of low-mass alkyl-halide and -dithioester adducts.

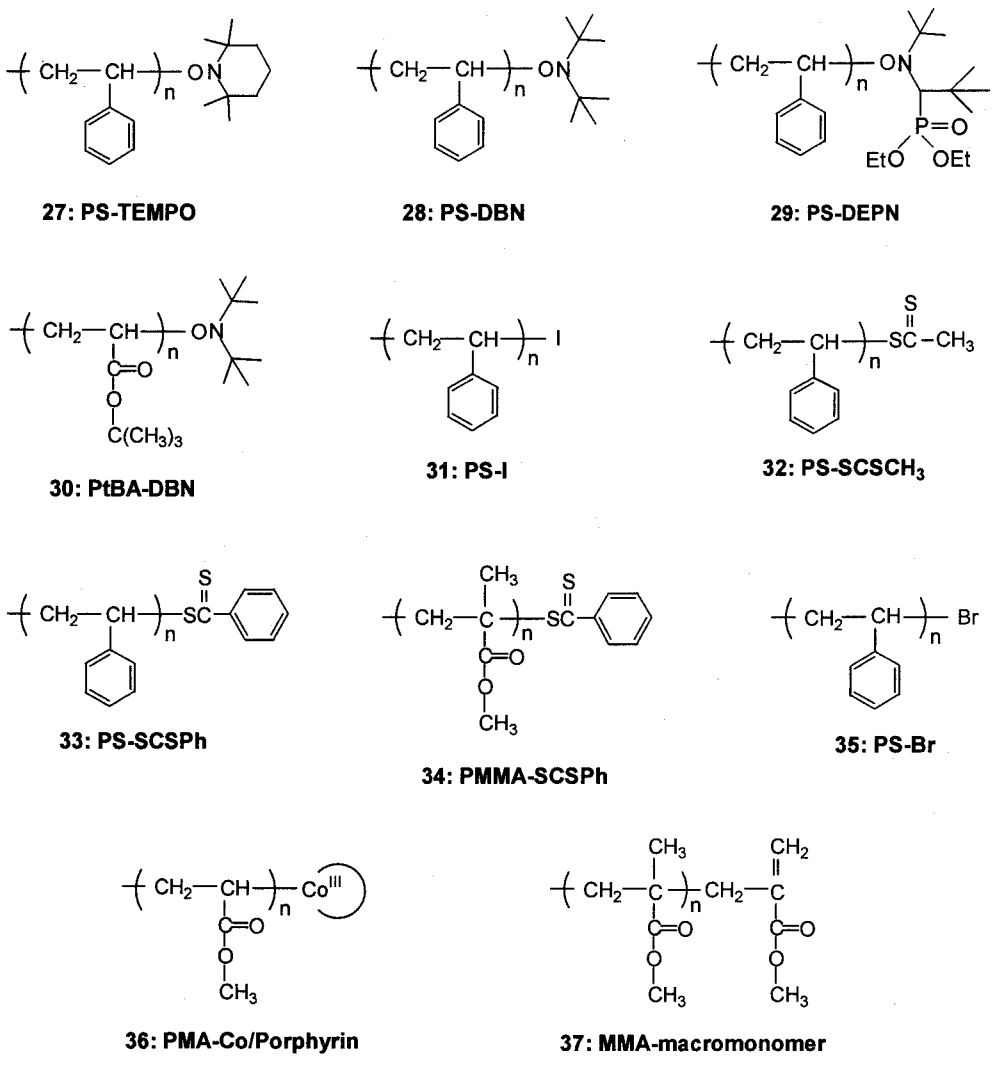

Figure 2.3. Examples of polymer adducts.

those of polymer adducts.

The methods useful to examine low-mass alkoxyamines (R-X) are based on a common concept. Namely, the alkyl radical R$^{\bullet}$ formed through the activation of R-X is scavenged by a chemical agent, e.g., a different nitroxide (X'$^{\bullet}$),[1-5] oxygen,[5-9] or deuterated styrene,[10] and the decay of the R-X concentration is followed. With a large excess of scavengers, the reformation of R-X is prevented, allowing the determination of k_{act} in the pseudo-first-order condition.

The nitroxide exchanging method (the use of X'$^{\bullet}$ as a scavenger) is one of the representative methods to study low-mass alkoxyamines. In this method, R-X is distinguished from other species by high performance liquid chromatography (HPLC). This method was first employed by Moad et al.,[1,2] who determined the half-lives of various adducts, e.g., **1**-**4**. In that study, they demonstrated that the k_{act} increases with an increase of the ring size for the cyclic nitroxides and that the alkoxyamines based on an open chain nitroxide, e.g., **4**, give the largest k_{act} values. They also noted that an increase of the solvent polarity enhances the activation of alkoxyamines. Other groups subsequently employed this method to examine **5**-**8**.[3-5] The systematic studies on **5**-**7** due to Scaiano et al.[3] clearly showed that

Table 2.1. Half-Life Times $t_{1/2}$ of Low-Mass Model Alkoxyamines

alkoxyamine	solvent	$t_{1/2}$ / min	T / °C	ref.
1	hexane	38	60	2
1	ethyl acetate	33	60	2
1	methanol	17	60	2
2	ethyl acetate	>1000	80	2
3	ethyl acetate	400	80	2
4	ethyl acetate	70	90	2
6	styrene (in bulk)	5~10	123	10
7	styrene (in bulk)	150	123	10
18	styrene (in bulk)	>300	123	10

Table 2.2. Arrhenius Parameters for k_{act} of Low-Mass Model Alkoxyamines

alkoxyamine	solvent	A_{act} / s^{-1}	E_{act} / kJ mol^{-1}	ref.
5	cyclohexane	1.0×10^{14}	114	3
5	*t*-butylbenzene	1.3×10^{14}	114.4	4
5	*t*-butylbenzene	2.0×10^{14}	115.7	7
6	cyclohexane	5.0×10^{13}	129	3
6	*t*-butylbenzene	2.5×10^{14}	133.0	7
7	cyclohexane	4.0×10^{13}	137	3
7	*t*-butylbenzene	2.6×10^{14}	145.7	7
7	*t*-butylbenzene	7.1×10^{11}	99	9
8	toluene	1.1×10^{14}	133.2	5
8	toluene	9.1×10^{14}	138.8	5
9	chrolobenzene	6.3×10^{14}	102.6	6
10	cyclohexane	1.1×10^{9}	92.1	6
10	methanol	1.2×10^{11}	96.3	6
11	*t*-butylbenzene	2.2×10^{14}	121.8	7
12	*t*-butylbenzene	1.9×10^{14}	124.5	7
13	*t*-butylbenzene	1.0×10^{14}	139.0	7
14	xylene	–	130	8
15	xylene	–	113	8
16	*t*-butylbenzene	5.8×10^{10}	97	9
17	*t*-butylbenzene	2.5×10^{10}	99	9

the strength of the C-O bond strongly depends on the steric hindrance of the alkyl moiety. The method using oxygen as a scavenger, which was developed by Howard et al.[6] and Bon et al.,[5] is another general tool to examine low-mass alkoxyamines. In this method, $R^{\bullet}$ reacts with oxygen to generate a peroxide (ROOR), and the resulting $X^{\bullet}$ (which reflects the decay of R-X) is monitored by electron spin resonance (ESR). By using this method, Fischer et al.[7] recently examined a variety of alkoxyamines, e.g., **5-7** and **11-13**, and provided

comprehensive information on the k_{act} of low-mass alkoxyamines. The third method, using deuterated styrene as a scavenger, was proposed by Hawker et al.[10] They determined the half-lives of alkoxyamines **6, 7**, and **18** by chasing the decay of R-X by proton magnetic resonance (^{1}H NMR).

Aside from these experimental studies, some groups have carried out semiempirical molecular orbital calculations.[2,12,13] It was demonstrated that those calculations generally provide a reliable, though qualitative, prediction of the experimentally observed trends in alkoxyamine dissociation rates.

2.3. Three Novel Methods for Determining k_{act}

2.3.1. GPC Direct Method (GPC Peak Resolution) for Polymer Adducts

The methods mentioned in Section 2.2 are useful to examine low-mass adducts but usually difficult to apply to polymer adducts. Here the author proposes two GPC methods, the direct and indirect one, which allow us to determine the k_{act} of polymer adducts in all the variants of LRP. In both methods, measurements are carried out in the monomer used in the actual LRP system. This is the largest advantage of these methods.

The direct method is based on the GPC observation of an early stage of polymerization containing a probe (initiating) polymer adduct P_0-X. When P_0-X is activated, the released polymer radical $P_0^{\bullet}$ will propagate until it is deactivated again by X to give a new adduct P_1-X. Here the subscript 1 denotes one activation-deactivation cycle. Since P_0-X and P_1-X (and other minor components) are generally different in chain length and its distribution, they may be distinguishable by GPC. By following the decay of the P_0-X concentration, k_{act} can be determined from the first-order plot

$$\ln(S_0/S) = k_{act}t \qquad (2.1)$$

where S_0 and S are the concentrations or GPC peak areas of P_0-X at time zero and t, respectively. In usual experimental conditions of LRP, however, the difference between P_0-X and P_1-X may not be large enough to allow accurate resolution of the GPC curve for this

purpose. A general method to increase this difference will be to decrease the rate of deactivation so that more monomers are added during a transient lifetime (the radical lifetime per activation-deactivation cycle). In the nitroxide-mediated LRP, for example, this can be achieved by intentionally decreasing the equilibrium concentration of X$^{\bullet}$ (or equivalently increasing that of P$^{\bullet}$) by, e.g., the use of a conventional initiator, as described in Chapter 1.2.3. A lower initial concentration of P_0-X is also effective to decrease the concentrations of the deactivating species, i.e., X$^{\bullet}$, P-X, and XA (see Scheme 1.1).

2.3.2. GPC Indirect Method (Polydispersity Analysis) for Polymer Adducts

The above-described method for determining k_{act} is free from any kinetic details, other than the existence of activation and propagation reactions, and for this reason, it was termed the direct method. An alternative approach described here is based on the use of GPC to follow the change in polydispersity. We focus on an early stage of polymerization started with a P_0-X, and analyze the polydispersity of the product polymer by using equations 1.4 and 1.5 which are valid for "ideal" LRP systems. In this analysis, equation 1.5 is cast into the form

$$F(C)\,[\,Y_B - (1/x_{n,B})\,]^{-1} = k_{act}\,t \qquad (2.2)$$

Since we can measure the overall number- and weight- average degrees of polymerization (x_n and x_w) and those of the subchain A or P_0-X ($x_{n,A}$ and $x_{w,A}$), we can calculate $x_{n,B}$ and Y_B of the incremental part of the product polymer according to equation 1.4, and then determine k_{act} according to equation 2.2.

This method is strictly valid when: (1) the rate constants k_{act}, k_{deact} (deactivation rate constant), and k_p (propagation rate constant) are independent of chain length, (2) [P$^{\bullet}$] is much smaller than [P-X], (3) there are no side reactions, and (4) [P$^{\bullet}$] is constant. Condition (1) is not usually questioned unless one deals with very short chains, for example. Condition (2) is met in most LRPs, in which [P$^{\bullet}$] = 10^{-8}-10^{-7} M and [P-X] = 10^{-3}-10^{-2} M, typically. Condition (3) would also approximately hold, since we are interested in an early stage of polymerization, in which the effects of side reactions are unimportant. This condition should be confirmed

to be valid in each examined system. Condition (4) requires careful considerations. The time-dependence of [P•] differs from system to system (cf. equations 1.12-1.18). The stationarity of [P•] can be checked by the easily accessible quantity R_p/[M] (= k_p[P•]), where R_p is the polymerization rate and M is monomer.

This method is an indirect one, since it totally depends on the accuracy of the theory and GPC and other kinetic details. However, unlike the direct method, it requires no particular resolution of GPC peaks (hence no special experimental conditions such as the addition of radical initiators). The only experimental requirement is to work at an early stage of polymerization to minimize the effects of side reactions.

2.3.3. Nitroxide Capping Method for the Initiators for ATRP

As mentioned above, there has been only one k_A value reported for an initiator for ATRP. This value was determined by Pascual et al.,[11] who examined the polymerization of styrene in the presence of **25** and Cu(I)Cl/2,2-bipyridine complex and followed the consumption of **25** by using vapor-phase chromatography. In Chapter 9, the author determines the k_A for various initiator/copper complex systems, in which the following method is employed.

The method used in Chapter 9 is analogous to the nitroxide exchanging method described above. Namely, a nitroxide is used as a scavenger in the activation of an alkyl halide initiator with a copper(I) complex. Since the alkyl halide is distinguishable from the formed alkoxyamine by means of ^{1}H NMR, the decay of the alkyl halide concentration can be chased. (This nitroxide capping method was originally used for the high-yield preparation of alkoxyamines from alkyl halides by Matyjaszewski et al.[14] The author applies it to the determination of k_A in this thesis.)

The concentration I of the initiator will follow the equation

$$-\mathrm{d}I/\mathrm{d}t = k_A I A \qquad (2.3)$$

where A is the concentration of the activator (the Cu(I)X complex). A is not generally constant but varies according to

$$A = A_0 - (I_0 - I) \tag{2.4}$$

where the subscript 0 denotes the initial state (t = 0). When $I_0 \neq A_0$, which is the case with the present experiments, equation 2.3 with equation 2.4 is solved to give

$$\ln(I_0/I) + \ln[(A_0 - I_0 + I)/A_0)] = (A_0 - I_0)k_A t \tag{2.5}$$

According to equation 2.5, k_A will be determined.

2.4. Conclusions

Two GPC methods, the direct and indirect ones, were proposed to determine the k_{act} of polymer adducts. They are applicable to substantially all the variants of LRP and thus can be powerful and versatile methods to study the activation processes of LRP in general. The nitroxide capping method with the use of ^{1}H NMR was also designed for determining the k_{act} of the initiators for ATRP. The adoption of these three methods will clarify details of the activation processes of individual systems, which will be described in the following chapters.

References

(1) Solomon, D. H.; Rizzardo, E.; Cacioli, P. *Eur. Pat. Appl. EP135280* (Chem. Abstr. **1985**, *102*, 221335q).

(2) Moad, G.; Rizzardo, E. *Macromolecules* **1995**, *28*, 8722.

(3) Skene, W. G.; Belt, S. T.; Connolly, T. J.; Hahn, P.; Scaiano, J. C. *Macromolecules* **1998**, *31*, 9103.

(4) Kothe, T.; Marque, S.; Martschke, R.; Popov, M.; Fischer, H. *J. Chem. Soc., Perkin Trans.* **1998**, *2*, 1553.

(5) Bon, S. A. F.; Chambard, G.; German, A. L. *Macromolecules* **1999**, *32*, 8269.

(6) Grattan, D. W.; Carlsson, D. J.; Howard, J. A.; Wiles, D. M. *Can. J. Chem.* **1979**, 57,

2834.

(7) Marque, S.; Mercier, C. L.; Tordo, P.; Fischer, H. *Macromolecules* **2000**, *33*, 4403.

(8) Veregin, R. P. N.; Georges, M. K.; Hamer, G. K.; Kazmaier, P. M. *Macromolecules* **1995**, *28*, 4391.

(9) Stipa, P.; Greci, L.; Carloni, P.; Damiani, E. *Polym. Degrad. Stab.* **1997**, *55*, 323.

(10) Hawker, C. J.; Barclay, G. G.; Orellana, A.; Dao, J.; Devonport, W. *Macromolecules* **1996**, *29*, 5245.

(11) Pascual, S.; Coutin, B.; Tardi, M.; Polton, A.; Vairon, J.-P. *Macromolecules* **1999**, *32*, 1432.

(12) Kazmaier, P. M.; Moffat, K. A.; Georges, M. K.; Veregin, R. P. N.; Hamer, G. K. *Macromolecules* **1995**, *28*, 1841.

(13) Puts, R. D.; Sogah, D. Y. *Macromolecules* **1996**, *29*, 3323.

(14) Matyjaszewski, K.; Woodworth, B. E.; Zhang, X.; Gaynor, S. G.; Metzner, Z. *Macromolecules* **1998**, *31*, 5955.

Part II

Nitroxide-Mediated Living Radical Polymerizations

Chapter 3

Activation Mechanism of Nitroxide-Mediated Living Radical Polymerization

Abstract

The pseudo-first-order activation rate constant k_{act} of polystyrene (PS)-TEMPO (2,2,6,6-tetramethylpiperidinyl-1-oxy) was determined as a function of the concentration of polymer radicals [P$^{\bullet}$] and temperature, by using the GPC direct and indirect methods. Well-defined values of k_{act} were obtained by both methods, and the results by the two methods were in good agreement. The k_{act} was found to be independent [P$^{\bullet}$], meaning that PS-TEMPO is activated (or dissociate) only thermally (Scheme 1.1a) and that degenerative chain transfer reaction (Scheme 1.1b) plays no detectable role in this system. The temperature dependence of the dissociation rate constant k_d was given by the Arrhenius equation, $k_d/s^{-1} = 3.0 \times 10^{13} \exp(-124 \text{ kJ mol}^{-1}/RT)$.

3.1. Introduction

In 1993, Georges et al. reported the nitroxide-mediated polymerization of styrene as the first successful living radical polymerization (LRP) system affording well-defined polymers with a low polydispersity (M_w/M_n = 1.1-1.3).[1] Since then, this system has attracted much attention in both academic and industrial fields and has been among the most extensively studied systems.[2,3] Important progress in understanding the mechanistic and kinetic aspect of this system can be found in the recent publication,[3] in which the polymerization rates R_p were fully examined as described in Chapter 1. However, details of the activation process in this system have never been disclosed, due to the lack of kinetic methods for studying this process. In Chapter 2, the author proposed two gel permeation chromatographic (GPC) methods for determining the activation rate constant k_{act} of polymer adducts. The purpose of this chapter is to adopt these methods to a styrene/nitroxide system and establish the activation mechanism of this system.

3.2. Definitions

Two activation processes have been postulated for styrene/nitroxide systems.[4-9] One is thermal dissociation (Scheme 1.1a), and the other is degenerative chain transfer (Scheme 1.1b). When both reactions are involved in the activation process, the pseudo-first-order activation rate constant k_{act} will take the form

$$k_{act} = k_d + k_{ex}[P^\bullet] \tag{3.1}$$

as discussed in Chapter 1. Here k_d and k_{ex} are the rate constants of dissociation and degenerative chain transfer, respectively. Thus the measurements of k_{act} as a function of $[P^\bullet]$ will allow us to discuss the contribution of the two processes on a quantitative basis. $[P^\bullet]$ hence R_p can be manipulated by the addition of a radical initiator such as *t*-butylhydroperoxide (BHP), as demonstrated in Chapter 1.

Among the disputes on the activation mechanism of this system, Hammouch and Catala have claimed the importance of degenerative transfer in controlling the molecular weights.[6]

On the other hand, the analysis of the M_w/M_n values of the TEMPO/styrene/BHP system given by the present author's group has showed some indirect evidence against the importance of degenerative transfer, where TEMPO is 2,2,6,6-tetramethylpiperidinyl-1-oxy.[7] On the basis of the polydispersity analyses of styrene/TEMPO systems, Veregin et al.[8] have also made a similar suggestion, while Greszta and Matyjaszewski[9] have indicated a difficulty of discussing this matter because of possible side reactions. It should be noted that the GPC direct method used in this chapter is independent of such side reactions. It allows to directly observe the activation process of a probe polymer-nitroxide adduct (P_0-X). Therefore, this method is expected to provide an unequivocal answer to the problem. The GPC indirect method will also be useful, since the measurement is made at an early stage of polymerization where the effects of side reactions are negligible in most cases.

3.3. Experimental Section

3.3.1. Materials

Styrene and BHP were purified by distillation. Benzoyl peroxide (BPO) was purified by recystallization from methanol. TEMPO (98 %, Aldrich) was used as received.

3.3.2. Preparation of PS-TEMPO Adduct

Styrene, BPO (72 mM), and TEMPO (86 mM) were charged in a glass tube, degassed with several freeze-thaw cycles, and sealed off under vacuum. To ensure complete decomposition of BPO, the mixture was preheated for 3.5 h at 95 °C, where no appreciable polymerization proceeded.[1] Then the system was heated at 125 °C for 4 h (conversion: 12 %), and the polymer was recovered as a precipitate from a large excess of methanol, purified by reprecipitation with a chloroform (solvent)/methanol (nonsolvent) system, and thoroughly dried. By GPC (see below), this polymer was found to have a M_n of 1700 and a M_w/M_n ratio of 1.11. According to a chain-extension test (the polymerization of styrene started with this sample), this sample is about 95 % pure; i.e., about 5 % of the chains are potentially inactive without a TEMPO moiety at the chain end (see Figure 3.1). This polystyrene (PS)-TEMPO adduct (**27**; $n \approx 15$: Figure 2.3) was used as a probe adduct P_0-X.

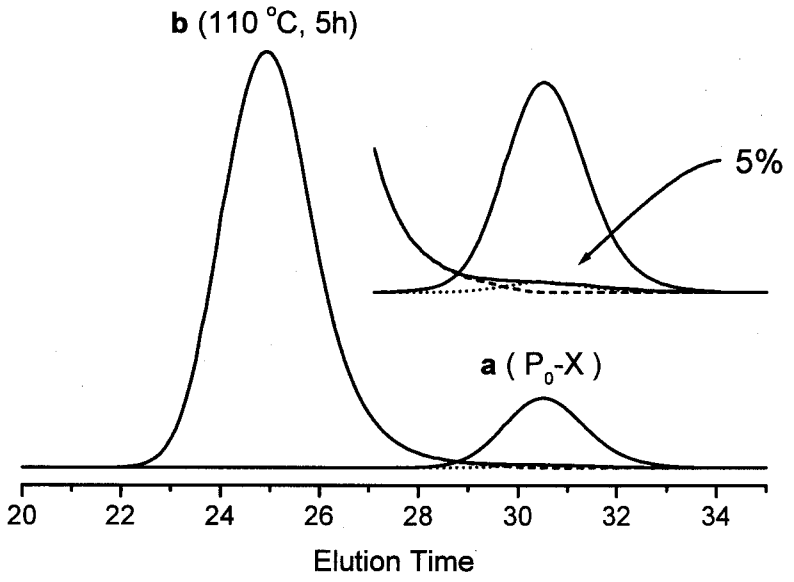

Figure 3.1. GPC elution curves for: (a) the PS-TEMPO adduct P_0-X and (b) the product obtained after a long enough (t = 5 h) polymerization of pure styrene "initiated" with P_0-X. The tail part of curve b contains about 5 % of P_0-X remaining unreacted, which means that P_0-X originally contains this much of potentially inactive species.

3.3.3. General Procedure and Kinetic Analysis of Polymerization

A styrene solution of a fixed amount of P_0-X (23 mM) and a variable amount of BHP (0-80 mM) was charged in a glass tube, degassed, and sealed off in vacuum. The solution was heated for a prescribed time t and quenched to room temperature. The reaction mixture was diluted with tetrahydrofuran (THF) to a known concentration, and a constant amount of the solution was injected to a GPC system for a quantitative analysis.

3.3.4. GPC

The GPC measurement was made on a Tosoh HLC-802 UR high-speed liquid chromatograph equipped with Tosoh gel columns G2500H, G3000H, and G4000H (Tokyo, Japan). THF was used as eluent, and temperature was maintained at 40 °C. The column system was calibrated with Tosoh standard polystyrenes. Sample detection and quantification were made with a Tosoh differential refractometer RI-8020 calibrated with known concentrations of polystyrenes in THF.

3.4. Results and Discussion

3.4.1. Determination of k_{act} by GPC Direct (Peak Resolution) Method

The author first determined the k_{act} values by the direct (peak-resolution) method. The details of this method were described in Chapter 2. Figure 3.2 shows the GPC curves of the reaction mixtures with various amounts of BHP, heated at 110 °C for 10 min. Each mixture contains the same amount of P_0-X at $t = 0$ ($[P_0\text{-X}]_0 = 23$ mM), as shown by the solid curve in the figure. After the heating, the curves show evident changes. When $[BHP]_0 = 0$, the curve becomes broader with the peak position shifted leftward or to the higher-molecular weight side. This is commonly observed at an *early* stage of this type of living radical polymerization with a small R_p. On the other hand, when $[BHP]_0 \geq 5$ mM, the curves become bimodal. These experimental conditions are so designed as to determine k_{act} by the peak-resolution method with the highest possible accuracy (and therefore they are far different from those in the usual work that aims at the preparation of well-defined, low-polydispersity polymers). The total area under each curve minus that of the $t = 0$ curve gives the amount of the monomer converted to polymer, i.e., the conversion. Figure 3.3 shows the

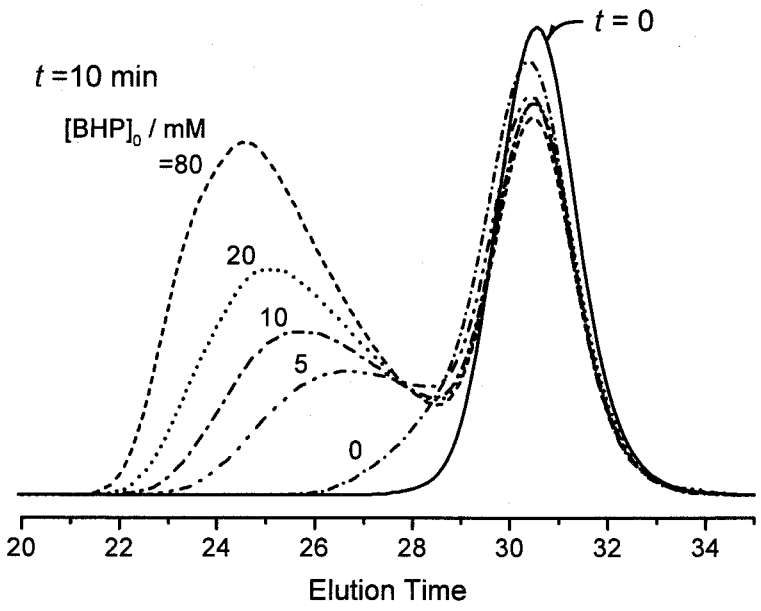

Figure 3.2. GPC elution curves of the styrene/PS-TEMPO(P_0-X)/BHP mixtures heated at 110 °C for 10 min: $[P_0\text{-X}]_0 = 23$ mM. The number attached on each curve indicates $[BHP]_0$ in mM. The solid curve is for the original ($t = 0$) solution, which contains only P_0-X as polymer species. All the curves were reduced to the same original P_0-X concentration.

plot of $\ln([M]_0/[M])$ vs t, where [M] is the monomer concentration. In all examined cases, the plot is approximately linear, showing that $R_p/[M]$ or $[P^\bullet]$ is nearly stationary for each value of $[BHP]_0$ in this range of t ($\leq$ 60 min).

Knowing the conversion and the overall M_n from the GPC curve, one can compute the concentration of polymer species, $[N_p]$, as a function of time, which is given in Figure 3.4. Within the experimental accuracy (about $\pm$ 10 %), $[N_p]$ is constant and equal to the initial value $[P_0\text{-}X]_0$.[10] This means that the observed changes in the GPC curves are due mainly to the activation of P_0-X and the subsequent polymerization starting from $P_0^\bullet$, rather than to the polymerization initiated by BHP. The role of BHP is to increase the stationary concentration of $P^\bullet$ or equivalently to decrease the stationary concentration of $X^\bullet$.[7] The number of BHP-originated polymer radicals to be stationarily supplied for this purpose can be trivial, if the desired level of $[P^\bullet]$ is not too high (note that typical value of $[P^\bullet]$ are 10^{-8}–10^{-7} M).[7] This is the main reason why the conversion and hence M_n increase with increasing $[BHP]_0$ without an appreciable increase in the number of polymers. We have made these interpretations just to avoid misunderstandings about the role of BHP and what happens at an early stage of this type of polymerizations. Actually, however, those details are not required in the direct method.

The bimodal GPC curves in Figure 3.2 clearly show that they are composed of two components, i.e., the first lower-molecular-weight component, unactivated P_0-X, and the second higher-molecular-weight component, activated and grown chain P_1-X. (The subscript 1 denotes one activation-deactivation cycle.) The second component can also include other minor species originated from BHP, thermal initiation, and a further activation of P_1-X. These curves in Figure 3.2 can be fairly accurately resolved into the two components, as illustrated in Figure 3.5, in which the shape of the curve at the lower-molecular-weight side almost exactly agrees with that of the original adduct (P_0-X) in all cases. This means that the lower-molecular-weight part of the curve is little contaminated by the second components and that we can unequivocally determine the P_0-X concentration by this peak resolution, without considering the details of the second components such as their origins and amounts. Thus this analysis allows us to determine k_{act} directly from the

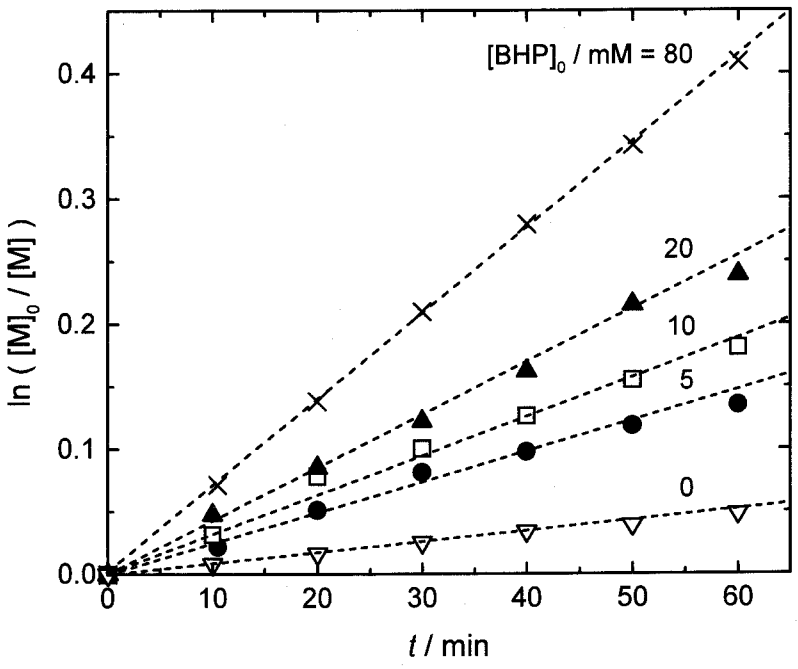

Figure 3.3. Plot of ln([M]$_0$/[M]) vs t for the styrene polymerization at 110 °C with the PS-TEMPO adduct (P_0-X) and the radical initiator BHP: [P_0-X]$_0$ = 23 mM and [BHP]$_0$ = 0(▽), 5(●), 10(□), 20(▲), and 80(×) mM.

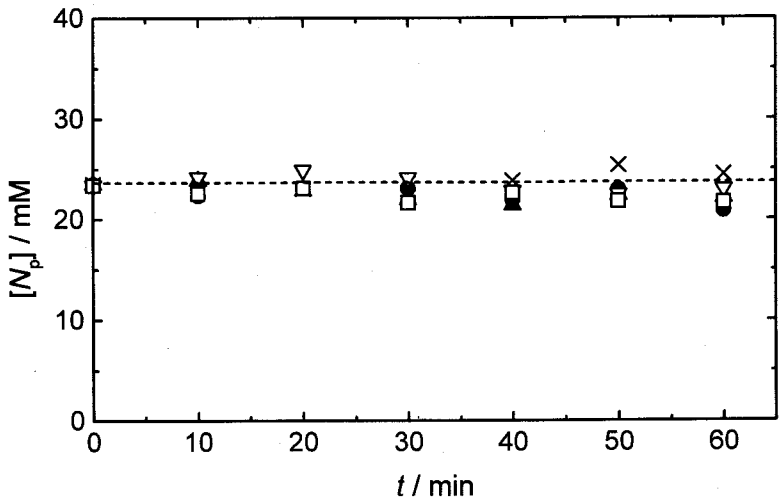

Figure 3.4. The total concentration [N_p] of polymer species as a function of reaction time: [N_p]$_0$ = [P_0-X]$_0$ = 23 mM. For symbols and reaction conditions, see Figure 3.3.

activation of P_0-X. (The unimodal curve for $[BHP]_0 = 0$ (Figure 3.2) is clearly difficult to resolve, if not impossible. The number of monomer units incorporated into the chain during one activation-deactivation cycle is too small, or [P•] is too small, in this system.)

The area (or the intensity) S of the resolved P_0-X curve relative to that at $t = 0$ (S_0) is shown in Figure 3.6 in the first-order plot. Since P_0-X originally contains 5 % of potentially inactive species (Figure 3.1), this has been corrected by subtracting $0.05S_0$ from both S_0 and S in equation 2.1. Figure 3.6 shows that all data points are approximately represented by a straight line, exhibiting no obvious trend with BHP concentration and hence [P•]. The slope of the line passing through the origin gives the k_{act} value of 3.8×10^{-4} s^{-1}.

Regarding the accuracy of these measurements, the possibility of decomposition of alkoxylamines at high temperatures should be noted: according to Li et al.,[11] S-TEMPO (**6**: Figure 2.1), a unimolecular model compound of PS-TEMPO, decomposes to styrene and hydroxylamine species via disproportionation of styryl and TEMPO radicals (Scheme 1.4e).

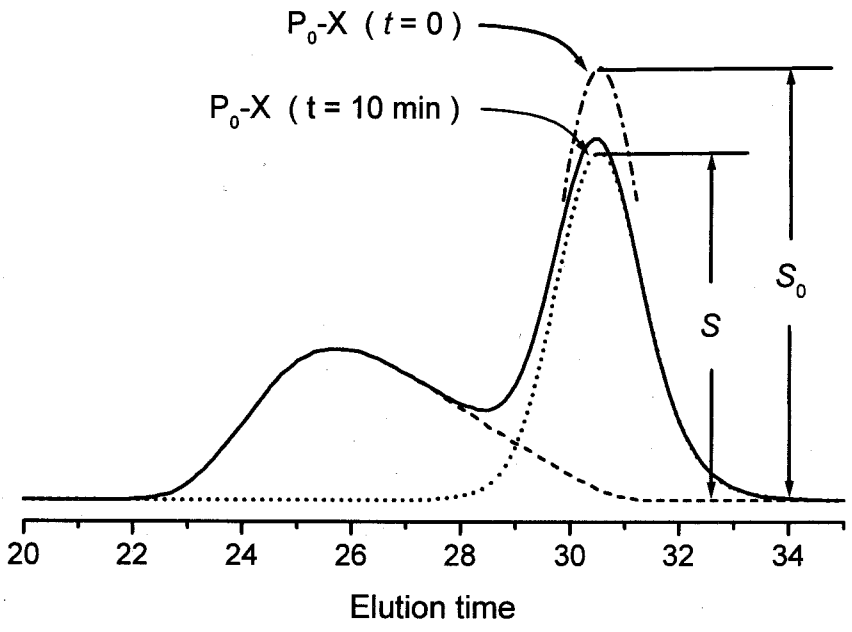

Figure 3.5. Resolution of the GPC elution curve (solid curve: $[BHP]_0 = 10$ mM, $t = 10$ min) into the two components P_0-X (dotted line) and the second one (broken line). The dot-dash curve indicates the P_0-X at $t = 0$.

The author's group recently examined this type of decomposition reaction using a PS-TEMPO adduct with $M_n \approx 1000$,[12] according to which the rate constant of decomposition of PS-TEMPO at 125 °C is 4.0×10^{-6} s^{-1}. It is expected from this value that the PS-TEMPO adduct used here in the k_{act} measurements can contain a maximum of about 5 % of decomposed species, produced and remaining unremoved during the preparation and purification stage of the adduct. This figure together with the possible contribution of bimolecularly terminated species (< 1 %)[3b] will reasonably compare to the fraction of the "dead" chains (about 5 %) estimated by the chain-extension test (Figure 3.1). Decomposed species possibly produced during the k_{act} experiments should be negligibly small in fraction (< 0.5 %). These confirm the reliability of the present analysis.

3.4.2. Determination of k_{act} by GPC Indirect (Polydispersity Analysis) Method

The direct method requires the addition of a conventional radical initiator in order to increase R_p so that the GPC peak-resolution is feasible. On the other hand, the indirect method

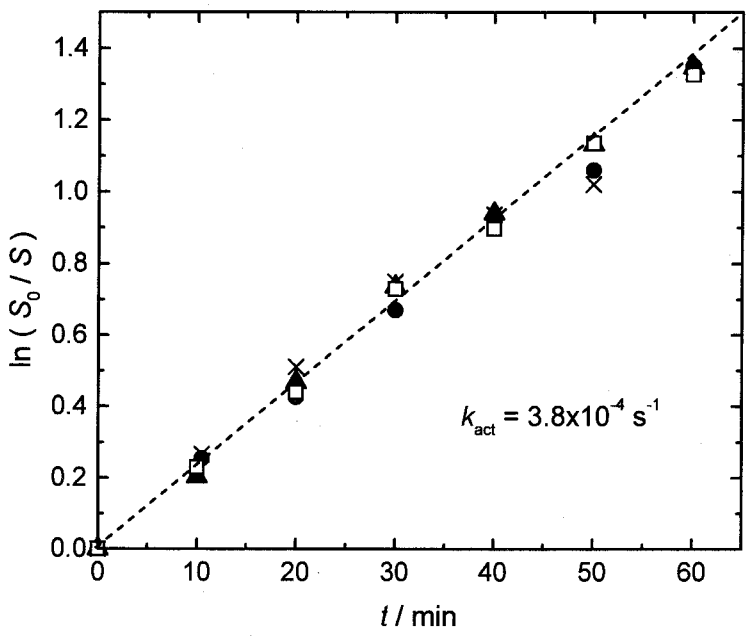

Figure 3.6. Plot of $\ln(S_0/S)$ vs t. The 5 % correction for the inactive P_0-X species has been made (see text). For symbols and experimental conditions, see Figure 3.3.

requires only the precise M_w/M_n values of the product polymers and thus is independent of the amount of a radical initiator. In this regard, the author attempted to adopt the indirect method to the BHP-free system where the adoption of the direct method was difficult. Figure 3.7 shows the GPC traces of this polymerization, i.e., containing only P_0-X (23 mM). The GPC trace at 10 min is reproduced from Figure 3.2.

Prerequisites for the indirect method to be valid are the absence of side reactions and the constancy of [P•] hence R_p/[M], as discussed in Chapter 2. As can be seen in Figure 3.4, $[N_p]$ is almost independent of t, which indicates that side reactions are negligible in this range of t ($\leq$ 60 min). This, coupled with the linear plot of $\ln([M]_0/[M])$ vs t given in Figure 3.3, confirms that the mentioned two conditions are approximately met in this experiment. Figure 3.8 shows the plot of $F(C)[Y_B - (1/x_{n,B})]^{-1}$ vs t according to equation 2.2, in which an appropriate correction was made for the inactive species included in P_0-X in about 5 %. The plot is almost strictly linear and the slope of the straight line gives a value of k_{act} of 4.1×10^{-4} s^{-1}. This value well agrees with the one determined by the direct method (3.8×10^{-4} s^{-1}).

Since this indirect method is valid irrespective of the shape of the chain length distribution curves, the author also attempted to analyze the data of the systems containing BHP (which were examined by the direct method above). As shown in Figures 3.3 and 3.4, the constancy of [P•] and $[N_p]$ are approximately met in these systems. The results, which will be shown in the next section, showed that the k_{act} values obtained by the indirect method are in agreement with those by the direct method within ± 10 %. (The validity of the indirect method was also confirmed at different temperatures (90-125 °C), as presented below.) Thus, despite its indirect nature, this method can provide sufficiently accurate k_{act} values as long as the mentioned conditions are met.

3.4.3. Activation Mechanism

The above observation in Figure 3.6 suggests that k_{act} is independent of [P•], i.e., $k_{ex} \cong 0$. For a more quantitative discussion, the author evaluated the k_{act} as a function of R_p/[M] (= k_p[P•]), for which equation 3.1 is cast into the form

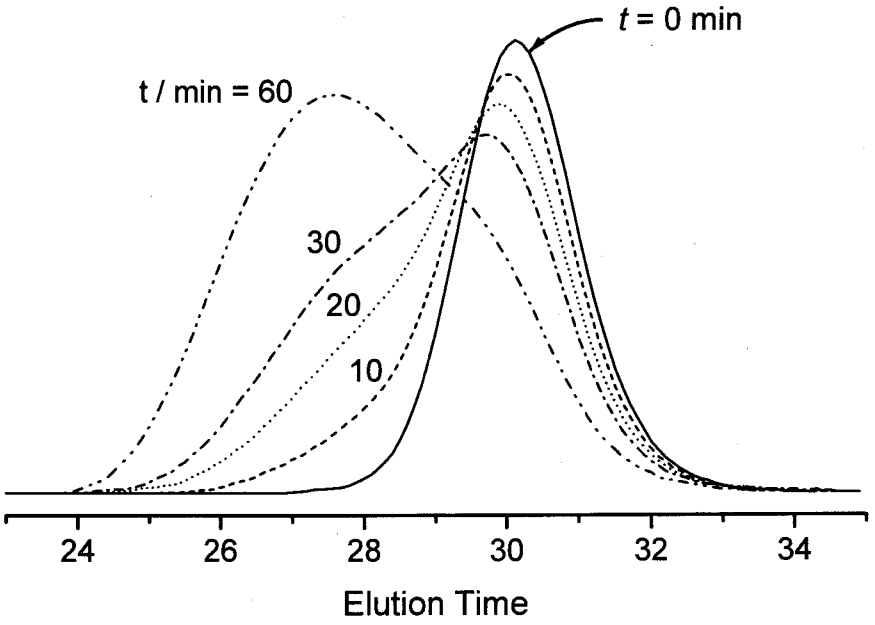

Figure 3.7. GPC elution curves of the styrene/PS-TEMPO(P_0-X) mixtures heated at 110 °C: $[P_0\text{-X}]_0$ = 23 mM. The number attached on each curve indicates the reaction time t in min. All the curves were reduced to the same original P_0-X concentration. The curve at 10 min is reproduced from Figure 3.2.

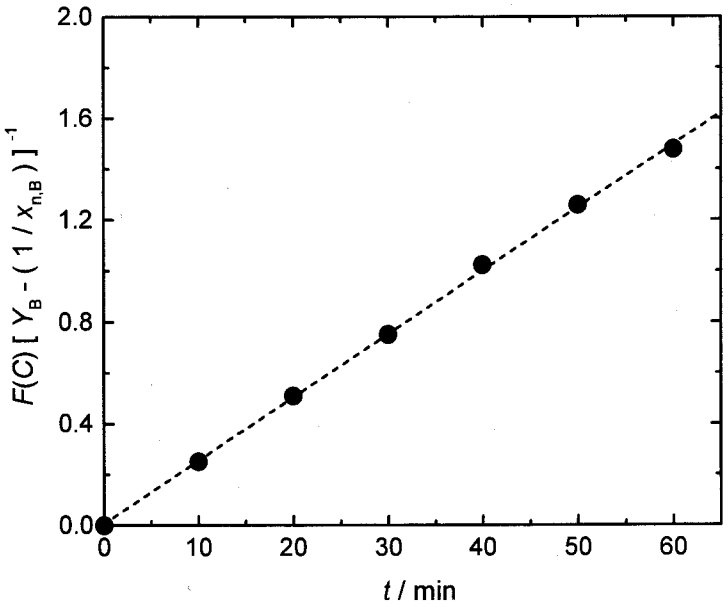

Figure 3.8. Plot of $F(C)[Y_B-(1/x_{n,B})]^{-1}$ vs t for the styrene polymerization at 110 °C with P_0-X: $[P_0\text{-X}]_0$ = 23 mM.

$$k_{act} = k_d + (k_{ex}/k_p)(R_p/[M]) \quad (3.2)$$

where k_p is the propagation rate constant. Figure 3.9 shows the plot of k_{act} vs R_p/[M]. Evidently, the data points obtained by the direct method (filled circles) form a horizontal straight line and the values obtained by the indirect method (open circles) gives almost same results. These results confirm that k_{act} may be identified with k_d in this system at least in the range of R_p/[M] $\leq 1\text{x}10^{-4}$ s^{-1} or [P$^\bullet$] $\leq 1\text{x}10^{-7}$ M, and thus the thermal dissociation process is virtually the only mechanism of activation in the styrene/TEMPO system.

3.4.4. Temperature dependence of k_d

The author also determined the k_{act} (= k_d) of PS-TEMPO at various temperatures. Figure 3.10 shows the k_d values obtained by the direct method (filled circles) and the indirect method (open circles). The results can be represented by the Arrhenius formula

$$k_d / s^{-1} = 3.0\text{x}10^{13} \exp(-124 \text{ kJ mol}^{-1} / RT) \quad (3.3)$$

The activation energy E_{act} of 124 kJ mol^{-1} is smaller than those (129-139 kJ mol^{-1})[15] of the TEMPO-based low-mass alkoxyamines **6** and **8** (Figure 2.1). This means that the chain length of the alkyl moiety gives a significant effect on the strength of the C-O bond. This would arise from the difference in steric factors.

3.4.5. Combination rate constant k_c

According to equation 3.3, the value of k_d at 125 °C is $1.6\text{x}10^{-3}$ s^{-1}, which, combined with the measured value[3b] of the equilibrium constant K (= k_d/k_c) of $2.1\text{x}10^{-11}$ M, gives $k_c = 7.6\text{x}10^7$ M^{-1} s^{-1}, where k_c is the combination rate constant (Scheme 1.1a). This k_c value for the PS-TEMPO combination may sound somewhat too small for a diffusion-controlled reaction involving a low-mass compound, for which k_c is on the order of 10^8 to 10^9, typically.[16,17] However, it is in fact comparable with the k_c values between TEMPO and low-mass model radicals such as[18] 1-phenylethyl (16 ± 4 or 19 ± 2), 1-phenyl-1-methylethyl (12 ± 1),

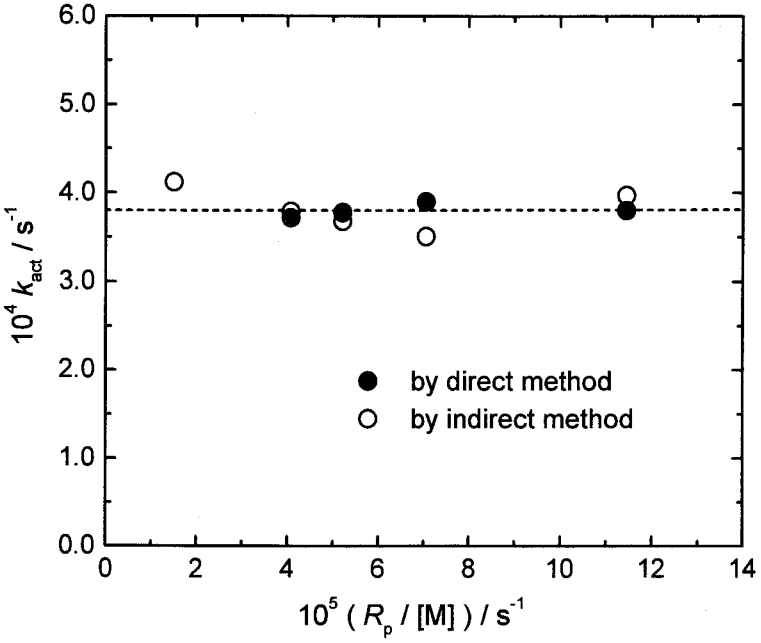

Figure 3.9. Plot of k_{act} vs R_p/[M]: (●) by the direct method and (○) by the indirect method. For experimental conditions, see Figure 3.3.

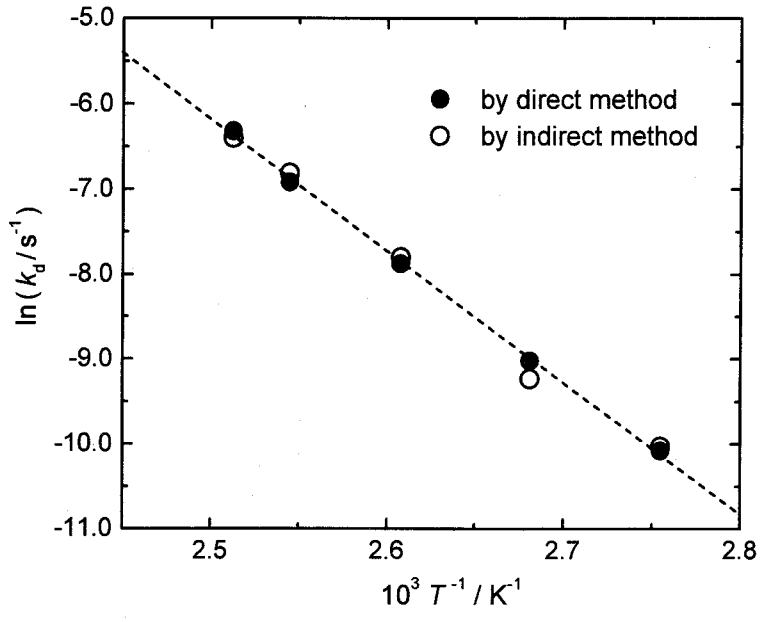

Figure 3.10. Plot of lnk_d vs T^{-1} for the thermal dissociation of PS-TEMPO: (●) by the direct method and (○) by the indirect method.

diphenylmethyl (4.63 ± 0.02), and 2-naphthylmethyl (5.7 ± 1.8), where the values in parentheses are k_c in unit of 10^7 M^{-1} s^{-1}. A polystyryl radical may thus be understood as among those radicals sterically hindered to a significant degree.

3.5. Conclusions

Within the present experimental conditions and the accuracy of k_{act} determination (about ± 10 %), degenerative transfer may be negligible, and k_{act} may be identified with k_d. This conclusion should be valid for the styrene/TEMPO polymerization at any other temperatures unless R_p is increased too much by the addition of a conventional radical initiator, since k_d, k_{ex} and k_p will change with temperature more or less similarly. From the temperature dependence of k_{act} (= k_d), it was also found that there are considerable polymer effects on the C-O bond dissociation energies, presumably due to the steric hindrance of polymers.

References and Note

(1) Georges, M. K.; Veregin, R. P. N.; Kazmaier, P. M.; Hamer, G. K. *Macromolecules* **1993**, *26*, 2987.

(2) (a) *Controlled Radical Polymerization*; Matyjaszewski, K., Ed.; ACS Symposium Series 685; American Chemical Society: Washington, DC, **1998**. (b) *Controlled/Living Radical Polymerization*; Matyjaszewski, K., Ed.; ACS Symposium Series 768; American Chemical Society: Washington, DC, **2000**.

(3) (a) Catala, J. -M.; Bubel, F.; Hammouch, S. O. *Macromolecules* **1995**, *28*, 8441. (b) Fukuda, T.; Terauchi, T.; Goto, A.; Ohno, K.; Tsujii, Y.; Miyamoto, T.; Kobatake, S.; Yamada, B. *Macromolecules* **1996**, *29*, 6393. (c) Greszta, D.; Matyjaszewski, K. *Macromolecules* **1996**, *29*, 7661. (d) Fischer, H. *J. Polym. Sci. Part A.: Polym. Chem.* **1999**, *37*, 1885. (e) Fukuda, T.; Goto, A.; Ohno, K. *Macromol. Rapid Commun.* **2000**, *21*, 151.

(4) Matyjaszewski, K.; Gaynor, S.; Greszta, D.; Mardare, D.; Shigemoto, T. *J. Phys. Org. Chem.* **1995**, *8*, 306.

(5) Greszta, D.; Mardare, D.; Matyjaszewski, K. *Macromolecules* **1994**, *27*, 638.

(6) Hammouch, S. O.; Catala, J. M. *Macromol. Rapid Commun.* **1996**, *17*, 683.

(7) Goto, A.; Fukuda, T. *Macromolecules* **1997**, *15*, 4272.

(8) Veregin, R. P. N.; Odell, P. G.; Michalak, L. M.; Georges, M. K. *Macromolecules* **1996**, *29*, 3346.

(9) Greszta, D.; Matyjaszewski, K. *Macromolecules* **1996**, *29*, 7661.

(10) A crude calculation suggests that $[N_p]$ will be larger than $[P_0\text{-}X]_0$ by about 10 % for the system with the highest $[BHP]_0$ at t = 60 min, which barely exceeds the limit of the present experimental accuracy.

(11) Li, I.; Howell, B. A.; Matyjaszewski, K.; Shigemoto, T.; Smith, P. B.; Priddy, D. B. *Macromolecules* **1995**, *28*, 6692.

(12) Ohno, K.; Tsujii, Y.; Fukuda, T. *Macromolecules* **1997**, *30*, 2503.

(13) Tsujii, Y.; Fukuda, T.; Miyamoto, T. *Polym. Prepr. (Am. Chem. Soc., Div. Polym. Chem.)* **1997**, *38(1)*, 657.

(14) Fukuda, T.; Goto, A.; Ohno, K.; Tsujii, Y. In *Controlled Radical Polymerization*; Matyjaszewski, K., Ed.; ACS Symposium Series 685; American Chemical Society: Washington, DC, 1998: Chapter 11.

(15) See references 3, 5, and 7 in Chapter 2.

(16) Beckwith, A. L. J.; Bowry, V. W.; Moad, G. *J. Org. Chem.* **1988**, *53*, 1632.

(17) Beckwith, A. L. J.; Bowry, V. W.; Ingold, K. U. *J. Am. Chem. Soc.* **1992**, *114*, 4983.

(18) Bowry, V. W.; Ingold, K. U. *J. Am. Chem. Soc.* **1992**, 114, 4992.

Chapter 4

Effects of the Structures of Nitroxides on Activation Rate Constants

Abstract

The pseudo-first-order activation rate constants k_{act} of polystyrene (PS)-DBN (di-*tert*-butylnitroxide), and -DEPN (*N*-*tert*-butyl-1-diethylphosphono-2,2-dimethylpropyl nitroxide) adducts were determined as a function of temperature by the GPC direct method, and compared with that of PS-TEMPO (2,2,6,6-tetramethylpiperidinyl-1-oxy) obtained in Chapter 3. The results showed that both the steric and polar factors associated with the structure of nitroxides strongly affect the magnitude of k_{act}. A steric factor significantly contributes to the entropy of the reaction, while a polar one takes part in the C-O bond energy. As a principle, nitroxides possessing bulkier and electron-donating substituents are more easily released from the corresponding adducts (i.e., larger k_{act}.) These results should be useful not only for a systematic understanding of existing systems but also for the design of new nitroxides.

4.1. Introduction

The nitroxide-mediated living radical polymerization (LRP) is one of the most extensively studied variants of LRP.[1] While this method is simple and robust and usually results in a well-controlled polymerization, its applicability has been limited mainly to styrenics[2] and styrenics-including random copolymerizations.[3] Recently, it was found that the polymerization of acrylates can be controlled by the proper choice of nitroxides[4-6] such as di-*tert*-butyl nitroxide (DBN: Figure 1.3)[4] and *N*-*tert*-butyl-1-diethylphosphono-2,2-dimethylpropyl nitroxide (DEPN: Figure 1.3),[5] instead of the more common nitroxide, 2,2,6,6-tetramethylpiperidinyl-1-oxy (TEMPO: Figure 1.3). (The details of the DBN-mediated acrylate polymerization are the topics of Chapter 5, in which another major problem of acrylate systems, i.e., slow polymerization rate R_p, is also considered.) These findings indicate that the nitroxide structure can play an important role in the success of controlled polymerization, and induce the exploration of new nitroxides. For the design of new high-performance nitroxides, quantitative knowledge about k_{act} (and k_{deact}) in relation to the nitroxide structure should be highly useful.

Semiempirical molecular orbital calculations[7,8] predict that k_{act} strongly depends on the nitroxide structure, and that steric factors are of prime importance. They also indicate that k_{act} increases with ring size for cyclic nitroxides and that alkoxyamines based on an open-chain nitroxide give the largest k_{act}. Although this has been partly confirmed experimentally for low-mass alkoxyamines,[7,9] there have been no studies on polymer-nitroxide adducts other than the TEMPO-related systems studied in Chapter 3. In this chapter, the author determines the k_{act} values of the two polystyrene-nitroxide adducts PS-DBN and PS-DEPN. Since DBN consists only of alkyl substituents as TEMPO does, the comparison of the k_{act} values of PS-DBN and PS-TEMPO will make clear the importance of steric effects on k_{act}. The study on PS-DEPN will provide useful information about the polar as well as steric effects on k_{act}. Although the molecular orbital calculations have suggested that the polar effects caused by electron withdrawing or donating groups in nitroxides are rather minor on the bond dissociation, the experimentally observed solvent dependence of k_{act} suggests that polar effects do contribute to alkoxyamine homolysis.[7]

4.2. Experimental Section

4.2.1. Materials

Styrene was purified by distillation. Benzoyl peroxide (BPO) was purified by recrystallization. TEMPO (98%) and DBN (98%) were used as received from Aldrich. DEPN was prepared according to the procedure of Tordo et al.[10]

4.2.2. Preparation of PS-Nitroxide Adducts

1-Phenylethyl-DBN (**11**: Figure 2.1) was prepared according to Matyjaszewski et al.[11] A styrene solution of S-DBN (40 mM) and BPO (1.7 mM) in a glass tube was degassed by several freeze-thaw-pump cycles, sealed off under vacuum, and heated at 80 °C for 90 min. After purification,[12] a PS-DBN was obtained with M_n and M_w of 2170 and 2600, respectively (M_w/M_n = 1.20), according to PS-calibrated gel permeation chromatography (GPC). A chain extension test[12] (the polymerization of styrene started with this sample) showed that this polymer contains 4 % of potentially inactive species (without DBN moiety at the chain end). The PS-DEPN prepared similarly had a M_n of 1960 and a M_w/M_n ratio of 1.11, and contained 5 % of potentially inactive species. Experimental data shown below have been corrected for these impurities.

4.2.3. General Procedure for Determination of k_{act}

The PS-nitroxide adducts described above were used as probe adducts (P_0-Xs). P_0-X and benzoyl peroxide (BPO) dissolved in styrene were charged in a glass tube, degassed, sealed off, and heated for a prescribed time t to allow polymerization to proceed. The reaction mixture was diluted with tetrahydrofuran (THF) to a known concentration and analyzed by GPC.

4.2.4. GPC

The GPC analysis was made on a Tosoh HLC-802 UR high-speed liquid chromatograph equipped with Tosoh gel columns G2500H, G3000H, and G4000H (Tokyo, Japan). THF

was used as eluent (40 °C). The column system was calibrated with Tosoh standard PSs. Sample detection and quantification were made with a Tosoh differential refractometer RI-8020 calibrated with known concentrations of PSs in THF.

4.3. Results and Discussion

4.3.1. Effects of Nitroxide Structures on k_{act}

The author determined the k_{act} values by the direct (peak-resolution) method. The details of this method were described in Chapter 2. Figure 4.1 shows the GPC chart of the styrene solution containing PS-DBN (2.0 mM) as a probe adduct P_0-X and BPO (5.0 mM) as a conventional radical initiator, heated at 70 °C for 10 min. With a proper amount of BPO added to the system, the GPC curve got separated into two definite peaks, thus allowing accurate resolution. This effect of conventional radical initiators was interpreted in Chapter 2. Clearly, the lower-molecular-weight peak in Figure 4.1 corresponds to the unactivated and remaining P_0-X, and the higher-molecular-weight one corresponds to the activated and grown chain P_1-X (and other minor components, e.g., arising from the decomposition of BPO

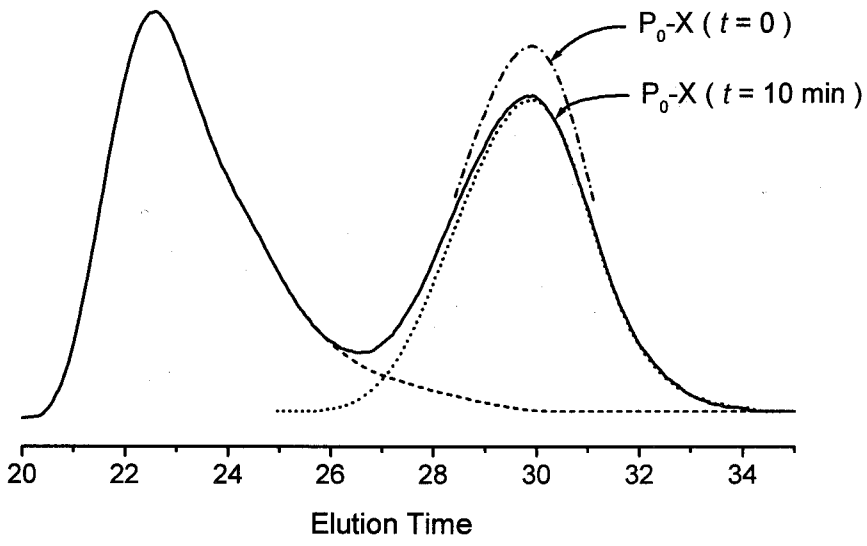

Figure 4.1. The GPC chart of the styrene/PS-DBN(P_0-X)/BPO mixture heated at 70 °C for 10 min (solid line): $[P_0\text{-X}]_0$ = 2.0 mM and $[BPO]_0$ = 5.0 mM, which is resolved into P_0-X (dotted line) and other components (broken line). The dot-dash line indicates the P_0-X at t = 0.

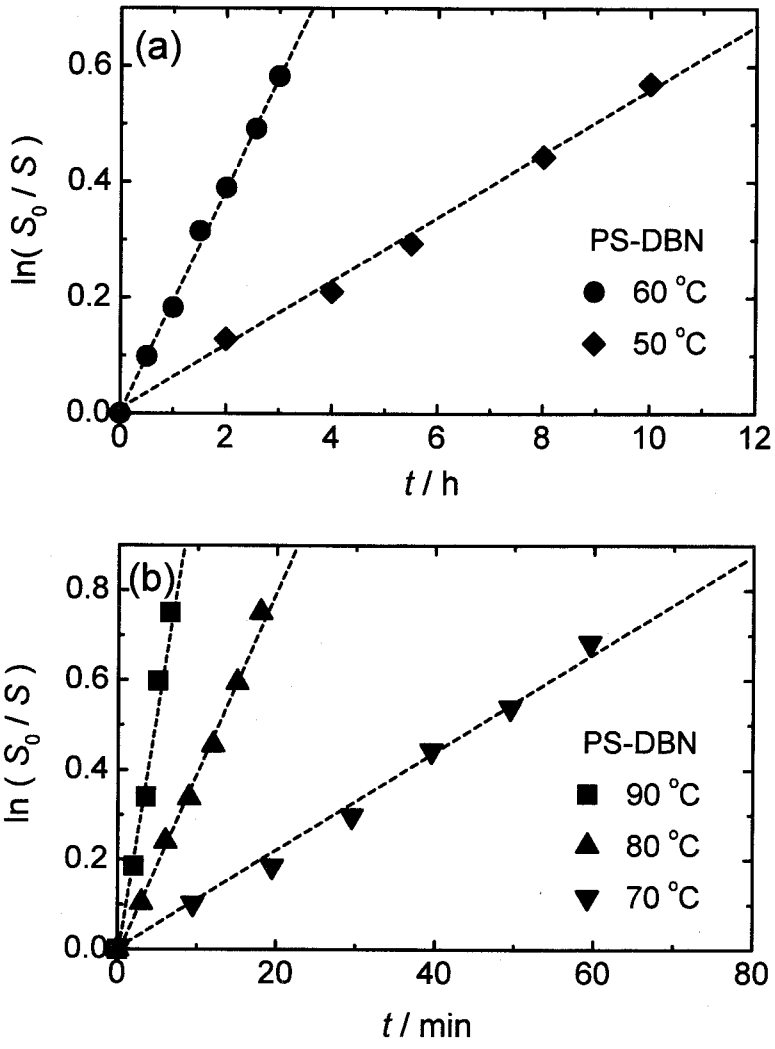

Figure 4.2. Plot of $\ln(S_0/S)$ vs. t for PS-DBN (a) at 50 (◆) and 60 (●) °C, and (b) at 70(▼), 80 (▲), and 90 (■) °C: $[P_0\text{-X}]_0$ = 2.0 mM in all cases, and $[BPO]_0$ = 2.0, 3.0, 5.0, 5.0, and 7.5 mM for 50, 60, 70, 80, and 90 °C, respectively.

and further activation of P_1-X). Here the subscript 1 denotes one activation-deactivation cycle. Figures 4.2 and 4.3 show the plot of $\ln(S_0/S)$ vs t at various temperatures for PS-DBN and PS-DEPN, respectively, where S_0/S is the ratio of the P_0-X concentration or the GPC peak area at time zero to that at time t. The plots are linear in all cases, which give well-defined values of k_{act} according to equation 2.1.

Figure 4.4 shows the temperature dependence of k_{act}. The Arrhenius parameters obtained thereby and the k_{act} values estimated at 120 °C are summarized in Tables 4.1 and 4.2,

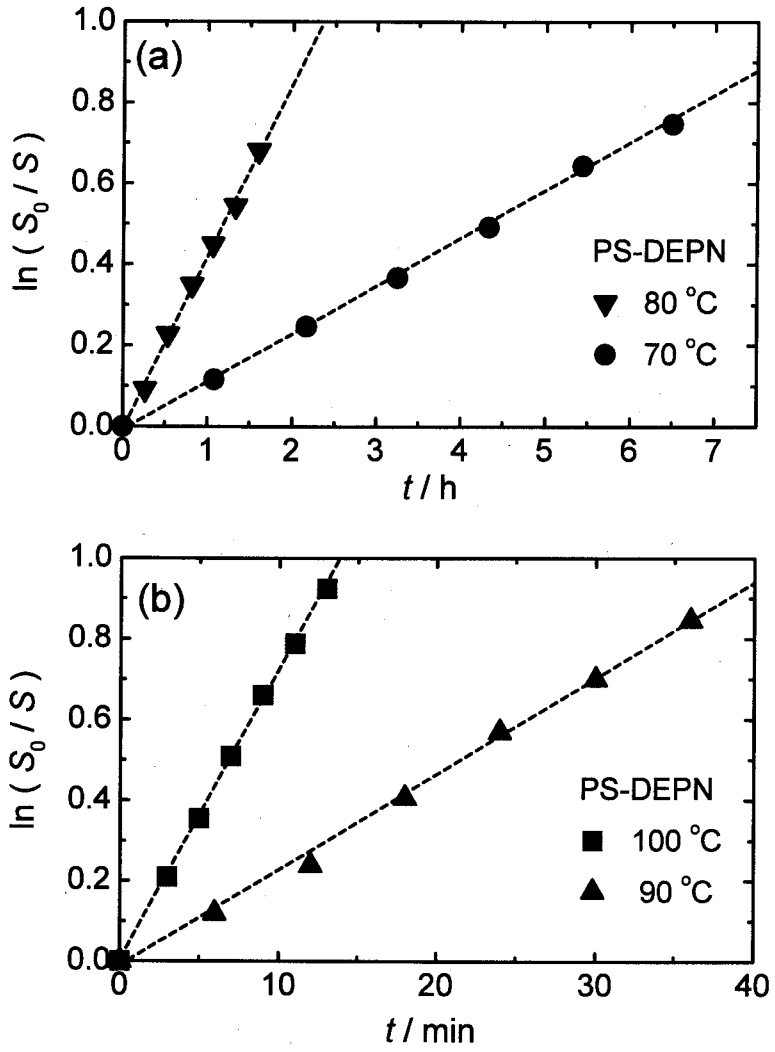

Figure 4.3. Plot of $\ln(S_0/S)$ vs. t for PS-DEPN (a) at 70 (●) and 80 (▼) °C, and (b) at 90 (▲) and 100 (■) °C: $[P_0\text{-}X]_0$ = 4.6 mM in all cases, and $[BPO]_0$ = 2.0 mM for 70, 80, and 90 °C and 6.0 mM for 100 °C.

respectively. In comparison among PS-nitroxide adducts, the open-chain nitroxide DBN gives a much larger k_{act} than the cyclic nitroxide TEMPO, meaning that steric factors are very important in determining k_{act}. The activation energy E_{act} of the PS-DBN dissociation is somewhat smaller than that for the PS-TEMPO adduct. Although the E_{act} values may be subject to a considerable error, their face values indicate that steric factors have a small effect on the strength of the C-O bond in this case. This is in good agreement with the result of the molecular orbital calculation which predicts that the C-O bond dissociation energy of an

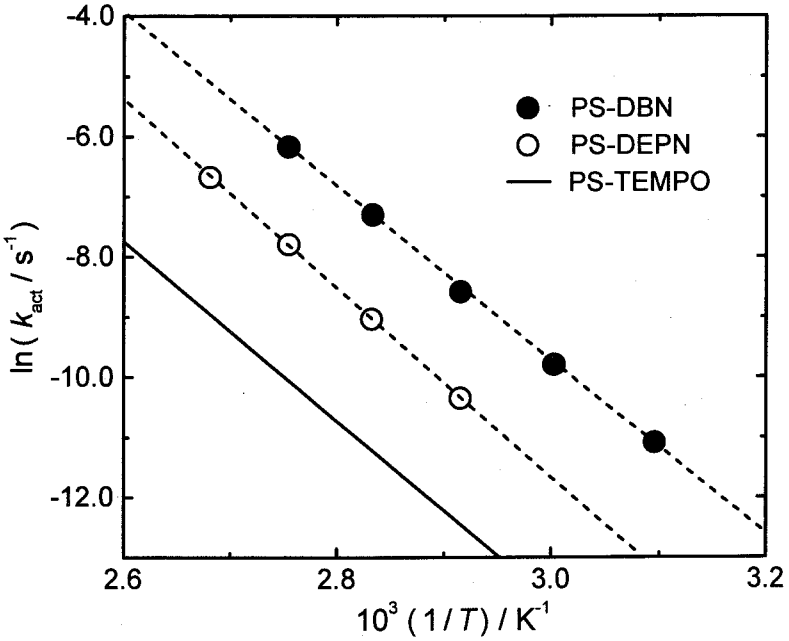

Figure 4.4. Plot of ln(k_{act}) vs. T^{-1} for the dissociation of (●) PS-DBN and (○) PS-DEPN. The solid line corresponds to the PS-TEMPO dissociation being determined in Chapter 3.

Table 4.1. Arrhenius Parameters for the k_{act} of Alkoxyamines

alkoxyamine	A_{act} [a] / s^{-1}	E_{act} [b] / (kJ mol^{-1})
PS-TEMPO[c]	3.0 x 10^{13}	124 ± 2
PS-DBN	3.8 x 10^{14}	120 ± 2
PS-DEPN	2.0 x 10^{15}	130 ± 2

[a] At 95 % confidence level, A_{act} = (1.6-6.4)x10^{13}, (2.5-6.4)x10^{14}, and (1.1-3.7)x10^{15} for PS-TEMPO, PS-DBN, and PS-DEPN, respectively. [b] At 95 % confidence level, statistical error smaller than 2 kJ mol^{-1}. [c] obtained in Chapter 3.

Table 4.2. The k_{act} of Alkoxyamines at 120 °C

alkoxyamine	10^3 k_{act} / s^{-1}
PS-TEMPO[a]	1.0
PS-DBN[b]	42
PS-DEPN[b]	11
PtBA-DBN[c]	1.0

[a] obtained in Chapter 3. [b] calculated from the Arrhenius parameters in Table 4.1. [c] obtained in Chapter 5.

alkyl-DBN adduct is only 3 to 6 kJ mol^{-1} smaller than that of the corresponding TEMPO adduct for any kind of alkyl components.[7] Steric factors will have a larger effect on E_{act} when a nitroxide has so bulky substituent(s) as to make the C-O bond considerably longer. On the other hand, the frequency factor A_{act} for the DBN adduct is much larger than that for the TEMPO analogue, meaning that steric factors are more strongly reflected on the reaction entropy.

One may expect from an entropic point of view that DEPN would give a larger k_{act} than DBN, since the former has a much bulkier side group than the latter. Interestingly, however, Table 4.2 shows that it is not the case at 120 °C. This suggests that while the entropic factor of the PS-DEPN dissociation is larger than that of the PS-DBN dissociation, the energetic factor of the former reaction must also be larger than that of the latter. This was in fact observed (Table 4.1). A larger E_{act} for PS-DEPN would be due to the electron-withdrawing effect of the phosphonate group, which results in a larger C-O bond energy. Polar factors can thus have a noticeable effect on the bond dissociation energy.

However, Fischer et al.[9] recently reported that the E_{act} for 1-phenylethyl-DEPN adduct (**12**: Figure 2.1) (124.5 kJ mol^{-1}) is smaller than that for the corresponding TEMPO adduct (**6**: Figure 2.1) (133.0 kJ mol^{-1}), as shown in Table 2.2. This is the opposite of our results. Fischer et al. examined low-mass adducts, while we examined the polymeric ones. It is unclear at this moment whether these opposite results should be ascribed to chain length or experimental error. For this reason, the above discussion on the effect of polar factors should be viewed with due reserve. However, the comparison of the absolute values of k_{act} of the polymeric and low-mass adducts unequivocally leads to the conclusion that the k_{act} of the polymeric adduct is larger than that of the low-mass homologue[9] by a factor of 2 to 3 in all the three cases. This stresses the importance of the effect of chain length on the bond dissociation problem.

The fairly large k_{act} values of PS-DBN and PS-DEPN indicate that the use of DBN or DEPN instead of TEMPO will allow LRP to proceed under a lower temperature than in the TEMPO systems (typically, ≥ 120 °C for TEMPO-mediated styrene polymerizations). However, it is important to note that a large k_{act} does not always guarantee a high performance

LRP because of possible side reactions. In particular, thermal degradation of alkoxyamines[13,14] should be considered in the choice of nitroxides for practical applications.

4.3.2. Effects of Polymer Structures on k_{act}

Molecular orbital calculations also predict that the magnitude of k_{act} depends on the polymer as well as nitroxide moieties.[7] In fact, poly(*t*-butyl acrylate) (PtBA)[4] and PS attached to the same nitroxide (DBN) make a large difference in k_{act}, as shown in Table 4.2. In this particular case, the stabilities of the polymer radicals (decreasing in order of: Ph > CO_2R) seem to take more part in k_{act} than the steric factor (decreasing in order of: CO_2R > Ph) does. Namely, the energetic rather than the entropic factor is primarily important in this case. Certainly, the entropic factor will have to be emphasized for polymers possessing a bulkier substituent, like a sugar residue,[15] instead of a simple Ph or CO_2R group in the side chain. The relative importance of the two factors should vary according to the structure of the polymer.

4.4. Conclusions

The activation rate constants k_{act} of PS-DBN and PS-DEPN adducts were determined by the GPC peak-resolution method and compared with the k_{act} values of PS-TEMPO obtained in Chapter 3. The results indicated that both steric and polar factors associated with the structure of nitroxides affect the magnitude of k_{act}. A steric factor significantly contributes to the reaction entropy, while a polar one influences the C-O bond energy. The relative importance of the two factors depends on nitroxides (as well as on polymers). These results should be useful not only for a systematic understanding of existing systems but also for the design of new nitroxides.

References

(1) See references 2 and 3 in Chapter 3.

(2) (a) Georges, M. K.; Veregin, R. P. N.; Kazmaier, P. M.; Hamer, G. K.

Macromolecules **1993**, *26*, 2987. (b) Yoshida E. *J. Polym. Sci. Part A.: Polym. Chem.* **1996**, *36*, 2937. (c) Kazmaier, P. M.; Daimon, K.; Georges, M. K.; Hamer, G. K.; Veregin, R. P. N. *Macromolecules* **1997**, *30*, 2228. (d) Jousset, S.; Hammouch, S. O.; Catala, J. M. *Macromolecules* **1995**, *28*, 8441.

(3) (a) Hawker, C. J. ; Elce, E.; Dao, J.; Volksen, W.; Russell, T. P.; Barclay, G. G. *Macromolecules* **1996**, *29*, 2686. (b) Fukuda, T.; Terauchi, T.; Goto, A.; Tsujii, Y.; Miyamoto, T.; Shimizu, Y. *Macromolecules* **1996**, *29*, 3050. (c) Butz, S.; Baethge, H.; Schmidt-Naake, G. *Macromol. Rapid Commun.* **1997**, *18*, 1049.

(4) Chapter 5 of this thesis; Goto, A.; Fukuda, T. *Macromolecules* **1999**, *32*, 618.

(5) Benoit, D.; Grimald, S.; Finet, J. P.; Tordo, P.: Fontanille, M.; Gnanou, Y. In *Controlled Radical Polymerization*; Matyjaszewski, K., Ed.; ACS Symposium Series 685; American Chemical Society: Washington, DC, 1998: Chapter 14.

(6) Benoit, D.; Chaplinski, V.; Braslau, R.; Hawker, C. J. *J. Am. Chem. Soc.* **1999**, *121*, 3904.

(7) Moad, G.; Rizzardo, E. *Macromolecules* **1995**, *28*, 8722.

(8) Kazmaier, P. M.; Moffat, K. A.; Georges, M. K.; Veregin R. P. N.; Hamer, G. K. *Macromolecules* **1995**, *28*, 1841.

(9) Marque, S.; Mercier, C. L.; Tordo, P.; Fischer, H. *Macromolecules* **2000**, *33*, 4403.

(10) WO 96/24620, invs.: Grimaldi, S.; Lemoigne, F.; Finet, J. P.; Tordo, P.; Nicol, P.; Plechot, M.

(11) Matyjaszewski, K.; Woodworth, B. E.; Zhang, X.; Gaynor, S. G.; Metzner, Z. *Macromolecules* **1998**, *31*, 5955.

(12) See the Experimental Section in Chapter 3.

(13) Li, I.; Howell, B. A.; Matyjaszewski, K.; Shigemoto, T.; Smith, P. B.; Priddy, D. B. *Macromolecules* **1995**, *28*, 6692.

(14) Ohno, K.; Tsujii, Y.; Fukuda, T. *Macromolecules* **1997**, *30*, 2503.

(15) Ohno, K.; Tsujii, Y.; Miyamoto, T.; Fukuda, T.; Goto, M.; Kobayashi, K.; Akaike, T. *Macromolecules* **1998**, *31*, 1064.

Chapter 5

Kinetic Studies on Nitroxide-Mediated Living Radical Polymerization of *tert*-Butyl Acrylate

Abstract

The nitroxide-mediated LRP of *tert*-butyl acrylate (tBA) was kinetically studied. It was demonstrated that the polymerization rate R_p can be increased by addition of a proper amount of a radical initiator, dicumyl peroxide (DCP), without causing any appreciable broadening of the polydispersity. The use of di-*tert*-butylnitroxide (DBN) allowed the controlled polymerization of tBA to proceed at a lower temperature than the polymerization controlled by a TEMPO (2,2,6,6-tetramethylpiperidinyl-1-oxy) derivative, which was conducted by Georges et al. (*Macromolecules* **1996**, *29*, 8993). The pseudo-first-order activation rate constant k_{act} of the poly(tBA)-DBN adduct was also determined by the GPC direct method to be 1.0×10^{-3} s^{-1} at 120 °C, which indicates that the adduct experiences activation-deactivation cycles frequently enough to achieve low polydispersity. Nevertheless, the polydispersity markedly increased and the R_p decreased at later stages of polymerization, due to the decomposition of the alkoxyamine and the subsequent hydrogen transfer.

5.1. Introduction

The nitroxide-mediated living radical polymerization (LRP) has been successfully applied to styrene[1] and its derivative[2] and also proved to be effective in random copolymerizations of styrenics with other monomers such as acrylates, methacrylates and acrylonitrile.[3] However, it has found limited success in controlling the homopolymerizations of these monomers other than styrenics: the first attempt with acrylates was made by Solomon et al.,[4] who obtained oligomers with rather high polydispersities ($M_w/M_n > 1.5$). More recently, Listigovers et al.[5] have carried out the homopolymerization of *t*- and *n*-butyl acrylates (tBA and nBA) at high temperatures (145–155 °C) using 4-oxo-2,2,6,6-tetramethylpiperidinyl-1-oxy (4-oxo-TEMPO) as a mediator, and obtained polymers with high molecular weights (e.g., $M_w \approx 27000$) and appreciably low polydispersities ($M_w/M_n < 1.5$). However, the maximum conversion achieved in their system was rather low (about 35 %). Benoit et al.[6] has used *N-tert*-butyl-*N*-(1-diethylphosphono-2,2-dimethyl)propylnitroxyl (DEPN: Figure 1.3) together with azobis(isobutyronitrile) (AIBN) to yield low-polydispersity poly(nBA)s (M_w/M_n = 1.1–1.2) with high conversions. However, this remarkable result was obtained at the expense of a long polymerization time (e.g., 42 h to reach conversions of 72–95 %).

In this Chapter, the author studies the polymerization of tBA mediated by di-*t*-butylnitroxide (DBN: Figure 1.3). The reason why we have chosen this nitroxide, rather than the more common nitroxide 2,2,6,6-tetramethylpiperidinyl-1-oxy (TEMPO: Figure 1.3), is the possibly larger rate of activation (homolysis) of the polymer-DBN adduct than that of the TEMPO counterpart.[7-10] There are two main purposes in this work. One is to confirm the role of a conventional radical initiator as an accelerator. As shown in Chapter 1, radical initiators such as *t*-butylhydroperoxide (BHP)[11] and dicumyl peroxide (DCP),[12] which have a moderate rate of decomposition at high temperatures, enhance the polymerization rate R_p of styrene in the presence of a styrenic-TEMPO adduct without causing any appreciable broadening of the chain length distribution, at least in a limited range of the initiator concentration. The tBA system is distinguished from the styrene system by the fact that the spontaneous (thermal) polymerization is appreciable in the bulk polymerization of styrene at high temperatures, whereas it is much less significant in that of tBA. Hence, the use of a

radical initiator is a possible way to manipulate the rate of polymerization of tBA. The other purpose of this work is to make clear the factors affecting the chain length distribution of this system. A preliminary result on the tBA polymerization in the presence of a poly(tBA)-DBN adduct (PtBA-DBN) has suggested that the chain length distribution of this system does not narrow as in a styrene-nitroxide system. The reason for this will be unequivocally established by determining the rate constant of activation k_{act} and comparing it to that in the styrene system. Results of such experiments will be presented below.

5.2. Experimental Section

5.2.1. Materials

Commercially obtained styrene, tBA, benzoyl peroxide (BPO), and DCP were purified by distillation or recrystallization. DBN was purchased from Aldrich and used without further purification. 2-Benzoyloxy-1-phenylethyl-DBN (**19**; BS-DBN: Figure 2.1) was prepared starting with BPO, styrene, and DBN in the same manner as described previously,[13] excepting that the reaction temperature was 60 °C.

5.2.2. General Procedure for Polymerization of tBA

BS-DBN (40 and 80 mM) and DCP (0, 1.0, and 3.0 mM) were dissolved in tBA, degassed, sealed off under vacuum, and heated at 120 °C for a prescribed time *t*. The mixture was then quenched to room temperature, diluted by tetrahydrofuran (THF) to a known concentration, and directly analyzed by gel permeation chromatography (GPC).

5.2.3. Preparation of PtBA-DBN Adduct

A tBA solution of BS-DBN (82 mM) and DCP (3.0 mM) in a glass tube was degassed and heated at 120 °C for 1 h (conversion: 20.2 %). The produced polymer was purified by reprecipitation with chloroform and methanol/water (8/2) used as a solvent and a nonsolvent, respectively, and then thoroughly dried. According to PS-calibrated GPC, M_n and M_w/M_n were found to be 2100 and 1.29, respectively. The chain extension test (see Chapter 3) showed that the fraction of potentially inactive species (without nitroxide moiety at the chain

end) is approximately 7 %. Another model adduct with M_n = 1200 and M_w/M_n = 1.16 was prepared similarly, excepting that the reaction was stopped at 20 min. This polymer was used for the decomposition experiments.

5.2.4. Measurements

Proton magnetic resonance (^{1}H NMR) spectra were obtained by a JEOL GSX-400 spectrometer operating at 400 MHz. These spectra were recorded at ambient temperature, and with flip angle of 45 degrees, spectral width of 7934 Hz, acquisition time of 4.129 sec, and pulse delay of 10 sec. The GPC measurement was made on a Tosoh HLC-802 UR high-speed liquid chromatograph equipped with Tosoh gel columns G2500H, G3000H, and G4000H. THF was used as eluent (40 °C). The column system was calibrated with Tosoh standard polystyrenes (PSs). Sample detection and quantification were made with a Tosoh differential refractometer RI-8020 calibrated with known concentrations of PtBA-DBN adducts in THF.

5.3. Results and Discussion

5.3.1. Enhancement of Polymerization Rate

Since TEMPO is most widely employed as a nitroxyl mediator, the author initially attempted the polymerization of tBA with TEMPO at 120 °C. However, the polydispersity index M_w/M_n of the resultant polymer remained approximately 2.0 throughout the course of polymerization. This was presumed to be due to a very small value of k_{act} in the tBA/TEMPO system at this temperature. It has been reported that k_{act} strongly depends on the structures of nitroxides. The (model) experiments[7,9,10] and molecular orbital calculations[7,8] showed that the k_{act} of the open-type nitroxide like DBN is larger than that of the ring-type one like TEMPO, mainly due to the difference in steric factors. This encouraged the author to use DBN instead of TEMPO.

Figure 5.1a shows the GPC traces for the bulk polymerization of tBA with BS-DBN adduct at 120 °C. It can be seen that the molecular weight increases with polymerization time t. However, the chains almost stopped growing after about 6 h, where the conversion

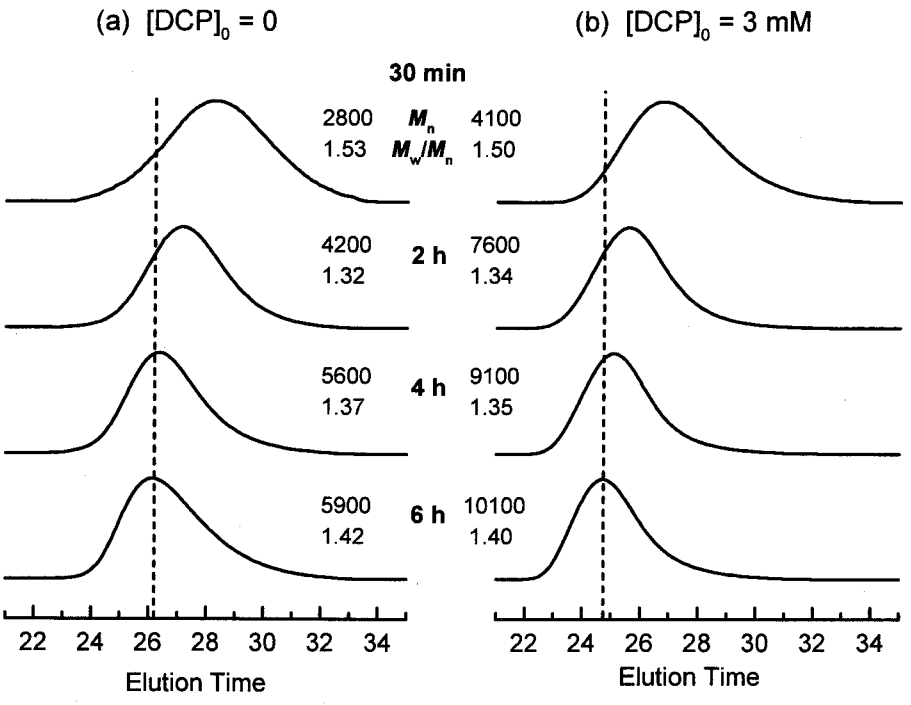

Figure 5.1. GPC charts for the tBA polymerization at 120 °C with $[BS\text{-}DBN]_0$ = 40 mM: (a) $[DCP]_0$ = 0 and (b) 3 mM. The broken vertical lines are just for the eye.

reached only about 30%. To increase the R_p and the chain length, we attempted to add a small amount of DCP as a radical initiator. It will supply new growing radicals to compensate the loss of P• through termination, resulting in a stationary rate of polymerization. This rate increases with increasing [DCP], as in a conventional system. (For more detail about the role of radical initiator, see Chapter 1.) DCP was chosen for its desirable decomposition rate at this temperature.[14] The resultant chromatograms are presented in Figure 5.1b. Clearly, the polymerization proceeded faster, and M_n and conversion exceeded 10000 and 50%, respectively, at 6 h. The polydispersity remained as small as that in the system without DCP. Thus the addition of a radical initiator has proved to be effective to increase R_p of the tBA/DBN system.

Figure 5.2 shows M_n and M_w/M_n of the product polymers as a function of conversion. Apparently, M_n increases linearly with conversion and agrees with the theoretical value (broken line in the figure) calculated from the conversion/$[BS\text{-}DBN]_0$ ratio, irrespective of DCP concentrations. This indicates that the number of DCP-initiated polymers is negligibly small compared with that of the BS-DBN-initiated molecules, and the role of DCP is only to

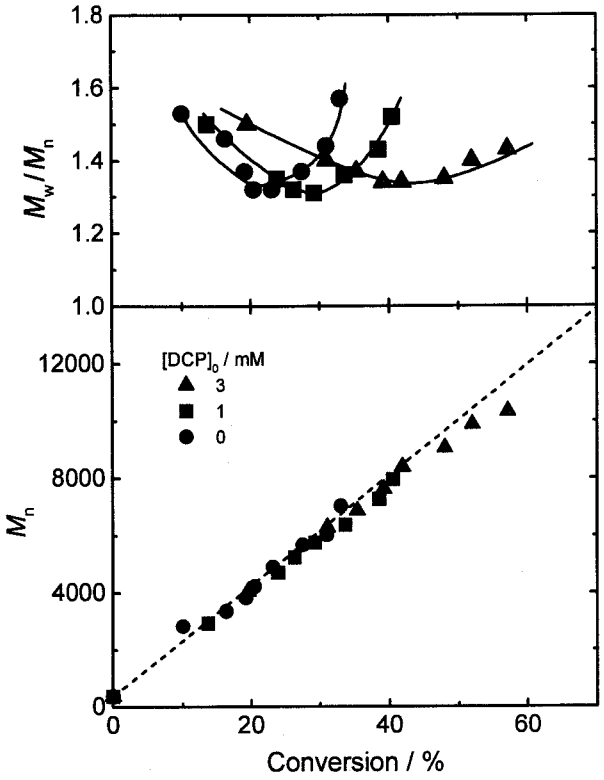

Figure 5.2. Plot of M_w/M_n and M_n (estimated by PS-calibrated GPC) vs monomer conversion for the tBA polymerization at 120 °C with $[BS\text{-}DBN]_0$ = 40 mM: $[DCP]_0$ = 0 (●), 1 mM (■), and 3 mM (▲). The broken line is theoretical, and the solid lines are just for the eye.

increase R_p. The M_w/M_n ratio also commonly becomes smaller with conversion in an initial stage and then tends to increase after passing through the minimum at which M_w/M_n is approximately 1.3. The increase in polydispersity in the later stage of polymerization would be ascribed to side reaction(s), which will be discussed below.

Since the presented values of M_n of PtBA were estimated by PS-calibrated GPC, they may be inaccurate on an absolute scale. ^{1}H NMR analysis will give more reliable M_n in this case. Figure 5.3 shows the spectrum of the model PtBA-DBN (see Experimental Section) with M_n of 2100 estimated by GPC, where the ortho protons of the benzoyloxy ring at the BPO-initiated chain end clearly appears at 7.9 ppm (peak **a**). The protons at the DBN moiety and tBA units are observed in a group at 1.0-2.5 ppm (peaks **e**), while the methine proton in the main chain neighboring to the DBN moiety appears at 4.05-4.15 ppm (peak **d**). Since DCP-initiated polymers are negligibly small in population as pointed out above, it can be assumed that all the polymers possess a benzoyloxy group at the initiating chain end. For the same reason, there must be very few polymers with two benzoyloxy groups at both chain

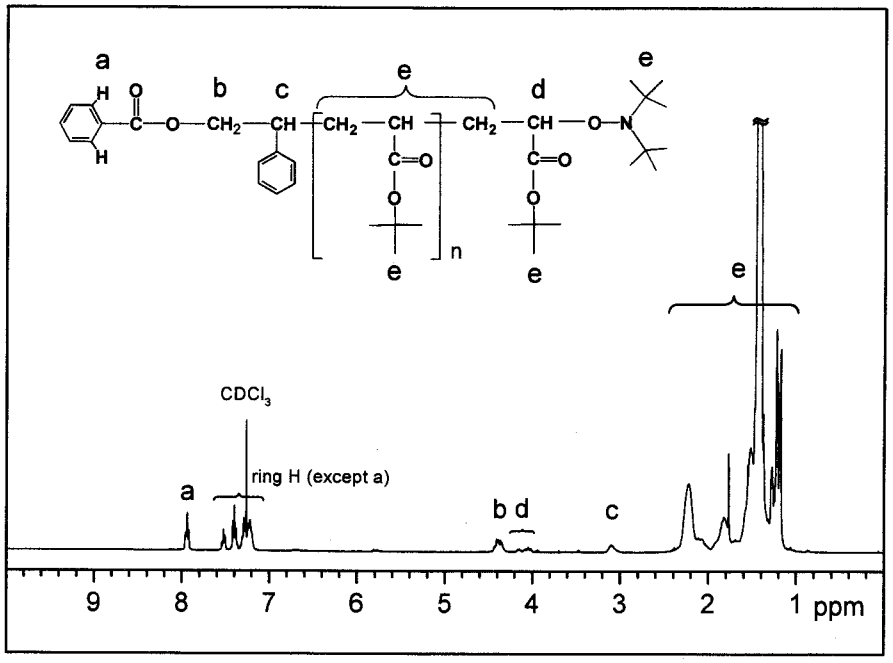

Figure 5.3. ^{1}H NMR spectrum of the model PtBA-DBN adduct (M_n = 2100 and M_w/M_n = 1.29).

ends (formed by combination of polymer radicals). Therefore, from the intensity of peak **a** relative to that of peaks **e,** we estimated the M_n to be 2100, which (accidentally) coincides with the GPC value. Thus it can be concluded that the M_n obtained by GPC is close to the actual values.

5.3.2. Effects of Hydrogen Transfer on Polymerization Rate

Figure 5.4 shows the $\ln([M]_0/[M])$ vs t plot for the polymerization with varying amounts of DCP, where M represents the monomer and the subscript zero denotes the initial state (t = 0). Clearly, R_p increases with an increase of [DCP]. However, even in the DCP-containing system, R_p became smaller and smaller as time elapsed. As discussed in Chapter 1, in the presence of initiation, a system with or without a polymer-nitroxide adduct should sooner or later reach the stationary state with respect to the concentrations of P$^\bullet$ and X$^\bullet$: the stationary-state [P$^\bullet$] is given by

$$[P^\bullet] = (R_i / k_t)^{1/2} \qquad (5.1)$$

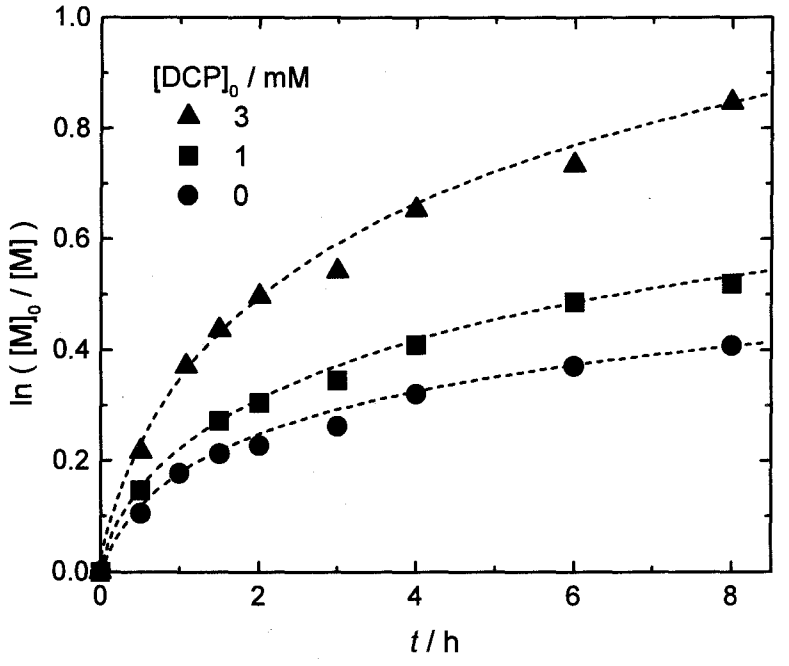

Figure 5.4. Plot of $\ln([M]_0/[M])$ vs t. For symbols and experimental conditions, see Figure 5.2.

where R_i is the rate of initiation and k_t is the rate constant of termination, respectively. This equation in fact holds in the styrene/TEMPO/BHP system, for example, as presented in Chapter 1. The decreasing trend in R_p observed here may be partly ascribed to the change of [DCP] with time. The decomposition rate constant k_{DCP} of DCP in dodecane is known in the range of 128 ~ 158 °C,[14] which allows us to estimate the k_{DCP} at 120 °C to be 3.9×10^{-5} s^{-1}. Since k_{DCP} is nearly independent of solvents,[14] we may use this value for the tBA system: the author thus expects that R_p after 8 h will become about half that at the initial stage of polymerization. However, the observed decrease in R_p is much more significant. This indicates that a side reaction may be a main cause for the decrease of R_p.

A possible one may be the decomposition of P-X, in which the nitroxyl radical X• abstracts the β-proton attached to the nitroxide moiety of P-X, forming a terminally-unsaturated polymer and a hydroxyamine XH.[15,16] It has been suggested that XH works as a retarder on R_p, since it reacts with P• through a hydrogen transfer to give a terminally-saturated polymer PH and X•, resulting in a decrease in [P•].[17] It was also reported that the rate of decomposition (formation of XH) depends on both monomers and nitroxides.[17] Since [XH] depends on the initial amount of BS-DBN as well as polymerization time, R_p will also

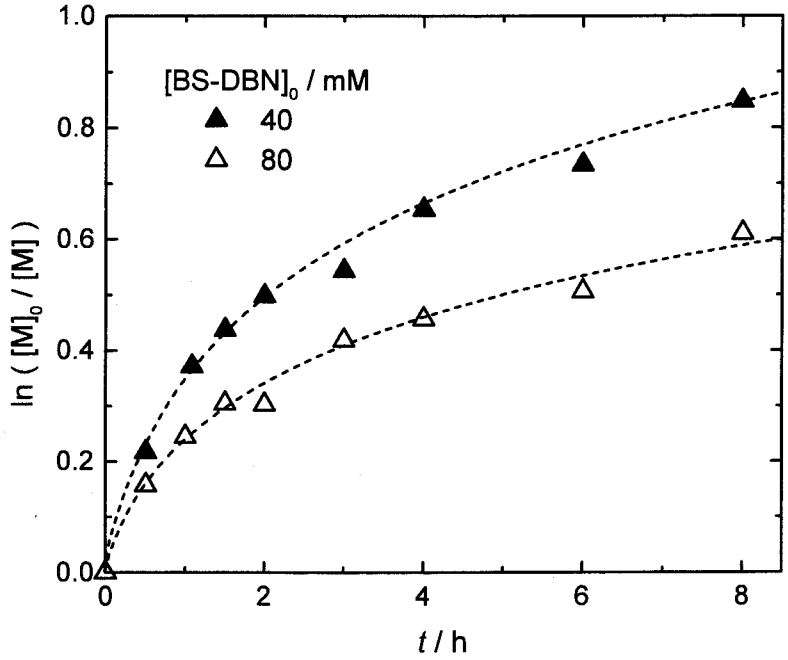

Figure 5.5. Plot of $\ln([M]_0/[M])$ vs t for the tBA polymerization at 120 °C with $[DCP]_0 = 3$ mM: $[BS\text{-}DBN]_0 = 40$ mM (▲) and 80 mM (△).

depend on them. Figure 5.5 shows the $\ln([M]_0/[M])$ vs t plot for the polymerization with varying amounts of BS-DBN and a fixed initial concentration of DCP. Clearly, the higher is $[BS\text{-}DBN]_0$, the smaller is R_p, as expected.

The decomposition of P-X into a terminally unsaturated polymer was directly confirmed by ^{1}H NMR spectroscopy. Figure 5.6 shows the ^{1}H NMR spectrum for the model PtBA-DBN adduct (M_n = 1200 and M_w/M_n = 1.16) dissolved in $CDCl_3$ and heated at 120 °C for 3 h. The peaks at about 5.8 and 6.7 ppm, which were absent before the heat treatment, can be assigned to the double-bond protons at the ω end of PtBA. (To avoid confusion, it should be noted that the PtBA-DBN adduct used for the decomposition study is different from the one used for other studies. Owing to the short preparation time (20 min), this adduct contains no detectable terminal unsaturation before the heat treatment.) Their intensities ($2D$) relative to that of the α-proton (A) next to the DBN moiety allow us to estimate the rate constant of decomposition k_{dec} from

$$\ln [A/(A+D)] = -k_{dec}\, t \qquad (5.2)$$

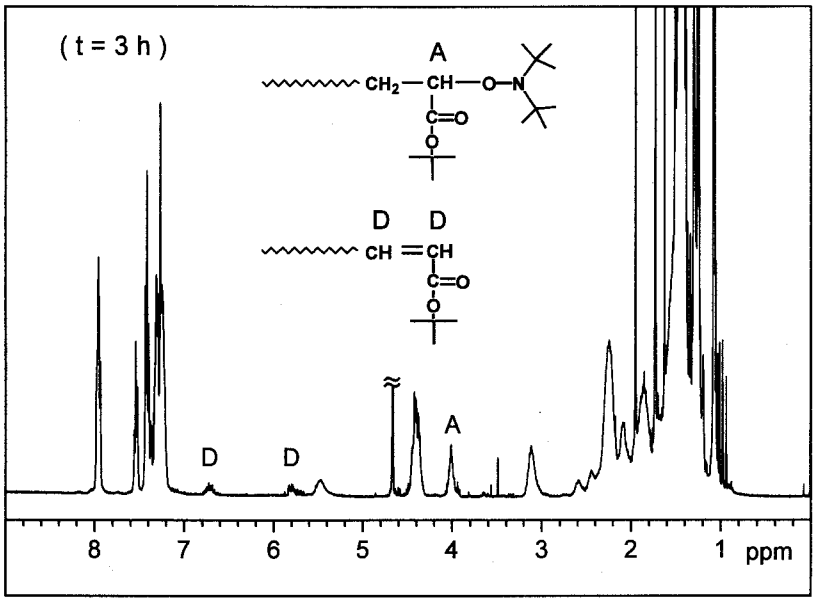

Figure 5.6. ^{1}H NMR spectrum of the model PtBA-DBN adduct (M_n = 1200 and M_w/M_n = 1.16) after the heat treatment at 120 °C. (This model adduct originally contained no detectable terminal unsaturation, unlike the one whose ^{1}H-NMR is given in Figure 5.3.)

An approximate value of k_{dec} thus obtained is 1.1×10^{-5} s^{-1}, which is about 4 times as large as that for the decomposition of PS-TEMPO adduct.[16] Thus, the decomposition of the active end in the tBA polymerization with PtBA-DBN should be more serious than that in the styrene polymerization with PS-TEMPO at the same temperature. (The decomposition rate is essentially independent of the concentration of free nitroxyl.[16] However, the monomer can exert a "solvent effect" on k_{dec},[15] so that k_{dec} in the actual polymerization system can be somewhat different from that in the model system.)

5.3.3. Determination of k_{act}

Now the author turns to another main subject of this work. He has attempted to determine the k_{act} of this system by the GPC direct (peak-resolution) method. The details of this method were described in Chapter 2. Here the PtBA-DBN adduct (M_n = 2100 and M_w/M_n = 1.29) was used as a probe P_0-X. P_0-X (15 mM) and DCP (1 mM) were dissolved in tBA and heated at 120 °C for a prescribed time t. (This experimental condition is an optimum one to facilitate the peak resolution (see below) and thus is far different from those aiming at the preparation of well-defined, low-polydispersity polymers as presented above.) Figure 5.7

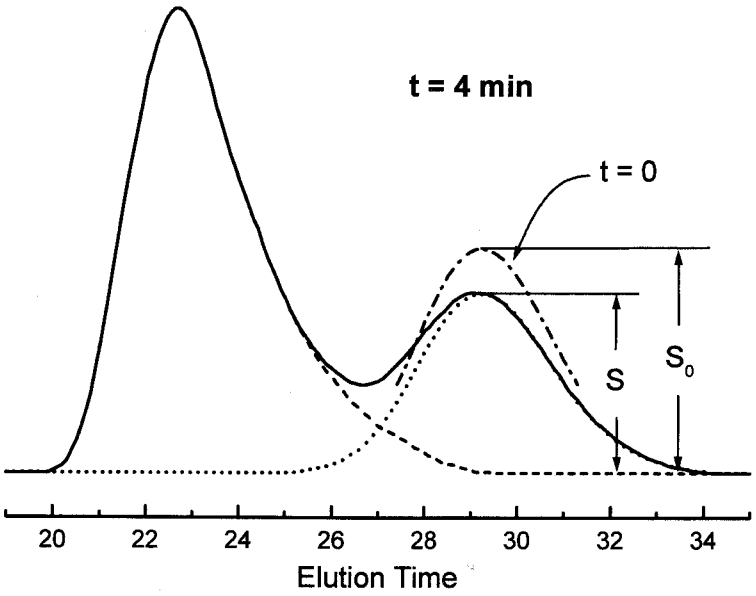

Figure 5.7. Two-component resolution of the GPC curve for the tBA polymerization at 120 °C for 4 min with $[P_0\text{-}X]_0$ = 15 mM and $[DCP]_0$ = 1 mM, where P_0-X is the PtBA-DBN adduct used as a probe.

shows the GPC trace of the solution quenched at t = 4 min. It composes two well-separated peaks. Clearly, the lower-molecular-weight peak is due to (the unactivated and remaining) P_0-X, while higher-molecular-weight one includes the activated and grown chain P_1-X and all the other minor components, e.g., stemming from the decomposition of DCP and further activation of P_1-X. Figure 5.8 shows the plot of $\ln(S_0/S)$ vs t, where S_0/S is the ratio of the P_0-X concentration (or the GPC peak area) at time zero to that at time t, according to equation 2.1. Since P_0-X contains 7 % of potentially inactive species (see Experimental Section), we have corrected the experimental data by subtracting $0.07S_0$ from both S_0 and S in equation 2.1. (Incidentally, the 7 % of inactive species is composed partly of a few percent of terminally unsaturated species, as is observed in the ^{1}H-NMR spectrum; Figure 5.3, at about 5.8 and 6.7 ppm.) As Figure 5.8 shows, the plot is linear passing through the origin, and its slope gives $k_{act} = 1.0\text{x}10^{-3}$ s^{-1}.

This value of k_{act} happens to be the same as the k_{act} value of $1.0\text{x}10^{-3}$ s^{-1} for the PS-TEMPO system at the same temperature obtained in Chapter 3. (For the PS-TEMPO system, k_{act} is identifiable with the rate constant of thermal homolysis k_d and the degenerative transfer plays no detectable role, as demonstrated in Chapter 3. This would also be the case with the

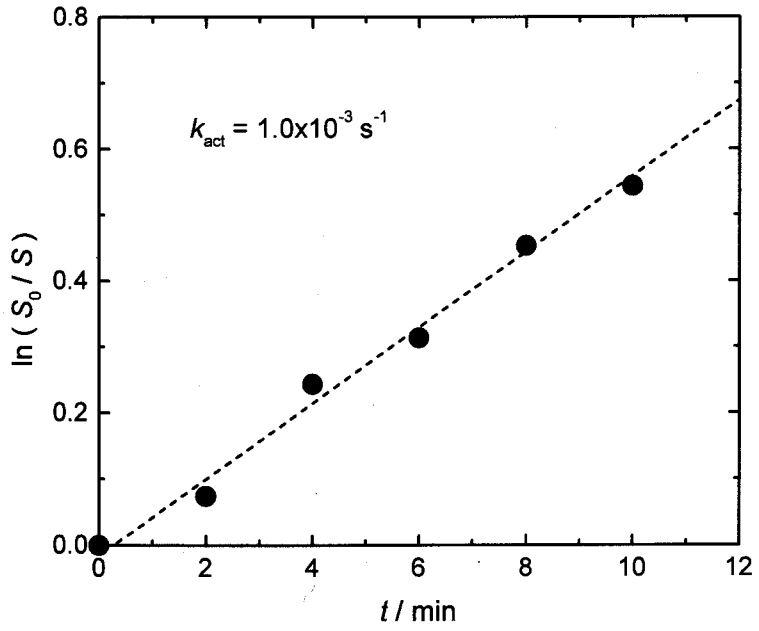

Figure 5.8. Plot of $\ln(S_0/S)$ vs t at 120 °C for the activation of PtBA-DBN.

PtBA-DBN system.) The PS-TEMPO system is known to provide low-polydispersity polymers (M_w/M_n < 1.2). The fact that the PtBA-DBN system does not give so low a polydispersity as in the PS-TEMPO system is, therefore, ascribed to the larger rate constant of decomposition in the former system than in the latter. If this is the case, the polydispersity in the PtBA-DBN system should be determined essentially by polymerization time, since both the activation and decomposition in this system are first-order reactions. Figure 5.9 shows the plot of M_w/M_n vs t for the PtBA polymers given in Figure 5.2. As expected, all the data points for different DCP concentrations (different conversions for the common t) fall on the same curve, showing that other reactions such as chain transfer and radical-radical termination, if any, have minor effects on the polydispersity of this system. The dotted line in the figure shows the value of M_w/M_n calculated with the relation taken from equations 1.5 and 1.6:

$$M_w/M_n = 1 + (2/k_{act}t) + (1/x_n) \qquad (5.3)$$

where x_n is the number-average degree of polymerization. This is valid for the "ideal" living

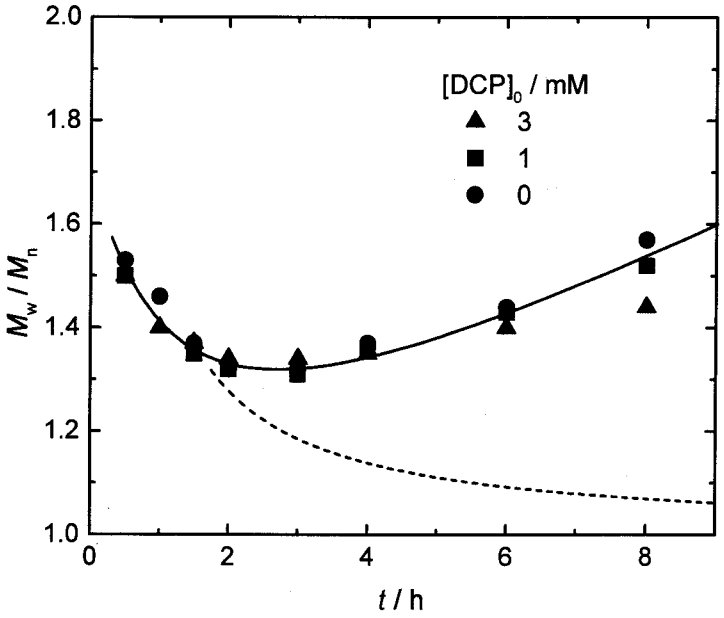

Figure 5.9. Plot of M_w/M_n vs t. The broken line shows equation 5.3, and the solid line is just for the eye: for symbols and experimental conditions, see Figure 5.2.

system with a constant R_p and no side reactions other than the activation, deactivation and propagation reactions. Deviations of the experimental points from the calculated curve are indeed more significant at larger polymerization time.

5.4. Conclusions

It was demonstrated that the polymerization rate of tBA in the presence of the alkoxyamine BS-DBN can be enhanced by the addition of a limited amount of radical initiator DCP without causing any appreciable broadening of polydispersities. The use of the nitroxide DBN allowed us to conduct a controlled polymerization at a relatively low temperature of 120 °C. The decomposition of the alkoxyamine into a terminally unsaturated compound and a hydroxyamine occurred to a rather serious degree, causing a decrease of the polymerization rate through the subsequent hydrogen transfer. Direct determination of k_{act} showed that a PtBA-DBN adduct will experience, during the course of polymerization, a sufficient number of activation-deactivation cycles to achieve as low a polydispersity as in the PS-TEMPO system. However, the observed M_w/M_n ratio showed a large deviation from what was expected from the k_{act} value alone, due to the mentioned decomposition of the alkoxyamine.

References

(1) Georges, M. K.; Veregin, R. P. N.; Kazmaier, P. M.; Hamer, G. K. *Macromolecules* **1993**, *26*, 2987.

(2) See references 2b-d in Chapter 4.

(3) See references 3a-c in Chapter 4.

(4) Solomon, D. H.; Rizzardo, E.; Cacioli, P. *Eur. Pat. Appl. EP135280* (Chem. Abstr. **1985**, *102*, 221335q).

(5) Listigovers, N. A.; Georges, M. K.; Odell, P. G.; Keoshkerian, B. *Macromolecules* **1996**, *29*, 8993.

(6) Benoit, D.; Grimald, S.; Finet, J. P.; Tordo, P.: Fontanille, M.; Gnanou, Y. In *Controlled Radical Polymerization*; Matyjaszewski, K., Ed.; ACS Symposium Series 685; American Chemical Society: Washington, DC, 1998: Chapter 14.

(7) Moad, G.; Rizzardo, E. *Macromolecules* **1995**, *28*, 8722.

(8) Kazmaier, P. M.; Moffat, K. A.; Georges, M. K.; Veregin R. P. N.; Hamer, G. K. *Macromolecules* **1995**, *28*, 1841.

(9) Marque, S.; Mercier, C. L.; Tordo, P.; Fischer, H. *Macromolecules* **2000**, *33*, 4403.

(10) Chapter 4 of this thesis; Goto, A.; Fukuda, T. *Macromol. Chem. Phys.* **2000**, *201*, 2138.

(11) Goto, A.; Fukuda, T. *Macromolecules* **1997**, *30*, 4272.

(12) Greszta, D.; Matyjaszewski, K. *J. Polym. Sci. Part A.: Polym. Chem.* **1997**, *37*, 1857.

(13) Ohno, K.; Tsujii, Y.; Miyamoto, T.; Fukuda, T.; Goto, M.; Kobayashi, K.; Akaike, T. *Macromolecules* **1998**, *31*, 1064.

(14) Kharasch, M. S.; Fono, A.; Nudenberg, W. *J. Org. Chem.* **1951**, *16*, 105.

(15) Li, I.; Howell, B. A.; Matyjaszewski, K.; Shigemoto, T.; Smith, P. B.; Priddy, D. B. *Macromolecules* **1995**, *28*, 6692.

(16) Ohno, K.; Tsujii, Y.; Fukuda, T. *Macromolecules* **1997**, *30*, 2503.

(17) Gridnev, A. A. *Macromolecules* **1997**, *30*, 7651.

Part III

Degenerative Chain Transfer-Based Living Radical Polymerizations

Chapter 6

Activation Mechanism of Iodide-Mediated Living Radical Polymerization

Abstract

The kinetics of the bulk polymerization of styrene in the presence of a model polystyryl iodide as a mediator and benzoyl peroxide (BPO) as a conventional radical initiator was studied. The polymerization rate R_p was found to be independent of the iodide concentration, showing that the stationary concentration of polymer radicals [P$^\bullet$] is determined by the balance of initiation and termination rates, as in the conventional (iodide-free) systems. The pseudo-first-order activation rate constant k_{act} of the model iodide was determined as a function of BPO concentration and temperature by both the GPC direct and indirect methods. The results showed that k_{act} is directly proportional to [P$^\bullet$], which means that degenerative chain transfer (Scheme 1.1b) is the only important mechanism of activation in this system. The activation energy for the transfer rate constant k_{ex} was found to be 27.8 kJ mol^{-1}, somewhat smaller than the known activation energy for the styrene propagation rate constant k_p of 32.5 kJ mol^{-1}. This indicates that lowering, rather than raising, the reaction temperature will be more effective to prepare polystyrenes with a narrower polydispersity by the iodide-mediated polymerization. This is because the most important parameter for determining the polydispersity of a degenerative-chain-transfer-type system is the k_{ex}/k_p ratio, as has been known for some time.

6.1. Introduction

Iodide-mediated living radical polymerization (LRP)[1-3] is one of the most simple and robust LRPs, since the experimental conditions is very close to those of conventional radical polymerization (e.g., it does not require high temperatures unlike the nitroxide systems). However, this polymerization has a major drawback: the chain length distribution of this system does not narrow as in the nitroxide, RAFT, and ATRP systems (Scheme 1.3). This would be due to the small k_{act} value of this system. Mechanistically, this polymerization is supposed to involve degenerative chain transfer (Scheme 1.1b) as an activation process.[3] However, no direct experimental evidence for it has been obtained yet. In Chapter 3, the author used two gel permeation chromatographic (GPC) methods to show that the main mechanism of activation in the 2,2,6,6-tetramethylpiperidinyl-1-oxy (TEMPO) mediated polymerization of styrene is the thermal dissociation (Scheme 1.1a) of the polystyrene (PS)-TEMPO adduct rather than degenerative chain transfer. In this chapter, the author adopts these methods to the iodide-mediated polymerization of styrene, and determines the pseudo-first-order activation rate constant k_{act} as a function of polymerization rate R_p and temperature. In this way, he will establish the activation mechanism and discuss the scope and limitation of this polymerization.

6.2. Experimental Section

6.2.1. Materials

Styrene and benzoyl peroxide (BPO) were purified by distillation or recrystallization. 1-Phenylethyl iodide (PEI) was prepared as described elsewhere[3a] and confirmed to be virtually 100 % pure by proton magnetic resonance (^{1}H NMR).

6.2.2. Synthesis and Characterization of ω-Polystyryl Iodide

A styrene solution of PEI (200 mM) and BPO (30 mM) in a glass tube was degassed by several freeze-thaw cycles, sealed off under vacuum, and heated at 80 °C for 70 min. After purification,[4] a PS-iodide adduct (PS-I; **31**: Figure 2.3) was obtained with M_n and M_w of 1500 and 1890, respectively (M_w/M_n = 1.26), according to PS-calibrated GPC. These values of M_w

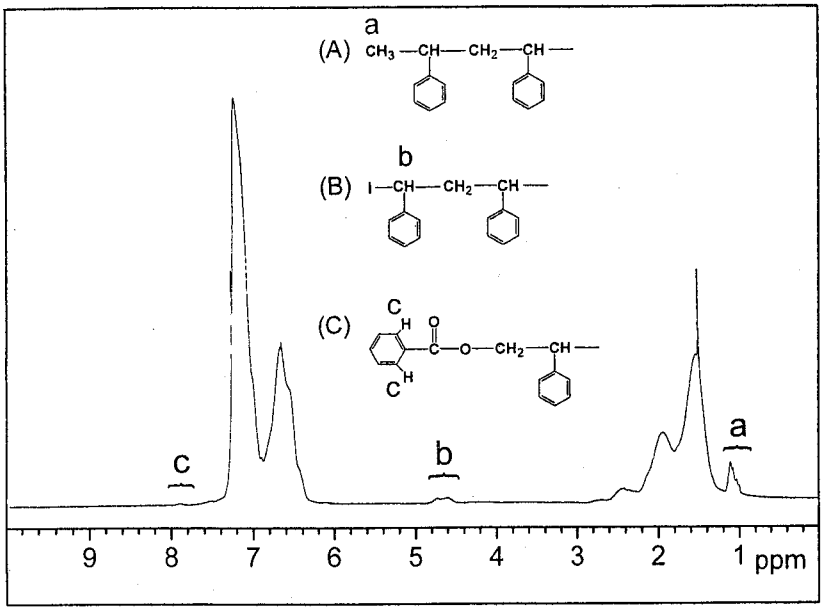

Figure 6.1. ^{1}H NMR spectrum of the model polystyryl iodide P_0-X. A, B, and C are the major three possible structures of the chain-ends, and a, b, and c denote the assignments of the signals.

and M_n are not necessarily reliable in an absolute scale because of the differences in the end groups between this sample and the anionically prepared standard PSs used for the GPC calibration.

^{1}H NMR analysis may give more reliable results in this particular case. The spectrum given in Figure 6.1 clearly shows the signals due to the methyl protons at the initiating chain end (0.9-1.2 ppm; peak a), the methine proton at the iodine end (4.5-4.8 ppm; peak b), and the ortho protons of the benzoyloxy ring at the BPO-initiated chain end (7.9 ppm; peak c). From the peak areas of the protons at the initiating chain ends (peaks a and c) relative to that of the methylene and methine protons in the main chain (1.2-2.8 ppm) and to that of the terminal methine (peak b), the author estimated the M_n of the PS moiety of the sample and the number fraction f_I of the iodine-capped chains to be 1900 and 0.98, respectively. Since peak a is slightly overlapped by the tail part of the main-chain protons, appropriate curve resolution was made in reference to the spectrum of a free-radically prepared PS with a high M_n (> 10^5), which showed no detectable chain-end signals. The author also notes that an elemental analysis showed that the sample contained 6.16 wt % of iodine, which, along with the M_n

value of 1900, gives f_I = 0.98 in agreement with the NMR value. On the other hand, the number fraction of the chains with a benzoyloxy chain end, f_B, is about 0.04 according to the above-mentioned NMR analysis. This value of f_B is consistent with the decomposition rate constant of BPO in styrene (see below) and the experimental conditions given above. Since the number of initiated chains is equal to that of the terminated (dead) chains (see below), and since the rate of thermal (spontaneous) initiation of styrene at this temperature (80 °C) is negligibly small compared to that of the BPO initiation, we can estimate that the fraction f_B of chains were terminated (mostly by combination in the case of styrene). This indicates that the fraction of active chains (f_I) does not exceed $1-f_B$ = 0.96, approximately.[5]

From all these results, one may conclude that the prepared PS-I sample, which will be used as a probe adduct P_0-X, is 96-98 % pure. In the following analysis, the author will correct the experimental data assuming that P_0-X includes 3 wt % of inactive species (without an iodine moiety). This correction, however, was generally small compared with other experimental errors. Even though the absolute values of molecular weights estimated by GPC may not be very accurate as suggested above, they can be used probably with less errors for the purpose of comparative studies such as are made in the determination of k_{act} by polydispersity analysis (see below). For example, the M_w/M_n ratio of 1.26 for P_0-X estimated by GPC should be a good approximation.

6.2.3. Kinetic Analysis of Polymerization

A fixed amount of P_0-X (17 mM) and a variable amount of BPO (0-30 mM) were dissolved in styrene, degassed, sealed off under vacuum, and heated at 80 °C for a prescribed time t. The mixture was then quenched to room temperature, diluted by tetrahydrofuran (THF) to a known concentration and directly analyzed by GPC.[4]

6.2.4. Measurements

^{1}H NMR spectra were obtained by a Varian VXR-200 spectrometer operating at 200 MHz. These spectra were recorded at ambient temperature, and with flip angle of 45 degrees, spectral width of 3001 Hz, acquisition time of 2.666 sec, and pulse delay of 2.0 sec.

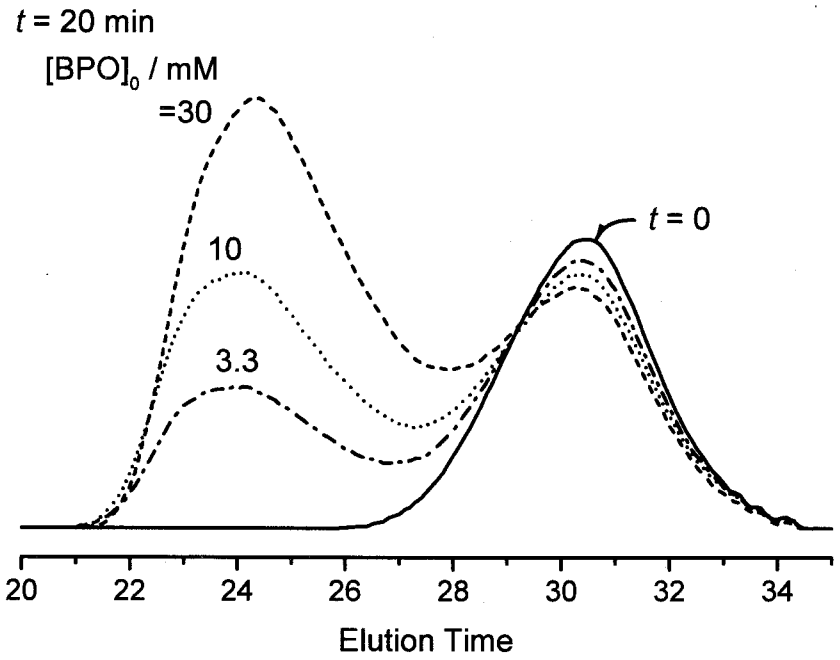

Figure 6.2. Examples of the GPC curves for the styrene/PS-I(P_0-X)/BPO mixtures heated at 80 °C for 20 min: $[P_0\text{-X}]_0$ = 17 mM; $[BPO]_0$ as indicated in the figure. The solid curve is for the original (t = 0) solution, which contains only P_0-X as polymer species. All the curves were reduced to the same original P_0-X concentration.

The GPC measurement was made on a Tosoh HLC-802 UR high-speed liquid chromatograph equipped with Tosoh gel columns G2500H, G3000H, and G4000H. THF was used as eluent (40 °C). The column system was calibrated with Tosoh standard polystyrenes (PSs). Sample detection and quantification were made with a Tosoh differential refractometer RI-8020 calibrated with known concentrations of PtBA-DBN adducts in THF.

6.3. Results and Discussion

6.3.1. Polymerization Rates

The author first examines the rate of polymerization R_p of this system. Figure 6.2 shows the examples of the GPC curves of the reaction mixtures obtained after the 20 min of heat treatment of the system with a fixed amount of P_0-X (17 mM) and varying amounts of BPO (0-30 mM). The total area under each curve relative to that of the t = 0 curve shows how much monomer was converted to polymer, i.e., the conversion. By independent experiments, it was confirmed that the RI (refractive index) detector response of PS-I does not depend on

chain length (for $M_n \geq 2000$), being the same as that of standard PSs within 1 or 2 %. Figure 6.3 gives the first-order plot of the monomer concentration [M]. In these relatively small conversion ranges, the plot is approximately linear, indicating that the system is in a stationary state with respect to the ratio R_p/[M] or the polymer radical concentration [P•]

$$[P^{\bullet}] = k_p^{-1} (R_p / [M]) \tag{6.1}$$

where k_p is the rate constant of propagation.

Figure 6.4 gives the values of $(R_p/[M])^2$ as a function of $[BPO]_0$, indicating that $[P^{\bullet}]^2$ is linear in $[BPO]_0$. The open circles in the figure for the conventional system (without the iodide P_0-X) fall on the same straight line as for the iodide system. This means that the iodide has no effect on the stationary rate of polymerization, and R_p, whether the iodide exists or not, may be given by the relations

$$(R_p / [M])^2 = (k_p^2 / k_t) R_i \tag{6.2}$$

$$R_i = R_{i,th} + 2f' k_{BPO} [BPO] \tag{6.3}$$

with $R_{i,th} = 2.2 \times 10^{-9}$ M^{-1} s^{-1}, and $2f'k_{BPO} = 7.2 \times 10^{-5}$ s^{-1}. In equations 6.2 and 6.3, k_t is the termination rate constant, and R_i is the total rate of initiation, which is the sum of the thermal initiation $R_{i,th}$ of styrene, and the initiation due to the decomposition of BPO with a rate constant k_{BPO} and an efficiency f'. The values of $R_{i,th}$ and $2f'k_{BPO}$ obtained here are reasonably compared to the literature values: $R_{i,th} = 2.5 \times 10^{-9}$ M^{-1} s^{-1},[6] and $k_{BPO} = 3.5 \times 10^{-5}$ s^{-1}.[7] In this work, use is made of the k_p value recommended by the IUPAC[8] and the k_p^2/k_t value due to Hui and Hamielec[6] ($k_p = 660$ and $k_p^2/k_t = 1.7 \times 10^{-3}$ M^{-1} s^{-1}, respectively).

6.3.2. Determination of k_{act} by GPC Direct (Peak-Resolution) Method

The k_{act} values of this system were determined by the direct (peak-resolution) method. (For the details of the method, see Chapter 2.) The GPC curves given in Figure 6.2 show two definite peaks. Clearly, the first lower-molecular-weight component corresponds to the

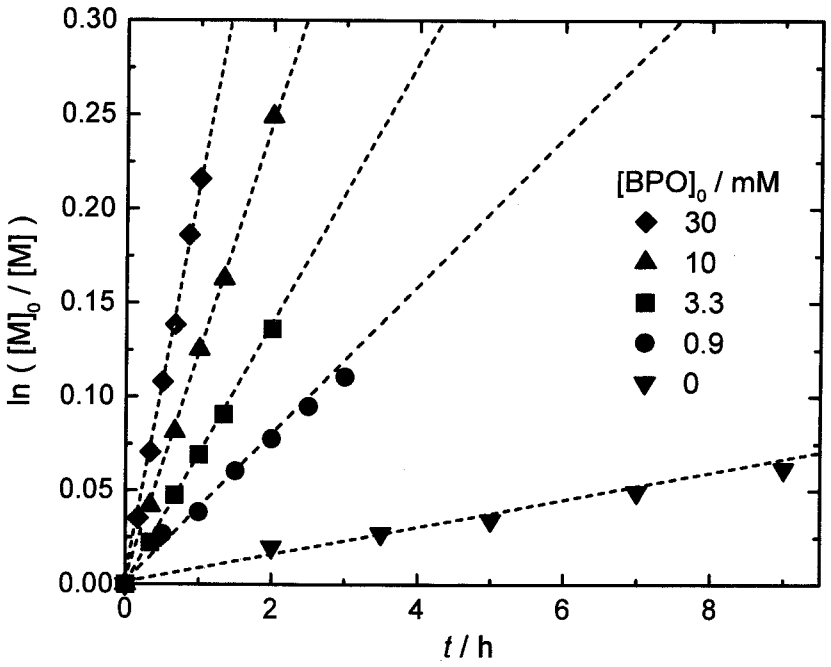

Figure 6.3. Plot of ln([M]$_0$/[M]) vs t: [P$_0$-X]$_0$ =17 mM; [BPO]$_0$ as indicated in the figure (80 °C).

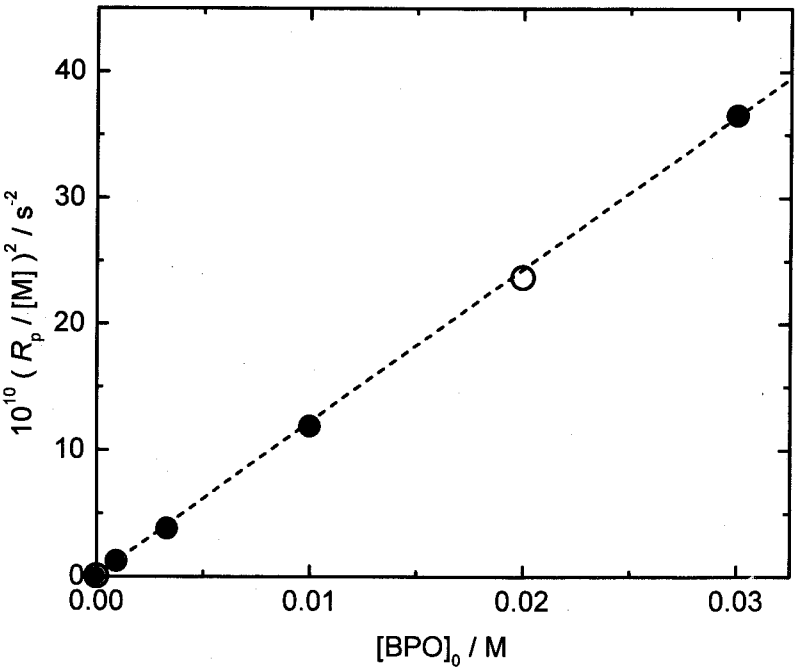

Figure 6.4. Plot of $(R_p/[M])^2$ vs [BPO]$_0$ for the polymerization of styrene at 80 °C in the presence of P$_0$-X ([P$_0$-X]$_0$ = 17 mM, filled circles) and the absence of it (open circles).

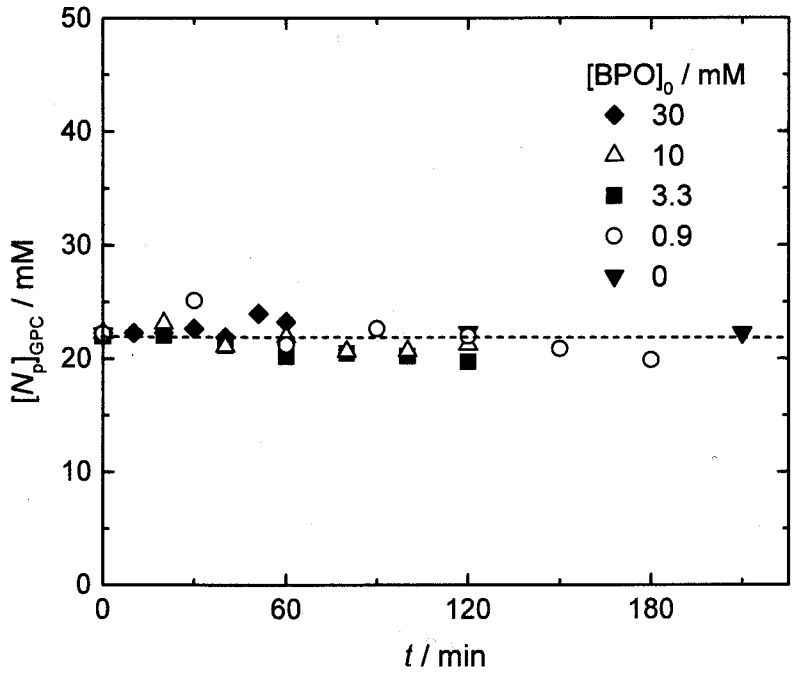

Figure 6.5. Plot of the concentration of polymer species $[N_p]_{GPC}$ of polymer vs t: $[P_0\text{-}X]_0$ = 17 mM; $[BPO]_0$ as indicated in the figure (80 °C). $[N_p]_{GPC}$ denotes the value of $[N_p]$ estimated by GPC.[16]

unactivated P_0-X. This peak was observed to become smaller with an increase in [BPO] when t was fixed (Figure 6.2) and with an increase in t when $[BPO]_0$ was fixed (not shown in the figure). The second, higher-molecular-weight component is ascribed mainly to the activated and grown chain P_1-X. This component can also include those species, albeit small in fraction, that originate from BPO, thermal initiation, and/or a further activation of P_1-X, where P_1-X is the PS-I produced from P_0-X after one cycle of activation-propagation-deactivation. Actually, the concentration of polymer species $[N_p]$, which can be estimated by the conversion and the overall M_n, is nearly constant and equal to $[P_0\text{-}X]_0$ within ± 10 % in the studied ranges of $[BPO]_0$ and t (Figure 6.5). This means that the cumulative number of BPO- (and thermally) originating chains is small compared with the number of P_0-X molecules. These details, however, are not required, since we are concerned here with the change of $[P_0\text{-}X]$ or the intensity S of the first peak. Accurate resolution was made on the well-separated peaks in Figure 6.2, which gave unequivocal values of S. Figure 6.6 shows the plot of $\ln(S_0/S)$ vs t for varying amounts of BPO. The plot is linear in all cases, giving a well-defined k_{act} value according to equation 2.1.

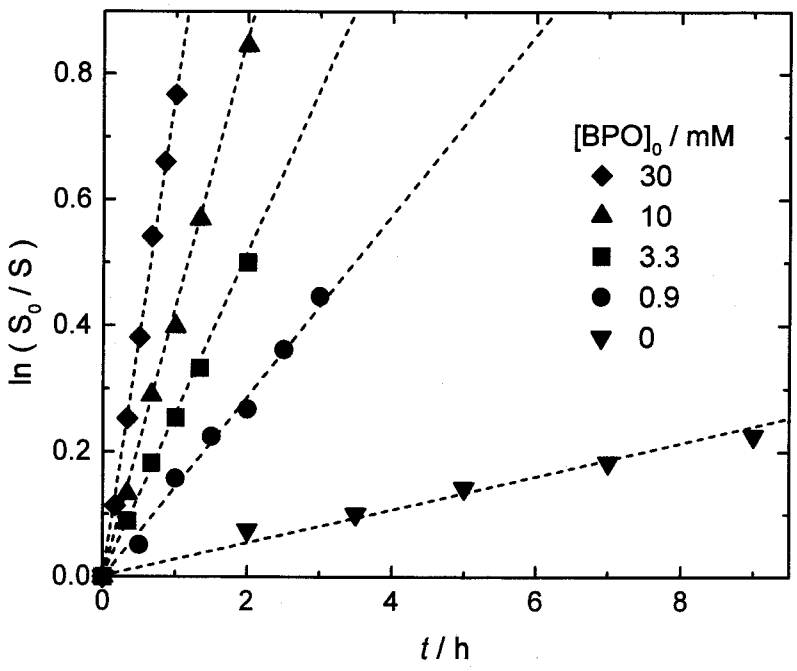

Figure 6.6. Plot of $\ln(S_0/S)$ vs t: $[P_0\text{-}X]_0$ = 17 mM; $[BPO]_0$ as indicated in the figure (80 °C).

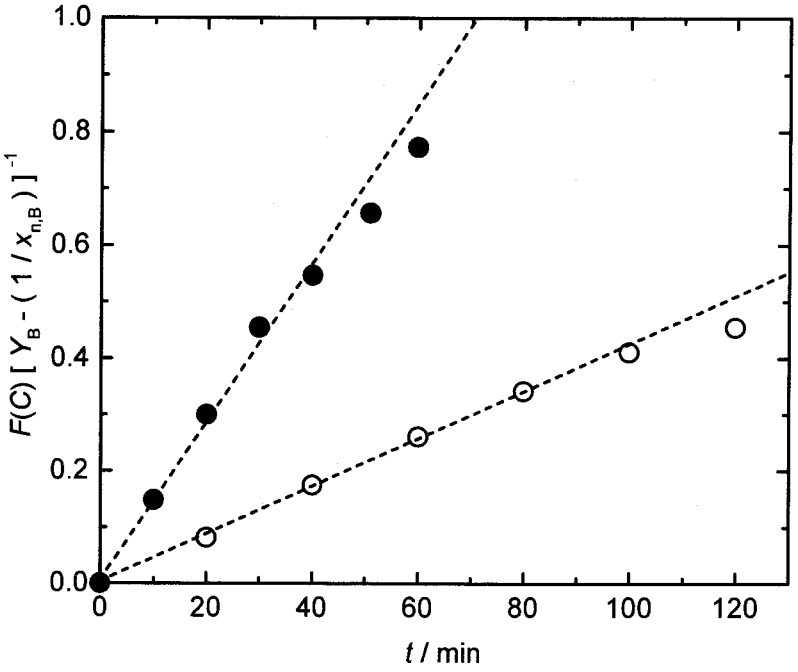

Figure 6.7. Plot of $F(C)[Y_B\text{-}(1/x_{n,B})]^{-1}$ vs t: $[P_0\text{-}X]_0$ = 17 mM; $[BPO]_0$ = 3.3 mM (○) and 30 mM (●) (80 °C).

6.3.3. Determination of k_{act} by GPC Indirect (Polydispersity Analysis) Method

The author next determined k_{act} by the indirect method. As discussed in Chapter 2, prerequisites for this method to be valid are the constancy of both [P•] and [N_p]. These conditions are approximately met in the present systems, as Figures 6.3 and 6.5 show. Two examples of the plot according to equation 2.2 are presented in Figure 6.7. The values of k_{act} estimated from the initial slopes of these curves are 7.1×10^{-5} and 2.3×10^{-4} s^{-1} for $[BPO]_0 = 3.3$ and 30 mM, respectively, which well agree with the values 7.2×10^{-5} and 2.2×10^{-4} s^{-1}, respectively, obtained by the direct method (Figure 6.6).

6.3.4. Mechanism of Activation

The activation, i.e., the cleavage of the C-I bond in this system can possibly occur by a thermal stimulus (thermal dissociation: Scheme 1.1a) and/or a chemical stimulus by a propagating radical P• (degenerative chain transfer: Scheme 1.1b). When both reactions are involved in the activation process, k_{act} will take the form

$$k_{act} = k_d + k_{ex}[P^\bullet] \tag{6.4}$$

as discussed in Chapter 3. Here k_d and k_{ex} are the rate constants of dissociation and degenerative chain transfer, respectively. Figure 6.8 shows the plot of k_{act} against $R_p/[M]$ (= $k_p[P^\bullet]$). It is evident that the data points obtained by the direct method (filled circles) and the indirect method (open circles) form a straight line passing through the origin, showing that $k_d = 0$ (within the accuracy of the present analysis) and $k_{ex} = 2400$ M^{-1} s^{-1}. These experiments establish that degenerative chain transfer is virtually the only mechanism of activation in the iodide/styrene system.

6.3.5. Temperature Dependence of k_{ex}

Figure 6.9 shows the k_{ex} values determined by the direct method at various temperatures. The result can be represented by the Arrhenius formula

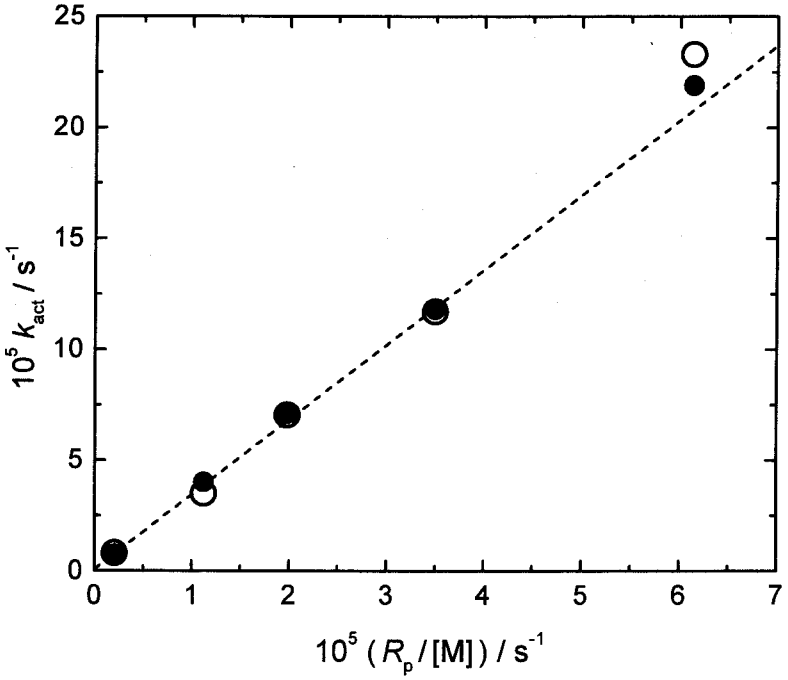

Figure 6.8. Plot of k_{act} vs R_p/[M]: (●) by the direct (curve-resolution) method and (○) by the indirect (polydispersity analysis) method (80 °C).

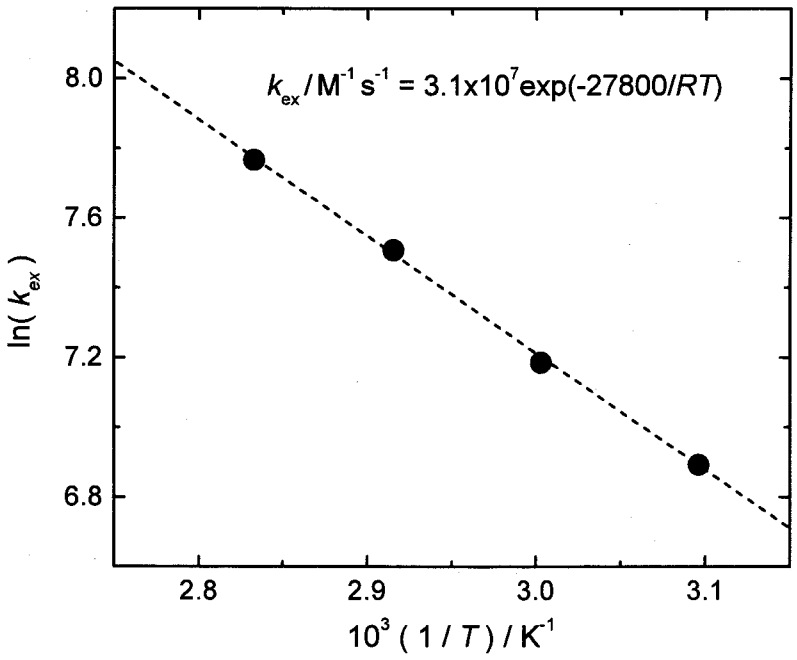

Figure 6.9. Plot of ln(k_{ex}) vs 1/T for the iodide-mediated polymerization of styrene.

$$k_{ex} / M^{-1} s^{-1} = 3.1x10^{7} \exp(-27.8 \text{ kJ mol}^{-1} / RT) \quad (6.5)$$

The activation energy of 27.8 kJ mol^{-1} obtained here is very small compared with those of homolytic bond-cleavage reactions, e.g., the PS-TEMPO dissociation reaction (124 kJ mol^{-1}),[9] but it seems reasonable in the order of magnitude for a transfer reaction. An increase in temperature does not give the iodide system such a large increase in activation rate as it gives the TEMPO system. The iodide-mediated polymerization at high temperatures (≥ 100 °C) is not recommended because of the possible isolation of iodine molecules.

6.3.6. Comments on the Narrowest Possible Polydispersity

In an ideal living system where side reactions such as initiation, termination and transfer reactions (other than degenerative one) have negligible effects on polydispersity, the polydispersity factor Y_B (= $M_w/M_n - 1$ of the incremental (or grown) portion B of the chain initiating from P_0-X, A chain) in a batch system (with constant R_p/[M]) is given by equation 2.2 with $F(C) = (1–2C^{-1})\ln(1–C)$[10,11]:

$$[Y_B - (1/x_{n,B})]^{-1} = (Ctk_{act})/[(C-2)\ln(1-C)] \quad (6.6)$$

where C is monomer conversion and $x_{n,B}$ is the number-average degree of polymerization of the B chain. In a nitroxide/styrene system, for example, $k_{act} = k_d$ = constant at a given temperature, and therefore Y_B can be manipulated by changing t for a given value of C. The smallest possible value of Y_B, which is equal to $x_{n,B}^{-1}$ is expectable for $t = \infty$ for any value of $C < 1$. Even though this limiting value of Y_B is difficult to realize due to side reactions, the author's group[12,13] previously demonstrated that the Y_B of a nitroxide/styrene system became smaller as t was increased while C was fixed.

The behavior of an iodide/styrene system is expected to be quite different from this, since $k_{act} = k_{ex}[P^{\bullet}]$ in this system. In reference to equations 6.1 and 6.6, we have

$$[Y_B-(1/x_{n,B})]^{-1}=(k_{ex}/k_p)[C/(2-C)] \qquad (6.7)$$

Namely, the polydispersity of this system is a function of C only (if side reactions are not considered). Similarly, equation 2.1 with $k_{act}=k_{ex}[P^\bullet]$ reads

$$\ln(S_0/S)=(k_{ex}/k_p)\ln[1/(1-C)] \qquad (6.8)$$

Again, this is a function of C only. Equations 6.7 and 6.8 are tested in Figures 6.10a and b, respectively. In both cases, experimental points varying in BPO concentration and hence $[P^\bullet]$ fall on a straight line, whose slope (k_{ex}/k_p) is 3.6 in both cases. With the aforementioned value of k_p of 660 M^{-1} s^{-1}, we can recover the k_{ex} value of 2400 M^{-1} s^{-1}.

As this discussion suggests, the polydispersity of the iodide system is determined essentially by conversion, and the smallest possible value of Y_B is expected for full conversion ($C = 1$), where equation 6.7 gives

$$Y_B = x_{n,B}^{-1} + (k_p / k_{ex}) \qquad (\text{at } C = 1) \qquad (6.9)$$

When the "initiating" A-chain and the $x_{n,B}^{-1}$ term are negligibly small, equation 1.4 with equation 6.9 simplifies to $Y = k_p/k_{ex}$ (at $C = 1$).[10,14] At 80 °C, $k_{ex}/k_p = 3.6$ (see above), and therefore the smallest value of M_w/M_n possibly achievable at 80 °C would be 1.28.[15] More generally, combination of the Arrhenius equations for k_{ex} (equation 6.5) and k_p[8] gives

$$k_p / k_{ex} = 1.38 \exp(-4.7 \text{ kJ mol}^{-1} / RT) \qquad (6.10)$$

The value of -4.7 kJ mol^{-1} may be subject to a considerable error, but it makes a striking contrast to, e.g., the large activation energy of the dissociation rate constant of a PS-TEMPO adduct (124 kJ mol^{-1}).[9] Taking equation 6.10 at its face value, it suggests that with respect to polydispersities, the iodide system would somewhat benefit from lowering the reaction temperature. At 20 °C, for example, the smallest possible value of M_w/M_n would be 1.20.

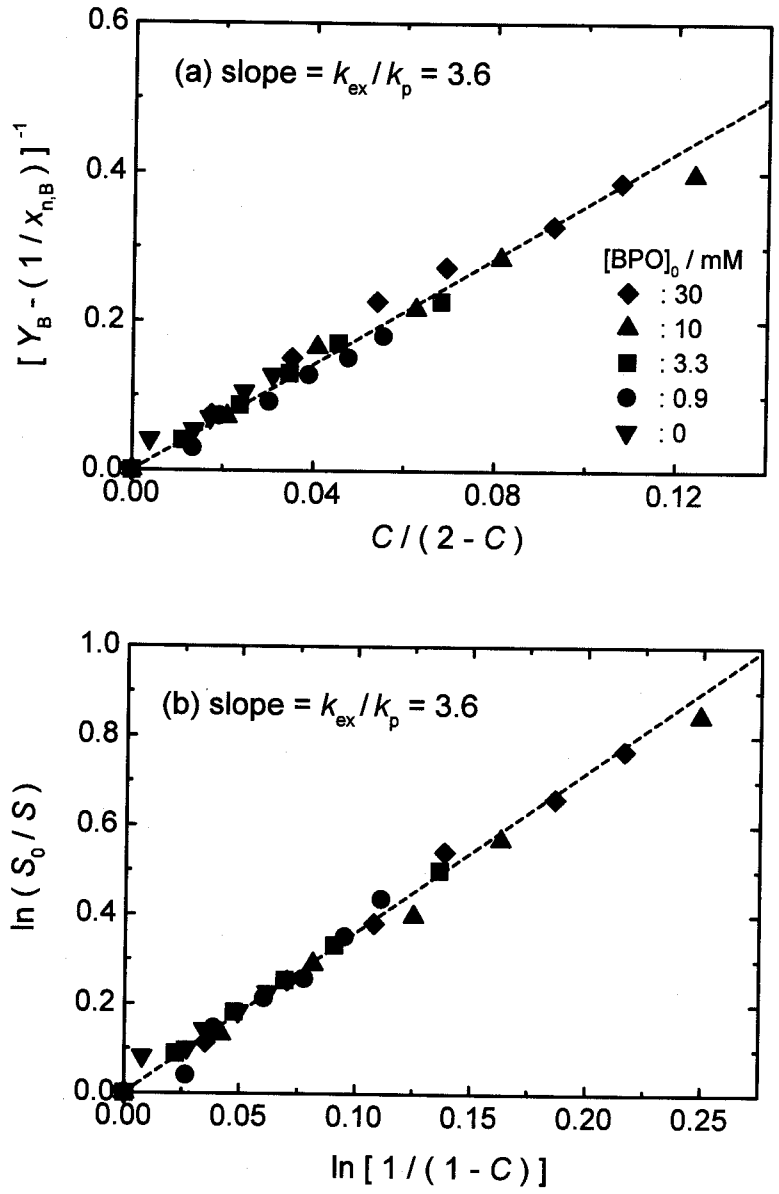

Figure 6.10. (a) Plot of $[Y_B-(1/x_{n,B})]^{-1}$ vs $C/(2-C)$ and (b) of $\ln(S_0/S)$ vs $\ln[1/(1-C)]$ for the iodide-mediated polymerization with varying $[BPO]_0$ as indicated in Figure 10a (80 °C).

Of course, side reactions would inevitably broaden the polydispersity over these limiting values. At lower temperatures, R_p is smaller and it takes more time to achieve the desired conversion. Optimization of experimental conditions based on the detailed kinetic information obtained here and elsewhere will be primarily important.

6.4. Conclusions

The bulk polymerization of styrene in the presence of a model PS-I as a mediator and BPO as a conventional radical initiator was kinetically studied with respect to the rate of polymerization R_p, the rate of activation of the mediator, and the change in the polydispersity of the polymerization product. It was found that: (1) as in the conventional (iodide-free) system, R_p is determined by the balance of initiation and termination rates. In other words, the iodide has no direct effect on the stationary concentration of P$^\bullet$. (However, as in a nitroxide-mediated polymerization,[17] the iodide can have some indirect effect on [P$^\bullet$] by, for example, lowering the average molecular weight of the product, which may be reflected on k_t and hence on [P$^\bullet$] through the stationary-state relation [P$^\bullet$] = $(R_i/k_t)^{1/2}$.) (2) Both the GPC curve-resolution and polydispersity-analysis methods allowed to determine the pseudo-first-order activation rate constant k_{act} of the PS-I adduct, showing that k_{act} is directly proportional to [P$^\bullet$], namely, degenerative chain transfer is the only important mechanism of activation in this system. (3) The fact that the k_{act} in the iodide system is proportional to [P$^\bullet$] hence R_p means that the polydispersity of this system is determined by conversion only (if effects of side reactions are disregarded), which is a unique feature that is not a characteristic of, e.g., a nitroxide system. (4) The minimum possible value of M_w/M_n ratio, achievable in a degenerative-type system with a high M_n, at a full conversion, and with negligible effects of side reaction, is equal to $1+(k_p/k_{ex})$,[10,14] which, for the iodide/styrene system, has turned out to be 1.28 at 80 °C. This limiting value becomes somewhat smaller by lowering the temperature. Since details of elementary reactions including the activation (deactivation), initiation, and termination processes are known, such properties as the chain length and its distribution of the polymers produced in the iodide system can now be predicted.

References and Notes

(1) Yutani, Y.; Tatemoto, M. *Eur. Pat. Appl.* 048937OA1, **1991**.

(2) (a) Kato, M.; Kamigaito, M.; Sawamoto, M.; Higashimura, T. *Polym. Prepr., Jpn.* **1994**, *43*, 255. (b) Ueda, N.; Kamigaito, M.; Sawamoto, M. *Polym. Prepr., Jpn.*

1996, *45*, 1267.

(3) (a) Matyjaszewski, K.; Gaynor, S.; Wang, J.-S. *Macromolecules* **1995**, *28*, 2093. (b) Gaynor, S.; Wang, J.-S.; Matyjaszewski, K. *Macromolecules* **1995**, *28*, 8051.

(4) See the Experimental Section of Chapter 3.

(5) More strictly, if the dead chains are produced by combination only, the *number* fraction f_1 does not exceed $1-(f_B/2) = 0.98$.

(6) Hui, A. W.; Hamielec, A. E. *J. Appl. Polym. Sci.* **1972**, *16*, 749.

(7) Molnar, S. *J. Polym. Sci., Part A-1* **1972**, *10*, 2245.

(8) Gilbert, R. G. *Pure Appl. Chem.* **1996**, *68*, 1491.

(9) Chapter 3 of this thesis; Goto, A.; Terauchi, T.; Fukuda, T.; Miyamoto, T. *Macromol. Rapid Commun.* **1997**, *18*, 673.

(10) Müller, A. H. E.; Zhuang, R.; Yan, D.; Litvinenko, G. *Macromolecules* **1995**, *28*, 4326.

(11) See the discussion in Chapter 1.2.2.

(12) Goto, A.; Fukuda, T. *Macromolecules* **1997**, *30*, 4272.

(13) Fukuda, T.; Goto, A. *Macromol. Rapid Commun.* **1997**, *18*, 682.

(14) Matyjaszewski, K. *Macromol. Symp.* **1996**, *111*, 47.

(15) The M_w/M_n ratio of the PS-I adduct (P_0-X) used for this study is 1.26 (see the Experimental Section), which is smaller than the limiting value. This is because some lower-mass components have been removed during the purification process. The raw product must have had a larger M_w/M_n ratio.

(16) The values of $[N_p]$ estimated by GPC can include a systematic error, since the large end-group effect observed for P_0-X (see the text) would become less and less significant as the chain length increases. Therefore the condition of constancy of $[N_p]$ may not be so well met as the figure suggests.

(17) Fukuda, T.; Terauchi, T.; Goto, A.; Ohno, K.; Tsujii, Y.; Miyamoto, T.; Kobatake, S.; Yamada, B. *Macromolecules* **1996**, *29*, 6393.

Chapter 7

Activation Mechanism of RAFT (Reversible Addition-Fragmentation Chain Transfer)-Based Living Radical Polymerizations

Abstract

The bulk polymerizations of styrene and methyl methacrylate in the presence of model polymer-dithiocarbonate adducts as mediators and benzoyl peroxide (BPO) as a conventional initiator were kinetically studied. The polymerization rate, hence the concentration of polymer radicals [P$^{\bullet}$], was proportional to [BPO]$^{1/2}$. The pseudo-first-order activation rate constants k_{act} were determined by the GPC direct and indirect methods. The results showed that k_{act} is directly proportional to [P$^{\bullet}$], indicating that reversible addition-fragmentation chain transfer (RAFT: Scheme 1.2) is the only important mechanism of activation. The magnitude of the exchange rate constant k_{ex} (= k_{act}/[P$^{\bullet}$]) was strongly dependent on both the structures of the dithiocarbonate group and the polymer. The k_{ex} values for the three RAFT systems examined in this work were all very large, which explains why these systems can provide low-polydispersity polymers from an early stage of polymerization. The activation energy of k_{ex} for a polystyryl dithioacetate (PS-SCSCH$_3$) was 21.0 kJ mol^{-1}, which is reasonable for a fast addition reaction.

7.1. Introduction

A novel living radical polymerization (LRP) using dithio compounds (Scheme 7.1a: e.g., Z = CH_3 and Ph) has recently been developed by CSRIO group.[1-7] The mechanism of activation is supposed to involve a reversible addition-fragmentation chain transfer (RAFT: Scheme 7.1a) process.[1,2] This polymerization has found to be applicable to a wide range of monomers,[1-4] and moreover it can afford low polydispersity polymers ($M_w/M_n < 1.1$) even at an early stage of polymerization,[1,2] which indicates that these RAFT processes are extremely fast. In this chapter, the author determines the pseudo-first-order activation rate constants k_{act} of the RAFT-based polymerizations of styrene and methyl methacrylate (MMA) as a function of polymerization rate R_p and temperature T. In this way, he will be able to obtain quantitative magnitudes of k_{act} and the related activation energies, and moreover establish the activation mechanism of these systems. The effects of the structures of dithiocarbonate groups and polymers on k_{act} will also be discussed.

(a) RAFT (e.g., Z = CH_3 and Ph)

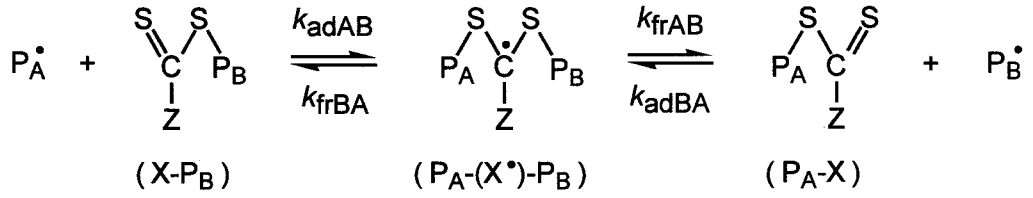

(b) Degenerative Chain Transfer

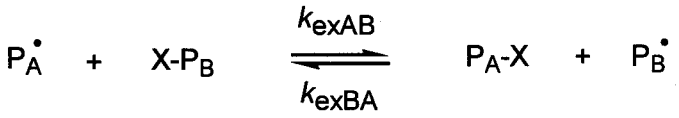

Scheme 7.1. RAFT and Degenerative Chain Transfer.

7.2. Experimental Section

7.2.1. Materials

Commercially available styrene, MMA, benzene, benzoyl peroxide (BPO), and azobisisobutyronitrile (AIBN) were purified by distillation or recrystallization. 1-Phenylethyl dithioacetate (**21**: Figure 2.2), 1-phenylethyl dithiobenzoate (**22**), and 2-phenylprop-2-yl dithiobenzoate (**23**) were prepared according to the published procedure.[1]

7.2.2. Preparation of Polymer-Dithiocarbonates

A styrene solution of **21** (17 mM) and BPO (10 mM) in a glass tube was degassed by several freeze-thaw-pump cycles, sealed off under vacuum, and heated at 60 °C for 3 h. After purification,[8] there was isolated a polystyryl dithioacetate (PS-SCSCH$_3$; **32**: Figure 2.3), which had a M_n of 1940 and a M_w/M_n ratio of 1.17 according to gel permeation chromatography (GPC). A chain extension test[8] showed that this polymer contains 6% (f_{dead} = 0.06) of potentially inactive species (without dithioacetate moiety at the chain end). Similarly, a styrene solution of **22** (41 mM) and BPO (7.5 mM) was heated at 80 °C for 3.5 h, giving a polystyryl dithiobenzoate (PS-SCSPh; **33**) with M_n = 1990, M_w/M_n = 1.07, and f_{dead} = 0.06. A MMA/benzene (3/1 v/v) solution of **23** (145 mM) and AIBN (30 mM) provided, after heat treatment at 60 °C for 7.5 h, a PMMA-dithiobenzoate (PMMA-SCSPh; **34**) with M_n = 1670, M_w/M_n = 1.20, and f_{dead} = 0.01.

7.2.3. Kinetic Analysis of Polymerization

The polymeric dithiocarbonates described above were used as probe adducts P_0-Xs. P_0-X and BPO were dissolved in monomer (styrene or MMA), degassed, sealed off under vacuum, and heated at a prescribed temperature for a prescribed time t. The reaction mixture was diluted by tetrahydrofuran (THF) to a known concentration and analyzed by GPC.

7.2.4. GPC

The GPC analysis was made on a Tosoh HLC-802 UR high-speed liquid chromatograph equipped with Tosoh gel columns G2500H, G3000H, and G4000H (Tokyo, Japan). THF

was used as eluent (40 °C). The column system was calibrated with Tosoh standard polystyrenes (PSs). Sample detection and quantification were made with a Tosoh differential refractometer RI-8020 calibrated with known concentrations of PSs in THF.

7.3. Results and Discussion

7.3.1. Polymerization Rate of Styrene/Polystyryl Dithioacetate (PS-$SCSCH_3$)/BPO System

The author first examines the polymerization of styrene including a fixed amount of PS-$SCSCH_3$ (0.45 mM) as a probe P_0-X and variable amounts of BPO (0–10 mM) as a conventional radical initiator. Figure 7.1 shows examples of the GPC curves for the mixtures heated at 60 °C for t = 10 min. The total area under each curve relative to that of the t = 0 curve shows the amount of the monomer converted to polymer, i.e., the conversion. An independent experiment confirmed that the GPC RI (refractive index) detector responses of PS-$SCSCH_3$s do not depend on chain length and agree with those of standard PSs within 1 or 2 % in the studied range of molecular weights ($M_n \geq 1600$).

Figure 7.2 shows the first-order plot of the monomer concentration [M]. In the studied range of conversions, the plot is approximately linear, indicating that the system is in a stationary state with respect to the ratio R_p/[M] (= k_p[P•]). Here k_p is the propagation rate constant. There was a few minutes of induction period when $[BPO]_0$ was zero. This system showed a non-zero value of R_p due to the spontaneous (thermal) initiation of styrene. This rate, however, was so small at 60 °C (see the ordinate scale in Figure 7.2) that even a usually unimportant amount of impurity seems to have brought about the detectable induction period.

Figure 7.3 shows the plot of $(R_p/[M])^2$ vs $[BPO]_0$, which confirms that $[P^•]^2$ is linear to $[BPO]_0$. In this regard, the RAFT process has no effect on R_p, as is usually the case with the polymerizations with a conventional chain transfer agent. However, independent experiments carried out with $[BPO]_0$ = 6 mM showed that the R_ps of the RAFT systems with $[PS\text{-}SCSCH_3]_0$ = 0.45 and 4.5 mM are about 5 % and about 20 %, respectively, smaller than

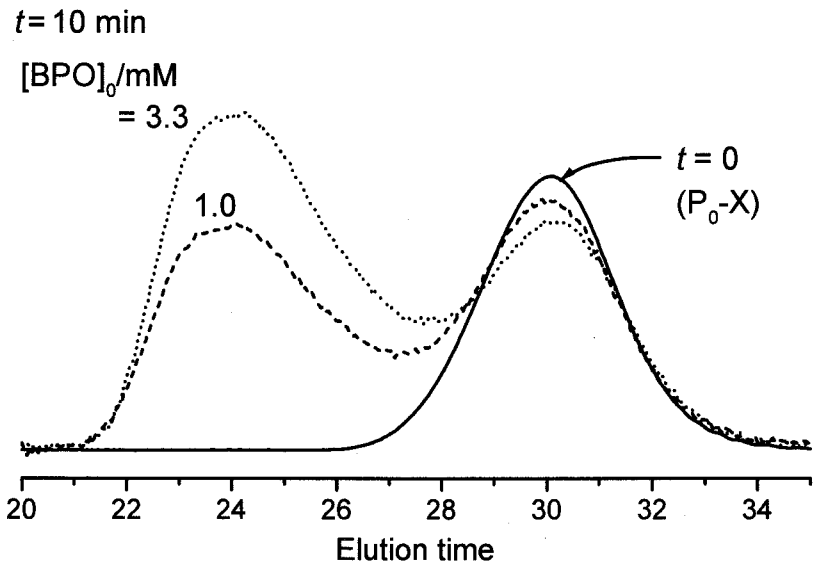

Figure 7.1. Examples of the GPC curves for the styrene/PS-SCSCH$_3$(P_0-X)/BPO mixtures heated at 60 °C for 10 min: $[P_0\text{-}X]_0$ = 0.45 mM; $[BPO]_0$ as indicated in the figure.

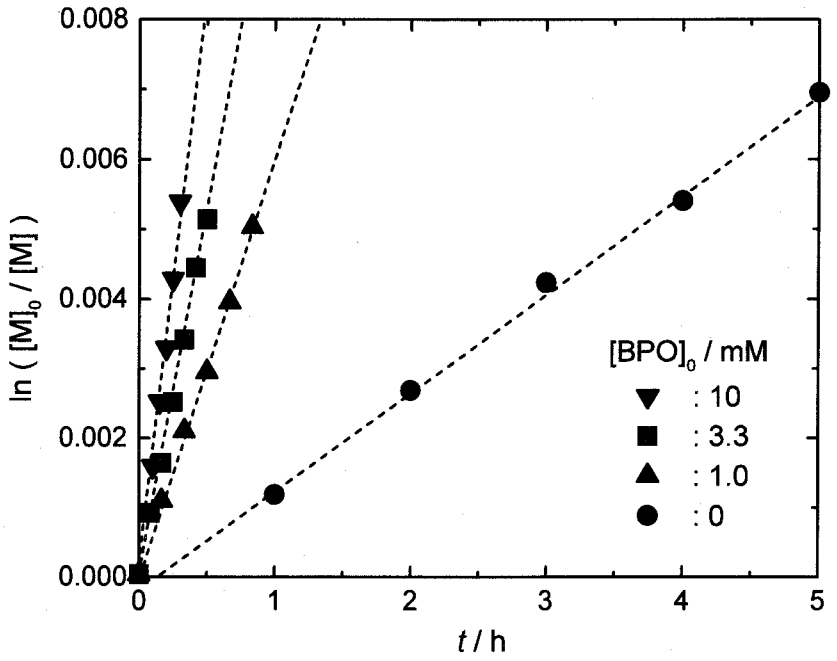

Figure 7.2. Plot of ln($[M]_0$/[M]) vs t (60 °C) for the styrene/PS-SCSCH$_3$(P_0-X) system: $[P_0\text{-}X]_0$ = 0.45 mM; $[BPO]_0$ as indicated in the figure.

that of the conventional (RAFT agent free) system. This rather weak dependence of R_p on the RAFT agent concentration suggests that a possible cause for this may be the chain length dependence of the termination rate constant k_t; as discussed in Chapter 1, in any variant of living radical polymerization with a sufficiently large rate R_i of (conventional) initiation, the stationary state is eventually reached in a predictable time after the onset of polymerization, where the system follows the conventional rate law

$$R_p = (k_p/k_t^{1/2})R_i^{1/2}[M] \qquad (7.1)$$

Since the number-average degree of polymerization x_n in living polymerization at a given conversion is inversely proportional to the concentration of living chains or the concentration of the initiating adduct P_0-X, and since k_t varies with x_n as $k_t \propto x_n^{-m}$ with m = 0.15~0.2,[9] the observed dependence of R_p on the RAFT agent concentration may possibly be ascribed to the chain length dependence of k_t. In the styrene/polystyryl iodide (PS-I)/BPO system studied in Chapter 6, a degenerative chain transfer-type system, such dependence of R_p on the PS-I concentration was not observed, even though the experiments were made for only one concentration of the PS-I. Presumably, the chain length difference between the iodide and iodide-free systems studied in this case happened to be small so that the mentioned dependence of k_t was unimportant.

7.3.2. Determination of k_{act} for Styrene/PS-SCSCH$_3$ System

The activation rate constant k_{act} was first determined by the GPC direct (peak resolution) method. The details of the method were described in Chapter 2. As discussed in Chapter 2, a lower initial concentration of P_0-X should lead to a larger number of monomer units added to $P_0^\bullet$ during an activation-deactivation cycle. In fact, with a sufficiently low $[P_0\text{-X}]_0$ (0.45 mM), the GPC curves were composed of two definite peaks such as those shown in Figure 7.1. The lower-molecular weight component corresponds to the unactivated P_0-X, and the higher-molecular weight one corresponds to the activated and grown chain P_1-X (plus other minor components such as those originated from BPO). These well-separated peaks in Figure 7.1

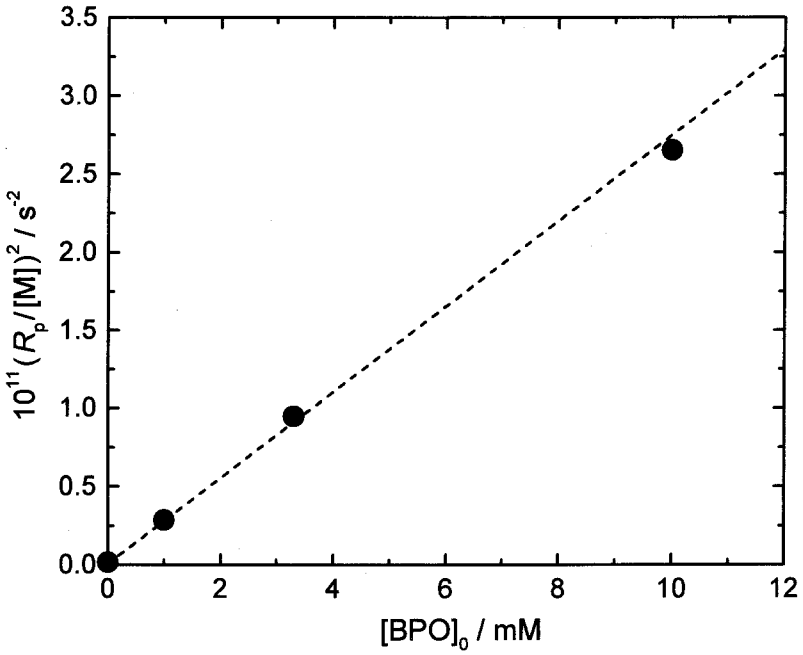

Figure 7.3. Plot of $(R_p/[M])^2$ vs $[BPO]_0$ (60 °C) for the styrene/PS-SCSCH$_3$(P_0-X) system: $[P_0\text{-X}]_0 = 0.45$ mM.

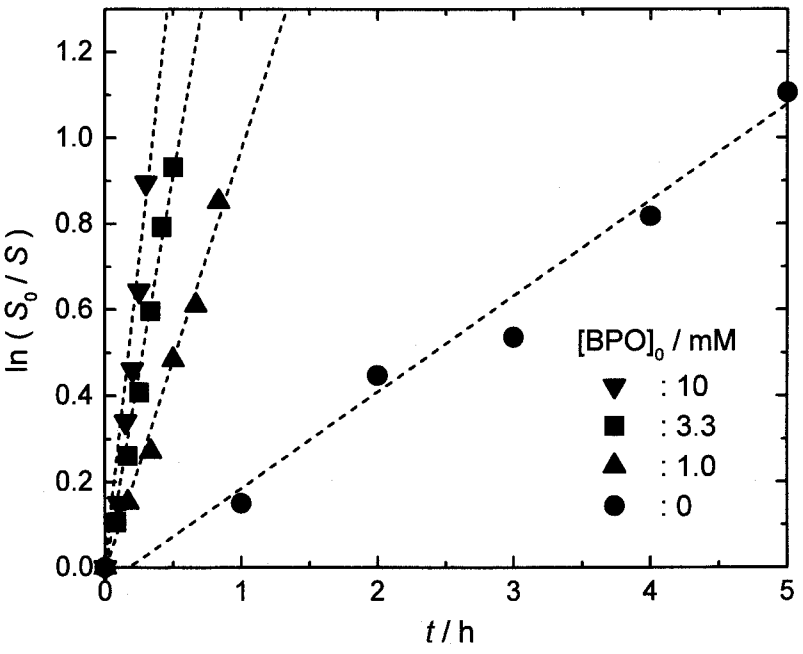

Figure 7.4. Plot of $\ln(S_0/S)$ vs t (60 °C) for the styrene/PS-SCSCH$_3$(P_0-X) system: $[P_0\text{-X}]_0 = 0.45$ mM; $[BPO]_0$ as indicated in the figure.

could accurately be resolved, allowing the author to unequivocally determine [P_0-X] or the intensity S of the first peak. Figure 7.4 shows the plot of $\ln(S_0/S)$ vs t for various concentrations of BPO. The plot is linear in all cases, giving a well-defined value of k_{act} according to equation 2.1. (A short induction period is observed for $[BPO]_0 = 0$; see above.) Since P_0-X originally contains 6 % of potentially inactive species (without the dithioacetate moiety: see the Experimental section), the data have been corrected by subtracting $0.06S_0$ from both S_0 and S. The primary oxygen-centered radical generated from BPO (PhCOO$^\bullet$) possibly attacks (or adds to) the C=S moiety. However, the concentration [PhCOO$^\bullet$] is estimated to be much far smaller than [P$^\bullet$] ([PhCOO$^\bullet$]/[P$^\bullet$] $\approx 10^{-3}$), and therefore the mentioned reaction should be totally unimportant.

The author next determined k_{act} by an alternative approach, the indirect (polydispersity analysis) method. Prerequisites for this method to be valid are the constancy of both [P$^\bullet$] (hence R_p/[M]) and the number of polymer chains N_p (Chapter 2). The [N_p] estimated by the conversion C and the overall x_n was nearly constant and exceeded in no case about 8 % of [P_0-X]$_0$ (Figure 7.5). This, coupled with the linear plot in Figure 7.2, confirms that the constancy of both N_p and [P$^\bullet$] is approximately met in this experiment. Figure 7.6 shows the plot of $F(C)[Y_B-(1/x_{n,B})]^{-1}$ vs t, according to equation 2.2. The plot is almost linear and the slope gives a well-defined value of k_{act} in all cases.

7.3.3. Mechanism of Activation

Scheme 7.1a shows a RAFT process, which involves the addition of radical $P_A^\bullet$ to the adduct P_B-X (rate constant = k_{adAB}) to form the intermediate radical, followed by the fragmentation of the intermediate to release either $P_A^\bullet$ (rate constant = k_{frBA}) or $P_B^\bullet$ (rate constant = k_{frAB}). This process, viewed as an exchanging or degenerative chain transfer process, is simplified to Scheme 7.1b, where k_{exAB}, for example, is the rate constant of the exchange reaction and related to the rate constants in Scheme 7.1a according to

$$k_{exAB} = P_{rB}k_{adAB} \qquad (7.2)$$

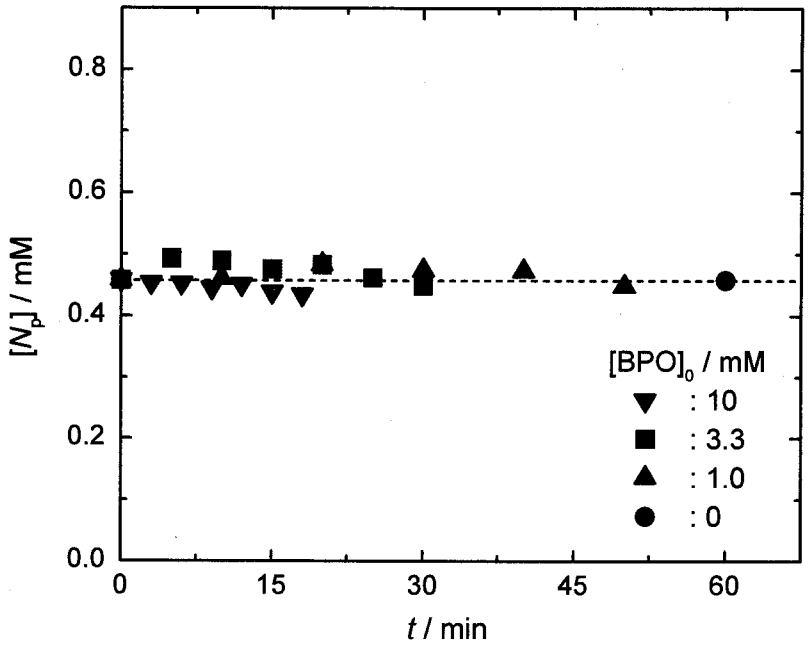

Figure 7.5. Plot of the number density $[N_p]$ of polymer vs t (60 °C) for the styrene/PS-$SCSCH_3(P_0\text{-}X)$ system: $[N_p]_0 = [P_0\text{-}X]_0 = 0.45$ mM; $[BPO]_0$ as indicated in the figure.

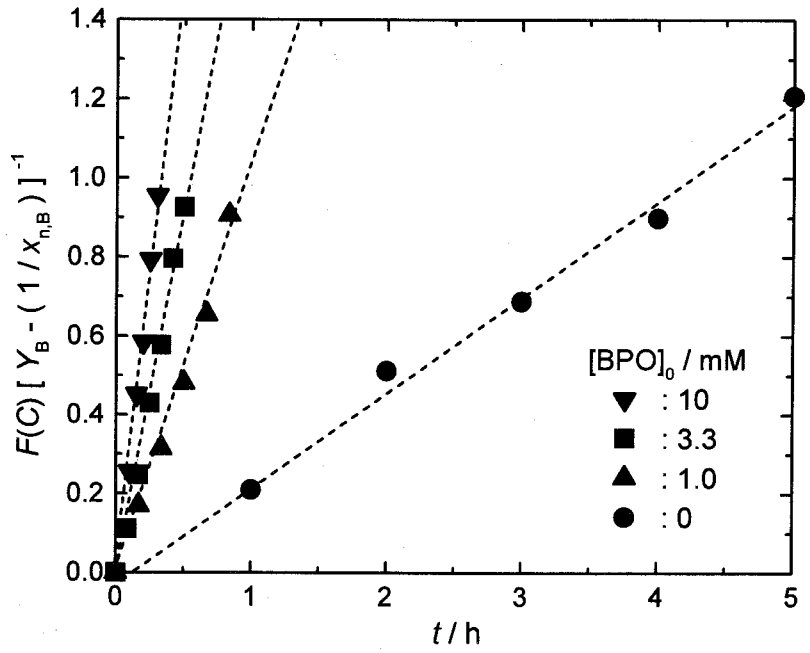

Figure 7.6. Plot of $F(C)[Y_B\text{–}(1/x_{n,B})]^{-1}$ vs t (60 °C) for the styrene/PS-$SCSCH_3(P_0\text{-}X)$ system: $[P_0\text{-}X]_0 = 0.45$ mM; $[BPO]_0$ as indicated in the figure.

Here P_{rB} (= $1-P_{rA}$) is the probability for the intermediate P_A-($X^\bullet$)-P_B to fragmentate into P_A-X and $P_B^\bullet$, and is given by

$$P_{rB} = \frac{k_{frAB}}{k_{frAB} + k_{frBA}} \tag{7.3}$$

When the polymer moieties P_A and P_B are kinetically identical as in homopolymerizations with sufficiently long chains, one can write $k_{exAB} = k_{exBA} = k_{ex}$, $k_{adAB} = k_{adBA} = k_{ad}$, and $k_{frAB} = k_{frBA} = k_{fr}$, which gives $P_{rA} = P_{rB} = 1/2$, i.e., equation 7.4.

$$k_{ex} = (1/2)\, k_{ad} \tag{7.4}$$

The existence of the intermediate radicals was confirmed by ESR spectroscopy for several RAFT systems (see below).[5] However, the C-S bond may possibly be cleaved by thermal homolysis (rate constant = k_d: Scheme 1.1a). If this process as well as the RAFT process are important, k_{act} will take the form

$$k_{act} = k_d + k_{ex}[P^\bullet] \tag{7.5}$$

(There is a small possibility of the degenerative chain transfer occurring directly to the C-S bond. However, this process, if any occurs, is difficult to kinetically distinguish from the RAFT process except that the former process does not accompany the intermediate radical. For this reason, the author simply neglects this process for the time being.)

Figure 7.7 shows the plot of k_{act} against $R_p/[M]$ (= $k_p[P^\bullet]$). Evidently, the data points obtained by the direct method (filled circles) and the indirect method (open circles) form a straight line passing through the origin, showing that $k_d = 0$ (within the accuracy of the present analysis) and the slope of the curve gives C_{ex} (= k_{ex}/k_p) = 180. This result suggests that the main mechanism of activation in this system is the RAFT process rather than thermal dissociation. With the known value of k_p (340 M^{-1} s^{-1}),[10] k_{ex} is estimated to be 61000 M^{-1} s^{-1}.

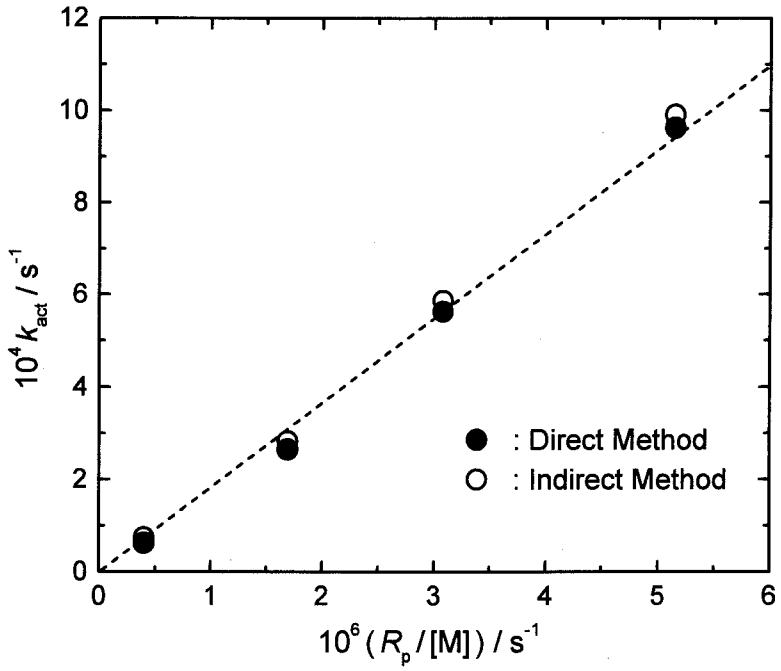

Figure 7.7. Plot of k_{act} vs (R_p/[M]) (60 °C) for the styrene/PS-SCSCH$_3$(P_0-X) system: (●) by the direct (curve-resolution) method, and (○) by the indirect (polydispersity analysis) method.

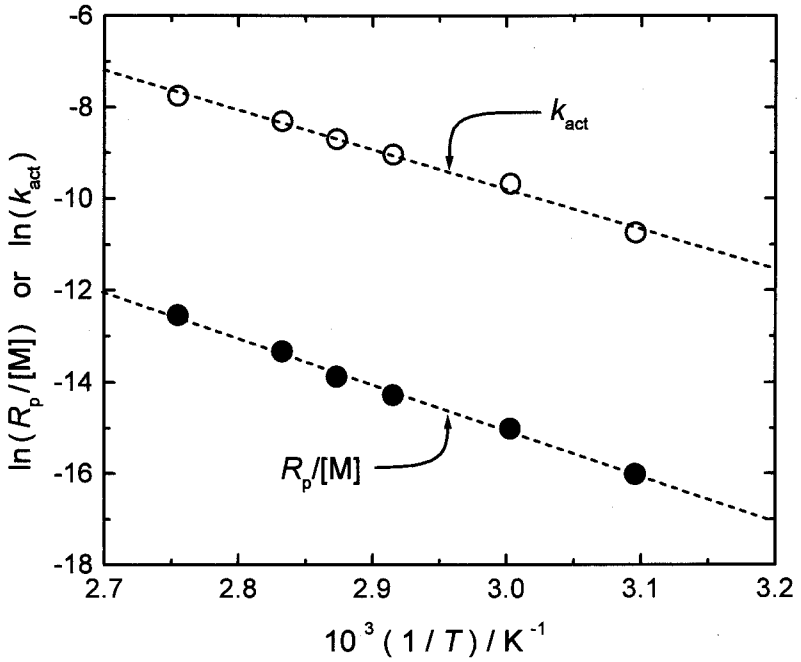

Figure 7.8. Plots of (○) ln(k_{act}) and (●) ln(R_p/[M]) vs 1/T for the styrene/PS-SCSCH$_3$(P_0-X) system: [P_0-X]$_0$ = 0.45 mM; [BPO]$_0$ = 0 at all examined temperatures.

7.3.4. Temperature Dependence of k_{ex} for Styrene/PS-SCSCH$_3$ System

The k_{act} values were determined by the direct method at various temperatures, all of which were carried out without BPO. Figure 7.8 shows the temperature dependence of k_{act} (= $k_{ex}[P^{\bullet}]$) and $R_p/[M]$ (= $k_p[P^{\bullet}]$). The results can be represented by

$$k_{act} / s^{-1} = 1.1\times10^{7} \exp(-72.1 \text{ kJ mol}^{-1}/RT) \quad (7.6)$$

$$(R_p/[M]) / s^{-1} = 3.6\times10^{6} \exp(-83.6 \text{ kJ mol}^{-1}/RT) \quad (7.7)$$

The constant C_{ex} (= k_{ex}/k_p) can be calculated with equations 7.6 and 7.7 to give

$$C_{ex} = 3.1 \exp(+11.5 \text{ kJ mol}^{-1}/RT) \quad (7.8)$$

With equation 7.8 and the known temperature dependence of k_p,[10] k_{ex} is given by

$$k_{ex} / M^{-1} s^{-1} = 1.3\times10^{8} \exp(-21.0 \text{ kJ mol}^{-1}/RT) \quad (7.9)$$

The activation energy of 21.0 kJ mol^{-1} is fairly small compared with those of homolytic bond cleavage reactions, e.g., the PS-TEMPO dissociation (124 kJ mol^{-1}),[11] but seems reasonable for addition reactions (k_p) such as those[10] for styrene (32.51 kJ mol^{-1}) and MMA (22.34 kJ mol^{-1}) and degenerative chain transfer reactions such as that relevant to PS-I (27.8 kJ mol^{-1}).[12]

7.3.5. Styrene/Polystyryl Dithiobenzoate (PS-SCSPh) System

The author also attempted to study the styrene polymerization with a PS-SCSPh adduct. The k_{act} in this system was extremely large, not allowing the author to determine its accurate value at this moment, but the GPC direct and indirect methods provided a crude estimate of C_{ex} = 6000 ± 2000 at 40 °C. This value is about 40 times as large as the corresponding acetate value given above, demonstrating a very large effect of the ester group on the RAFT velocity.

A comment may be due regarding the large C_{ex} value estimated here. With equation 7.4 and the k_p value of 160 for styrene[10] at 40 °C, one has $k_{ad} = 2k_{ex} = 2C_{ex}k_p \approx 1.9\times10^{6}$ M^{-1} s^{-1}

(for C_{ex} = 6000). This value of k_{ad} is exceptionally large for an addition reaction, perhaps near the "diffusion-controlled" limit. Examples of similarly large rate constant of addition can be found in some copolymerizations. For example, the rate constant k_{12} for vinyl acetate (1)/styrene (2) system is estimated as $k_{12} = k_{11}/r_1 \approx 0.6\times10^6$ M^{-1} s^{-1} with k_{11} = 6300[13] and r_1 = 0.01[14] at 40 °C.

7.3.6. MMA/PMMA-Dithiobenzoate (PMMA-SCSPh) System

Besides the ester group, the polymer moiety would also affect the magnitude of k_{act}. The author examined the polymerization of MMA including a fixed amount of PMMA-SCSPh (P_0-X: 0.56 mM) and variable amounts of BPO (0.1–1.0 mM). BPO was added, since MMA has no appreciable spontaneous (thermal) initiation unlike styrene. The first-order plot of [M] was approximately linear with no induction period in all examined cases (data not shown). The plot of $(R_p/[M])^2$ vs $[BPO]_0$ shown in Figure 7.9 confirms that $[P^\bullet]^2$ is proportional to $[BPO]_0$. The GPC chromatograms were composed of two well-separated peaks, which were used to determine k_{act} by the direct method. Figure 7.10 shows the plot of

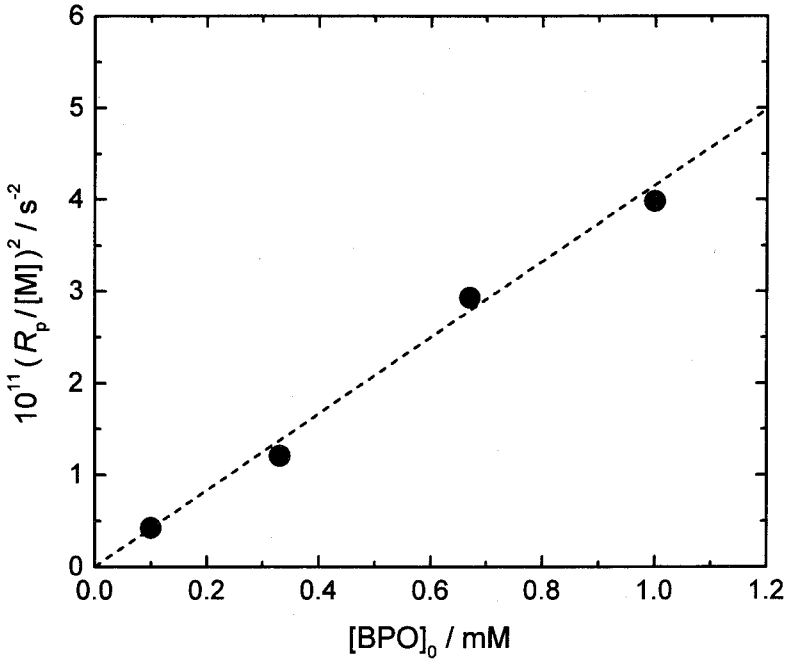

Figure 7.9. Plot of $(R_p/[M])^2$ vs $[BPO]_0$ (60 °C) for the MMA/PMMA-SCSPh(P_0-X) system: $[P_0\text{-}X]_0$ = 0.56 mM.

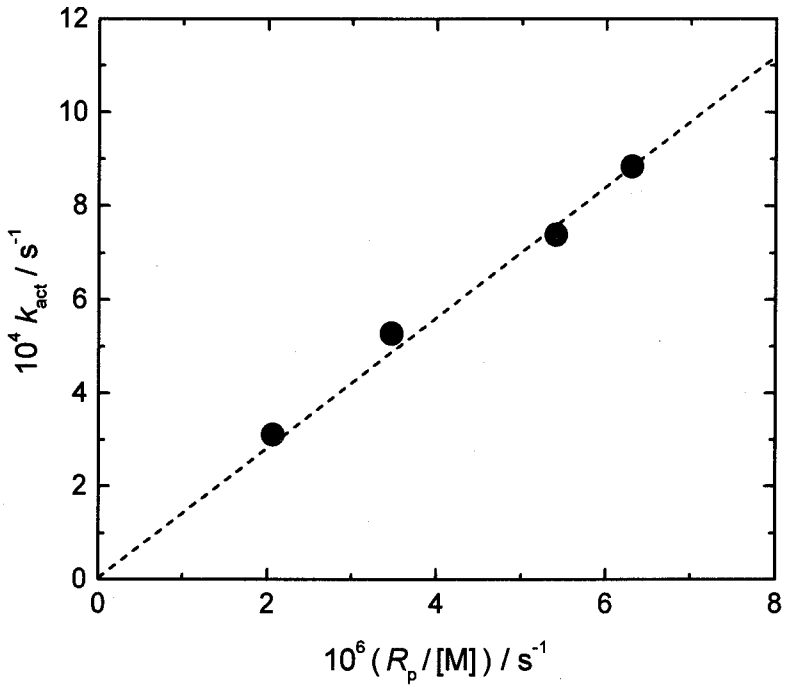

Figure 7.10. Plot of k_{act} vs (R_p/[M]) (60 °C) for the MMA/PMMA-SCSPh(P_0-X) system: k_{act} was determined by the direct (curve-resolution) method.

k_{act} vs R_p/[M] (= k_p[P•]). The intercept of the straight line gives k_d = 0, indicating that RAFT is virtually the only mechanism of activation in the MMA system as well as in the styrene system. The slope of the straight line gives C_{ex} = 140. This value is much smaller than that for the styrene/PS-SCSPh system discussed above, clearly showing that k_{act} is strongly dependent on the polymer (alkyl) moiety as well as the carbonate moiety.

7.3.7. Comments on Intermediate Radicals and Block Copolymerization

Referring to Scheme 7.1a again, it is easy to show that the stationary-state concentration of the intermediate P_A-(X•)-P_B is given by

$$[P_A\text{-}(X^\bullet)\text{-}P_B] = \frac{k_{adAB}[P_B\text{-}X][P_A^\bullet] + k_{adBA}[P_A\text{-}X][P_B^\bullet]}{k_{frAB} + k_{frBA}} \qquad (7.10)$$

When P_A and P_B are kinetically identical, equation 7.10 reduces to

$$[P-(X^{\bullet})-P]=\frac{k_{ad}}{k_{fr}}[P-X][P^{\bullet}] \quad (7.11)$$

In comparison of the styrene/PS-SCSPh and MMA/PMMA-SCSPh systems, we found that k_{ad}(styrene) » k_{ad}(MMA). In analogy to C-ON and C-halogen bonds, the bond energy of the PS-SC bond will be larger than that of the PMMA-SC bond or k_{fr}(styrene) will be smaller than k_{fr}(MMA). Hence one can expect that

$$[PS-(X^{\bullet})-PS] \gg [PMMA-(X^{\bullet})-PMMA] \quad (7.12)$$

In fact, the intermediate radical for the styrene system was clearly detected by ESR, while that for the *n*-butyl methacrylate system was undetectable.[5] This difference has been attributed to that in k_{fr},[5] but as equation 7.11 indicates, the difference in k_{ad} is also important. The author will come back to this point below.

Another comment concerns block copolymerization. For a smooth block copolymerization of monomer B to polymer A, for example, the exchange rate constant k_{exBA} must be large enough. The author showed in Chapter 6 that for a degenerative chain transfer-type system *by a batch process*, the polydispersity of the B block as a function of conversion C is given, in the ideal limit, by

$$[Y_B-(1/x_{n,B})]^{-1}=C_{exBB}[C/(2-C)] \quad (7.13)$$

where Y_B (= $M_{w,B}/M_{n,B}$ – 1) is the polydispersity index of the B block. Let us require that $x_{n,B}^{-1} \approx 0$ and Y_B = 0.1 for C = 1, for which equation 7.13 gives C_{exBB} = k_{exBB}/k_{pB} = 10. By taking this value as a measure and referring to equation 7.2, the condition of smooth block copolymerization reads

$$\frac{k_{exBA}}{k_{pB}}=\frac{P_{rA}k_{adBA}}{k_{pB}} \geq 10 \quad (7.14)$$

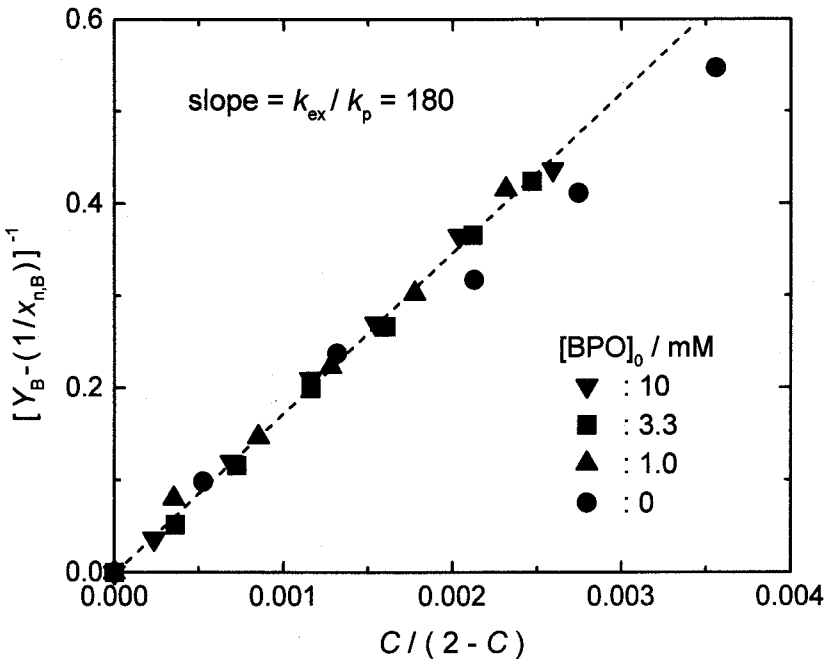

Figure 7.11. Plot of $[Y_B-(1/x_{n,B})]^{-1}$ vs $C/(2-C)$ (60 °C) for the styrene/PS-SCSCH$_3$(P_0-X) system: $[P_0\text{-X}]_0$ = 0.45 mM; $[BPO]_0$ as indicated in the figure. The three points for zero [BPO] show some deviation from the line, but the deviation is ascribed to the experimental error arising from the extremely small R_p for the BPO-free system.

Since k_{adBA} may presumably be approximated by k_{adBB} without too much error, equations 7.4 and 7.14 give

$$P_{rA} \geq 5C_{exBB}^{-1} \tag{7.15}$$

Regarding MMA/styrene/dithiobenzoate systems, we already know that C_{ex}(MMA) = 140 and C_{ex}(styrene) ≈ 6000. Equation 7.15 obviously holds for the PS radical adding to PMMA-X. On the other hand, in order for the PMMA radical to exchange with PS-X, P_r(styrene) has to be larger than about 5×(1/140) ≈ 0.04. The block copolymerization in this direction did not go smoothly,[7] which suggests that P_r(styrene) < 0.04 or that k_{fr}(MMA) is at least 25 times larger than k_{fr}(styrene). Putting this and the about 20 times difference in k_{ad} (about 40 times difference in C_{ex} with k_p(MMA)/k_p(styrene) = 2.4 at 60 °C[10]) into equation 7.11, we can estimate that the concentration of the intermediate radical in the MMA polymerization is at least 500 times smaller than that in the styrene polymerization, when other conditions are the

same. This would explain why the intermediate radical was not observed for the methacrylate system.[5]

Figure 7.11 shows the plot indicated by equation 7.13 for all the data of styrene/PS-$SCSCH_3$ system with different BPO concentrations, and hence different R_ps. In this conversion range, all the data points approximately fall on a single straight line passing through the origin with a slope of 180 (= C_{ex}), which naturally agrees with the value from Figure 7.7. Another example of such a plot, which extends to much higher conversions, was presented in Chapter 6 for the iodide-mediated polymerization of styrene.

Table 7.1. Comparison of C_{ex} (60 °C)

P-X	C_{ex}
1. PS-$SCSCH_3$	180
2. PS-SCSPh	6000 ± 2000[a)]
3. PMMA-SCSPh	140
4. PS-I[12]	4.0
5. PMMA-macromonomer[15]	0.20

[a)] Preliminary result at 40 °C.

7.4. Conclusions

The bulk polymerizations of styrene and MMA in the presence of polymer-dithiocarbonate adducts and BPO were kinetically studied. The polymerization rate R_p, hence [P•], was proportional to $[BPO]^{1/2}$ as in the conventional (RAFT agent-free) systems. The pseudo-first-order activation rate constant k_{act} determined by both the GPC direct and indirect methods was directly proportional to [P•], meaning that the main mechanism of activation in the present systems is RAFT rather than thermal dissociation. As summarized in Table 7.1, the exchange rate constants C_{ex} (= k_{ex}/k_p) for RAFT was strongly dependent on both the structures of the dithiocarbonate group and the polymer. In comparison with the C_{ex} values for the PS-I[12] and PMMA-macromonomer[15] systems, those for the examined RAFT systems are exceptionally large. This explains why these RAFT systems can yield low-polydispersity polymers from an early stage of polymerization.

References

(1) International Pat. Appl. PCT/US97/12540 WO9801478, invs.: Le, T. P. T.; Moad, G.; Rizzardo, E.; Thang, S. H.

(2) Chiefari, J.; Chong, Y. K.; Ercole, F.; Krstina, J.; Jeffery, J.; Le, T. P. T.; Mayadunne, R. T. A.; Meijs, G. F.; Moad, C. L.; Moad, G.; Rizzardo, E.; Thang, S. H. *Macromolecules* **1998**, *31*, 5559.

(3) Ganachaud, F.; Monteiro, M. J.; Gilbert, R. G.; Dourges, M.-A.; Thang, S. H.; Rizzardo, E. *Macromolecules* **2000**, *33*, 6738.

(4) International Pat. Appl. PCT/US98/26428 WO993114, invs.: Chiefari, J.; Mayadunne, R. T. A.; Moad, G.; Rizzardo, E.; Thang, S. H.

(5) Hawthorne, D. G.; Moad, G.; Rizzardo, E.; Thang, S. H. *Macromolecules* **1999**, *32*, 5457.

(6) Rizzardo, E.; Chiefari, J.; Chong, Y. K.; Ercole, F.; Krstina, J.; Jeffery, J.; Le, T. P. T.; Mayadunne, R. T. A.; Meijs, G. F.; Moad, C. L.; Moad, G.; Thang, S. H. *Macromol. Symp.* **1999**, *143*, 291.

(7) Chong, Y. K.; Le, T. P. T.; Moad, G.; Rizzardo, E.; Thang, S. H. *Macromolecules* **1999**, *32*, 2071.

(8) See the Experimental Section of Chapter 3.

(9) Olaj, O. F.; Vana, P. *Macromol. Rapid Commun.*, **1998**, *19*, 433.

(10) Gilbert, R. G. *Pure Appl. Chem.* **1996**, *68*, 1491.

(11) Chapter 3 of this thesis; Goto, A.; Fukuda, T. *Macromolecules* **1997**, *30*, 5183.

(12) Chapter 6 of this thesis; Goto, A.; Ohno, K.; Fukuda, T. *Macromolecules* **1998**, *31*, 2809.

(13) Ma, Y.-D.; Won, Y.-C.; Kubo, K.; Fukuda, T. *Macromolecules* **1993**, *26*, 6766.

(14) Nakata, T.; Otsu, T.; Imoto, M. *J. Polym. Sci., Part A, Polym. Chem.* **1965**, *3*, 3383.

(15) Moad, C. L.; Moad, G.; Rizzardo, E.; Thang, S. H. *Macromolecules* **1996**, *29*, 7717.

Part IV

Atom Transfer Radical Polymerization

Chapter 8

Activation Mechanism of Atom Transfer Radical Polymerization (ATRP)

Abstract

The activation process in the atom transfer radical polymerization (ATRP) of styrene with the cuprous bromide complex Cu(I)Br/2L (L = 4,4'-di-*n*-heptyl-2,2'-bipyridine) was kinetically studied by the GPC direct method using a polystyryl bromide (PS-Br) as a probe adduct. The mechanistic scheme of ATRP (Scheme 1.1c) was experimentally evidenced, and the second-order activation rate constant k_A for atom transfer was found to be 0.45 M^{-1} s^{-1} at 110 °C. This value is large enough to account for the observed production of low-polydispersity polymers even from an early stage of polymerization.

8.1. Introduction

Transition-metal-catalyzed living radical polymerization,[1-4] so-called "atom transfer radical polymerization (ATRP)",[2] developed by Sawamoto's[1] and Matyjaszewski's[2] groups independently has attracted much attention due to its applicability to a wide variety of monomers. Mechanistically, this polymerization is supposed to involve atom transfer (Scheme 1.1c) in its activation process, where a transition metal such as Ru,[1] Cu,[2,3] and Ni[4] acts as an activator to cleave the carbon-halogen bond of the alkyl halide P-X (typically, X = Cl or Br). As has been reported, the homogeneous ATRP of styrene catalyzed by a Cu(I) complex can yield polymers with predetermined degrees of polymerization up to DP $\approx$ 100 and polydispersity indices M_w/M_n as low as 1.04-1.05 even from an early stage of polymerization.[5] This indicates that the magnitude of the pseudo-first-order activation rate constant k_{act} in this system is also very large. In this chapter, the author confirms this by directly determining k_{act} by the gel permeation chromatographic (GPC) method. At the same time, this work presents experimental evidence for the mechanistic scheme of atom transfer to be involved in the activation process.

8.2. Experimental Section

8.2.1. Materials

Styrene and *tert*-butylhydroperoxide (BHP) were purified by fractional distillation. Cu(I)Br (99.999 %, Aldrich) was used as received without further purification. 4,4'-Di-*n*-heptyl-2,2'-bypyridine (dHbipy) was prepared by the dilithiation of 4,4'-dimetyl-2,2'-bypyridine followed by coupling with *n*-hexyl bromide, according to Matyjaszewski et al.[5] 1-Phenethyl bromide (**24**; PEBr: Figure 2.2) was used as received from Tokyo Kasei, Japan.

8.2.2. Preparation of Polystyryl Bromide

A styrene solution of PEBr (160 mM), Cu(I)Br (80 mM), and dHbipy (160 mM) in a glass tube was degassed and heated at 110 °C for 30 min. After purification,[6] there was isolated a polystyryl bromide (PS-Br; **35**: Figure 2.3), which had a M_n of 1400 and a M_w/M_n ratio of 1.06 according to GPC. A chain extension test[6] showed that this polymer contains 6 % of

potentially inactive species (without a halogen atom at the chain end).

8.2.3. Kinetic Analysis of Polymerization

The PS-Br described above was used as a probe adduct P_0-X. In a typical run, a Schlenk flask was charged with a predetermined amount of Cu(I)Br/2L (in this work, L = dHbipy), to which 4 mL of styrene solution of BHP (20 mM) and P_0-X (12 mM) dissolved in advance was quickly added. The flask with a glass stopper was immediately attached to a vacuum line and followed by three cycles of evacuation and dry-argon introduction. The system was then heated at 110 °C and stirred magnetically. After a prescribed time *t*, an aliquot (0.1 mL) of the solution was taken out by a syringe and quenched to air. The reaction mixture was then diluted by tetrahydrofuran (THF) to a known concentration and analyzed by GPC.

8.2.4. GPC

The GPC analysis was made on a Tosoh GPC-8020 high-speed liquid chromatograph equipped with Tosoh gel column G2500H, G3000H, and G4000H. THF was used as eluent

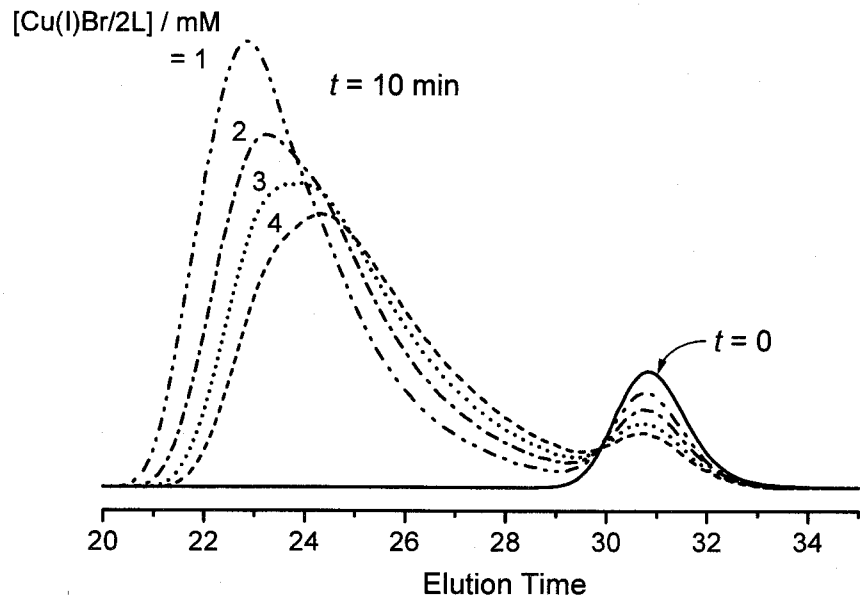

Figure 8.1. GPC charts for the PS-Br (P_0-X)/styrene/BHP mixture with different Cu(I)Br/2L concentrations heated at 110 °C for 10 min: $[P_0\text{-X}]_0$ = 12 mM; $[BHP]_0$ = 20 mM; $[Cu(I)Br/2L]_0$ as indicated in the figure.

(40 °C). Sample detection and quantification were made with a Tosoh differential refractometer RI-8020 calibrated with a known concentration of THF solution of a PS-Br adduct.

8.3. Results and Discussion

8.3.1. Determination of k_{act} by GPC Direct (Peak-Resolution) Method

A styrene solution of a probe adduct P_0-X (PS-Br: 12 mM), BHP (20 mM), and Cu(I)Br/2L (1-4 mM: L = dHbipy) was heated at 110 °C. As in this experiment, with a sufficiently low concentration of P_0-X and an addition of a conventional radical initiator such as BHP, a number of monomers will be added to $P_0^\bullet$ before it is deactivated with X (see Chapter 2). Figure 8.1 shows the GPC curves of the reaction mixtures at 10 min. All curves are clearly bimodal with the first lower-molecular-weight component corresponding to the unactivated adduct P_0-X and the second higher-molecular-weight one composed of the activated and grown chain P_1-X (plus other minor species). These well-separated peaks could accurately be resolved, allowing the unequivocal determination of [P_0-X] or the intensity S of the first peak. Figure 8.2 shows the plot of $\ln(S_0/S)$ vs t for various concentrations of Cu(I)Br/2L. The plots are linear in all cases, which give well-defined values of k_{act} according to equation 2.1. Since P_0-X originally contains about 6 % of potentially inactive species, it was corrected by subtracting $0.06S_0$ from both S_0 and S.

8.3.2. Mechanism of Activation

As mentioned above, the activation process of this system is supposed to be atom transfer (Scheme 1.1c). However, the cleavage of the C-Br bond can possibly occur by degenerative chain transfer (Scheme 1.1b). For the cleavage of the C-I bond, this process is in fact important, as shown in Chapter 6. When these two reactions are involved in the activation process, k_{act} will take the form

$$k_{act} = k_A[A] + k_{ex}[P^\bullet] \qquad (8.1)$$

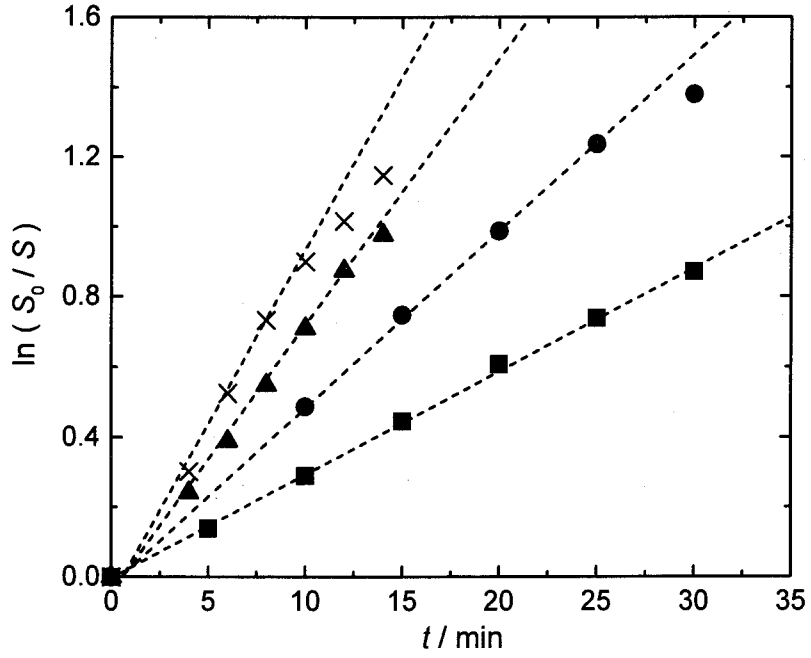

Figure 8.2. Plot of $\ln(S_0/S)$ vs t for the PS-Br activated by cuprous halide (110 °C): $[Cu(I)Br/2L]_0$ = 1 (■), 2 (●), 3 (▲), and 4 (×) mM.

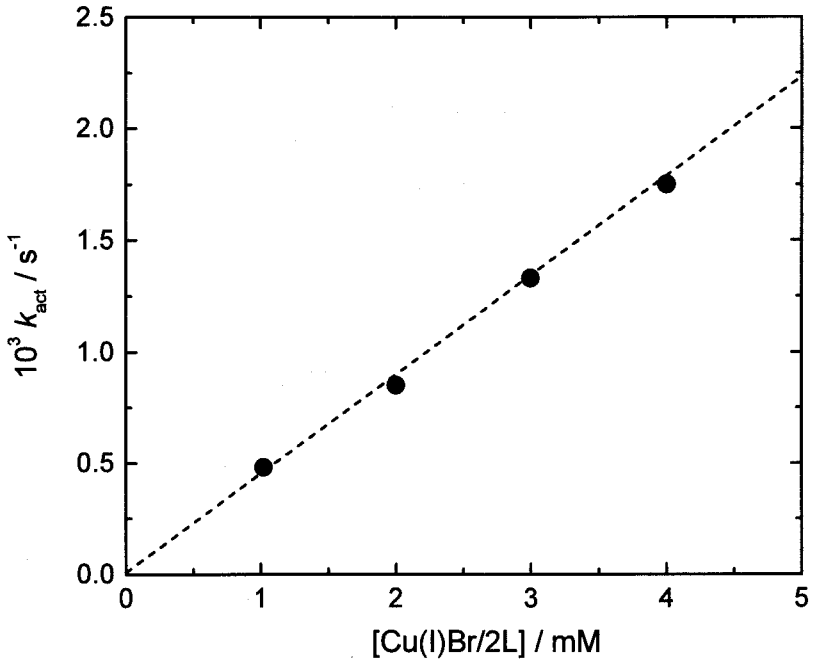

Figure 8.3. Plot of k_{act} vs $[Cu(I)Br/2L]_0$: data from Figure 8.2. The slope of the straight line gives the k_A of 0.45 M^{-1} s^{-1}.

where A is an activator (Cu(I)Br/2dHbipy in this work), and k_A and k_{ex} are the rate constants of atom transfer and degenerative chain transfer, respectively.

Figure 8.3 shows the plot of k_{act} vs $[Cu(I)Br/2L]_0$. The data points form a straight line passing through the origin, meaning that the degenerative chain transfer is negligible in this system. From the slope of the straight line, k_A can be estimated to be 0.45 M^{-1} s^{-1}. (The author assumes here that the equilibrium concentration [Cu(I)Br] is equal to the initial one $[Cu(I)Br]_0$. This is justified as follows: the radical concentration is estimated to be about $2.0x10^{-8}$ M from the plot of $\ln([M]_0/[M])$ vs t (data not shown), where [M] is the monomer concentration. The equilibrium constant K (= $[P^\bullet][Cu(II)Br_2/2L]/[P\text{-}X][Cu(I)Br/2L]$) of $3.9x10^{-8}$ estimated by Matyjaszewski et al.[5] suggests that [Cu(I)Br] is smaller than the initial value only by approximately 5%, which is negligibly small compared with other experimental errors.) With using the cited K (= k_A/k_{DA}) value of $3.9x10^{-8}$, the k_A value obtained here (0.45 M^{-1} s^{-1}) gives $k_{DA} = 1.1x10^7$ M^{-1} s^{-1}.

8.3.3. Comments on k_A Value

With a typical Cu(I)Br concentration of 0.1 M, the k_A of 0.45 M^{-1} s^{-1} gives $k_{act} = 0.045$ s^{-1}, meaning that a PS-Br adduct is activated once every 22 s. This figure is much smaller than, e.g., the k_{act}^{-1} value of 45 min for a PS-TEMPO (2,2,6,6-tetramethylpiperidinyl-1-oxy) adduct at the same temperature (see Chapter 3), and explains why the ATRP system provides low-polydispersity polymers *from an earlier stage of polymerization.*[5] The activation frequency in the TEMPO system is not so large that it takes a rather long time before the PS-TEMPO adduct experiences a sufficiently large number of activation-deactivation cycles to achieve a low polydispersity.[7]

8.3.4. Estimation of k_{act} by GPC Indirect (Polydispersity-Analysis) Method

To confirm the validity of the k_A value obtained by the direct method, the author also attempted to determine k_A by the indirect method. As discussed in Chapter 2, the indirect method is valid only for the system where $[P^\bullet]$ is constant and side reactions are absent. Therefore its adoption is limited to the initial stage of *stationary-state* polymerization where

the effects of side reactions are minor. Unfortunately, the polymerization rate (hence [P$^{\bullet}$]) of the present system was observed to vary seriously at an early stage of polymerization, and thus it was not possible to determine k_{act} rigorously by this method. However, it is possible to estimate the lower limit of k_{act} on the basis of the polydispersities observed at relatively large conversions, where the effect of the initial non-stationarity would be unimportant and the contribution of the "initiating" P_0-X would be minor if P_0-X is a low-mass compound. For example, in the bulk polymerization of styrene at 110 °C with $[P_0\text{-X}]_0 = [\text{Cu(I)Br/2L}]_0 = 87$ mM (P_0-X = PEBr), the polydispersity observed at 30 % conversion ($t \cong 2300$ s, and the degree of polymerization $x_n \cong 30$) was $M_w/M_n = 1.05$.[5] Application of these data to equation 2.2 gives $k_{act} = 0.05\ s^{-1}$ or $k_A = 0.6\ M^{-1}\ s^{-1}$, which is in remarkable agreement with the directly determined value. At higher conversions, the estimated value of k_A rapidly decreases, indicating that side reactions have a more serious effect as conversion increases.

It should be remembered that for the technical reason, the direct determination of k_{act} was conducted at unusually low concentrations of Cu(I)Br/2L. The value of k_A for ordinary (high-concentration) systems could be somewhat different, if the assumed kinetic linearity should break due to potential effect of the concentration of Cu(I)Br/2L on its structure and reactivity. However, this difference should not be very large, since the value of k_A estimated by the polydispersity analysis (the indirect method) for an ordinary system reasonably agreed with the one obtained at the low concentrations of Cu(I)Br/2L.

8.4. Conclusions

The second-order activation rate constant k_A in Cu(I)Br/2dHbipy-catalyzed ATRP of styrene at 110 °C was determined by the GPC direct method to be 0.45 $M^{-1}\ s^{-1}$. This figure is large enough to account for why this ATRP system can yield low-polydispersity polymers even from an early stage of polymerization. Mechanistically, ATRP was found to include only atom transfer in its activation process.

References

(1) Kato, M.; Kamigaito, M.; Sawamoto, M.; Higashimura, T. *Macromolecules* **1995**, *28*, 1721.

(2) Wang, J. S.; Matyjaszewski, K. *J. Am. Chem. Soc.* **1995**, *117*, 5614.

(3) See references 33-36 in Chapter 1.

(4) (a) Granel, C.; Dubois, Ph.; Jérôme, R.; Teyssié, Ph. *Macromolecules* **1996**, *29*, 8576. (b) Uegaki, H.; Kotani, Y.; Kamigaito, M.; Sawamoto, M. *Macromolecules* **1997**, *30*, 2249.

(5) Matyjaszewski, K.; Patten, T. E.; Xia, J. *J. Am. Chem. Soc.* **1997**, *119*, 674.

(6) See the experimental Section of Chapter 3.

(7) Goto, A.; Fukuda, T. *Macromolecules* **1997**, *30*, 4272.

Chapter 9

Activation Rate Constants of Initiators for Atom Transfer Radical Polymerization (ATRP)

Abstract

The second-order activation rate constants for atom transfer (Scheme 1.1c), k_A, for low-mass alkyl halides catalyzed by cuprous halide complexes Cu(I)X/2L (X = Cl or Br; L = 4,4'-di-*n*-heptyl-2,2'-bipyridine) were determined by the nitroxide capping method along with ^{1}H NMR. The k_A for 1-phenylethyl bromide, a typical initiator for atom transfer radical polymerization (ATRP), with the Cu(I)Br complex was found to be close to the known value of the k_A for a polystyryl bromide, being large enough for the initiation to be completed at an early stage of polymerization. It was also found that k_A strongly depends on the kind of halogen and the steric factor of the alkyl halide in question.

9.1. Introduction

Atom transfer radical polymerization (ATRP) is one of the most promising living radical polymerizations due to its applicability to a wide variety of monomers and its high controllability of the product polymers.[1] Among several transition metals successfully available in ATRP, copper(I) species has most widely been employed. In Chapter 8, the author examined the activation process of Cu(I)Br-catalyzed ATRP of styrene by measuring the pseudo-first-order activation rate constant k_{act} of a polystyryl bromide (PS-Br) by the GPC curve-resolution method. The result showed that the atom transfer mechanism (Scheme 1.1c) is the only important activation process in ATRP (hence $k_{act} = k_A$[Cu(I)Br]), and that the magnitude of k_A is large enough to explain the observed production of low-polydispersity polymers from an early stage of polymerization.[2] (Here k_A is the rate constant of atom transfer.)

Another requisite for obtaining such low-polydispersity polymers is a fast initiation. Figure 2.2 shows examples of ATRP low-mass initiators (**24-26**). The activation of such an alkyl halide initiator should occur in a relatively short time compared to the overall polymerization duration. This calls for kinetic studies on the activation of initiators, but no such studies other than the one due to Pascual et al.[3] have been reported in ATRP. In this chapter, the author determines the k_A of the low-mass alkyl halides **24-26** with Cu(I)X/2L (X = Cl or Br; L = di-*n*-heptyl-2,2'-bipyridine (dHbipy)) used as an activator, and discusses the factors affecting the initiation rate of ATRP. The method applied in this work is the nitroxide capping method, whose details were shown in Chapter 2.

9.2. Experimental Section

9.2.1. Materials

Cu(I)Br (99.999%) and Cu(I)Cl (99.99%) were purchased from Aldrich and Acros, respectively, and used as received. dHbipy was prepared by the dilithiation of 4,4'-dimethyl-2,2'-bipyridine followed by coupling with *n*-hexyl bromide, according to Matyjaszewski et al.[2] All other reagents were commercially obtained and used without further purification.

9.2.2. General Procedure for Determination of k_A

In a typical run, a Schlenk flask was charged with Cu(I)Br/2dHbipy (4 mM), to which a toluene-d_8 solution with **24** (1 mM) and 2,2,6,6-tetramethypiperidinyl-1-oxy (TEMPO; 16 mM) dissolved in advance was quickly added. The flask with a glass stopper was immediately attached to a vacuum line, followed by three cycles of evacuation and dry-argon introduction. The system was then kept at a preset temperature and stirred magnetically. After a prescribed time t, an aliquot of the solution was taken out by a syringe, quenched in the air, and examined by proton magnetic resonance (^{1}H NMR) at room temperature.

9.2.3. Proton Magnetic Resonance (^{1}H NMR)

^{1}H NMR spectra were obtained by a JEOL GSX-400 spectrometer operating at 400 MHz. These spectra were recorded at ambient temperature, and with flip angle of 45 degrees, spectral width of 7934 Hz, acquisition time of 4.129 sec, and pulse delay of 10 sec.

9.3. Results and Discussion

9.3.1. Determination of k_A for PEBr/CuBr System

1-Phenylethyl bromide (**24**; PEBr: 1 mM) was heated at 110 °C together with Cu(I)Br/2dHbipy complex (4 mM) and TEMPO (16 mM) in toluene-d_8. With such a large excess of TEMPO, the phenyl ethyl radical PE$^\bullet$ from PEBr will primarily be trapped by TEMPO to form PE-TEMPO rather than deactivated by Cu(II)Br_2 back to PEBr. Figure 9.1 shows the ^{1}H NMR spectra (in the range of 4.6-4.9 ppm) of the solution during the heat treatment. The signals at 4.73 and 4.80 ppm are assigned to the α-methine protons of PEBr and PE-TEMPO, respectively. The intensities of signals became smaller for PEBr and larger for PE-TEMPO as time elapsed, while the total intensity of the two signals is kept constant. The peak for PEBr disappeared completely in 150 min, meaning that the reaction proceeds quantitatively.

From the intensity of the signal, the concentration I of the initiator (PEBr) could be definitely obtained. Figure 9.2 shows the plot according to equation 2.5 with using the

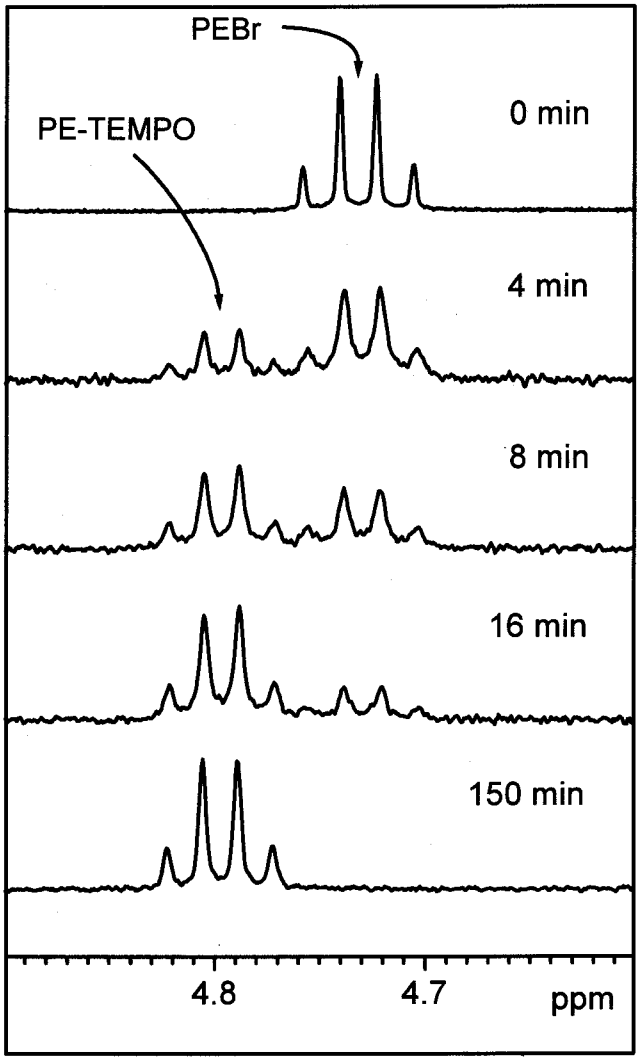

Figure 9.1. ^{1}H NMR spectra (in the range of 4.6-4.9 ppm) for the PEBr/Cu(I)Br/dHbipy/ TEMPO mixture in toluene-d_8 heated at 110 °C: $[PEBr]_0$ = 1 mM, $[Cu(I)Br/2dHbipy]_0$ = 4 mM, and $[TEMPO]_0$ = 16 mM: the signals at 4.73 and 4.80 ppm are assigned to the α-methine protons of PEBr and PE-TEMPO, respectively.

values of I. The plot is linear passing through the origin, and its slope with the known A_0 (= $[Cu(I)Br/2dHbipy]_0$) and I_0 gives k_A = 0.42 M^{-1} s^{-1}. This value combined with the typical Cu(I)Br concentration of 0.1 M used in the actual ATRP runs gives k_{act} = 0.042 s^{-1}; i.e., the half-life time of PEBr is as short as 17 s. This result indicates that the use of this concentration of Cu(I)Br allows complete "initiation" of PEBr at an early stage of polymerization. The k_A obtained here is very close to that for the PS-Br/Cu(I)Br system (0.45 M^{-1} s^{-1}),[4] which indicates that k_A is nearly independent of the chain length.

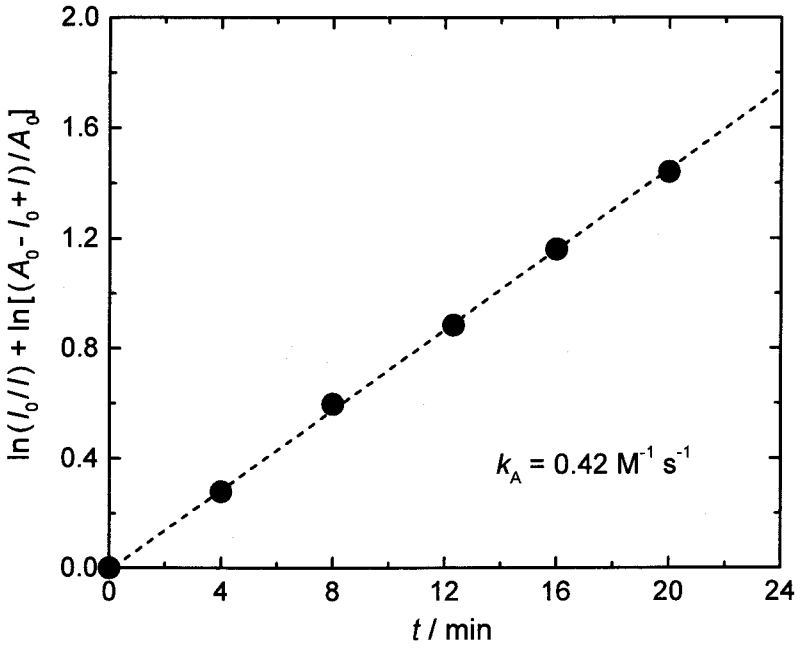

Figure 9.2. Plot of $\ln(I_0/I)+\ln[(A_0-I_0+I)/A_0)]$ vs. t for the activation of PEBr catalyzed by Cu(I)Br in toluene-d_8 at 110 °C: For the experimental condition, see Figure 9.1.

Regarding the accuracy of the measurement, two issues associated with the use of TEMPO should be noted. In order to examine possible interactions (e.g., coordination) of TEMPO with copper species, electron spin resonance (ESR) measurements of the TEMPO species in the presence of Cu(I)Br and Cu(II)Br_2 complexes were made. The results showed that the shape and intensity of the spectrum are almost identical with those observed in the absence of the copper species, indicating that TEMPO does not interact with the copper species. Consequently TEMPO should not give any effect on the activity of Cu(I)Br hence the value of k_A. Alkoxyamines such as PE-TEMPO suffer decomposition into an alkene and a hydroxylamine at high temperatures. The rate constants of this reaction known so far[5,6] suggest that decomposed species possibly produced during the k_A experiment is negligible in fraction (< 3%) at the examined temperature (110 °C).

9.3.2. Temperature Dependence of k_A for PEBr/CuBr system

Figure 9.3 shows the k_A values determined for the PEBr/Cu(I)Br system at various temperatures. The result can be represented by the Arrhenius formula

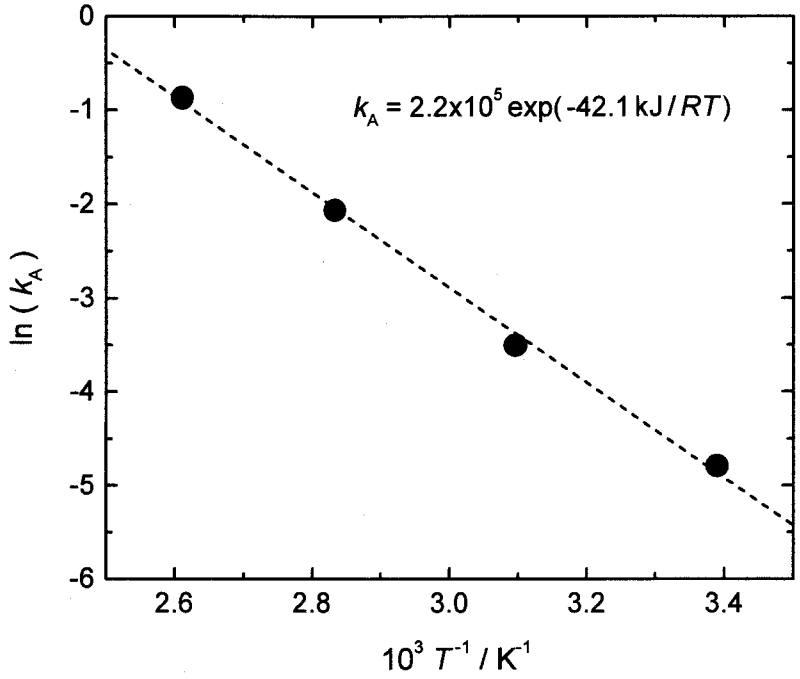

Figure 9.3. Plot of $\ln(k_A)$ vs. T^{-1} for the PEBr/Cu(I)Br system.

$$k_A / M^{-1} s^{-1} = 2.2x10^5 \exp(-42.1 \text{ kJ mol}^{-1}/RT) \quad (9.1)$$

It is interesting to note that this activation energy of 42.1 kJ mol^{-1} is much smaller than those of homolytic bond cleavage reactions such as that of PS-TEMPO dissociation (**27**: 124 kJ mol^{-1}),[7] but larger than those of chain transfer reactions, e.g., the degenerative transfer reactions related to PS-I (**31**: 27.8 kJ mol^{-1})[8] and PS-SCSCH$_3$ (**32**: 21.0 kJ mol^{-1}).[9]

9.3.3. Effects of Halogen and Alkyl Group on k_A

Table 9.1 lists the k_A values for several systems. For PECl (**25**) with Cu(I)Cl, k_A is much smaller than that for the PEBr/Cu(I)Br system, indicating that the C-Cl bond is much stronger than the C-Br bond. The value of 0.018 M^{-1} s^{-1} for the Cl system is in good agreement with that estimated by Pascual et al. (0.020 M^{-1} s^{-1}),[3] although the latter system includes 2,2-bipyridine as a ligand and the mixture of styrene and *N*,*N*-dimethylformamide as a solvent. Regarding Cu(I)Br-mediated systems, PEBr and BzBr (**26**) make a large difference in k_A,

suggesting that the α-methyl substituent in PEBr exerts a strong effect on the release of bromine.

Matyjaszewski et al. have recently reported that the mixed halogen system with an alkyl bromide (R-Br) and Cu(I)Cl gives a better control of polymerization than the homo-halogen (R-Br/Cu(I)Br) system, and explained it in terms of an increase of the relative rate of initiation to that of propagation.[10,11] Such a mixed halogen system has also been studied by Haddleton et al.[12] Compared with the homo-halogen system, propagation rate is certainly smaller in the mixed halogen system, since R-Cl, which has a stronger carbon-halogen bond than R-Br, is preferentially formed.[10] However there is no direct knowledge about initiation. For this reason, the author attempted to examine the initiation in the PEBr/Cu(I)Cl system. As Table 9.1 shows, the k_A for the PEBr/Cu(I)Cl is somewhat larger than that for the PEBr/Cu(I)Br system; namely, the use of Cu(I)Cl with R-Br does not only lead to slower propagation but also faster initiation. The lowest k_A in the PECl/Cu(I)Br system in addition to the highest k_A in PEBr/Cu(I)Cl system infers that Cu(I)Cl is a stronger reducing agent than Cu(I)Br.

Table 9.1. Values of Rate Constant k_A

Adduct	Activator (CuX)	k_A / M^{-1} s^{-1}
PS-Br (**35**)	CuBr	0.45[4]
PEBr (**24**)	CuBr	0.42
PEBr (**24**)	CuCl	0.52
PECl (**25**)	CuCl	0.018
PECl (**25**)	CuBr	0.010
BzBr (**26**)	CuBr	0.18

9.4. Conclusions

The activation rate constants for low-mass alkyl halides in the presence of Cu(I)X were determined by the nitroxide capping method along with the use of ^{1}H NMR. The initiation in the PEBr/Cu(I)Br system was found to be fast enough compared to propagation. It also turned out that k_A is only weakly dependent on chain length, that the C-Br bond is more labile than the C-Cl bond, and that the bromine bonded to secondary carbon is easier to be released than that bonded to primary carbon.

References

(1) See references 1-4 in Chapter 8.

(2) Matyjaszewski, K.; Patten, T. E.; Xia, J. *J. Am. Chem. Soc.* **1997**, *119*, 674.

(3) Pascual, S.; Coutin, B.; Tardi, M.; Polton, A.; Vairon, J.-P. *Macromolecules* **1999**, *32*, 1432.

(4) Chapter 8 of this thesis; Ohno, K.; Goto, A.; Fukuda, T.; Xia, K.; Matyjaszewski, K. *Macromolecules* **1998**, *31*, 2699.

(5) Li, I.; Howell, B. A.; Matyjaszewski, K.; Shigemoto, T.; Smith, P. B.; Priddy, D. B. *Macromolecules* **1995**, *28*, 6692.

(6) Ohno, K.; Tsujii, Y.; Fukuda, T. *Macromolecules* **1997**, *30*, 2503.

(7) Chapter 3 of this thesis; Goto, A.; Fukuda, T. *Macromolecules* **1997**, *30*, 5183.

(8) Chapter 6 of this thesis; Goto, A.; Ohno, K.; Fukuda, T. *Macromolecules* **1998**, *31*, 2809.

(9) Chapter 7 of this thesis; Goto, A.; Sato, K.; Tsujii, Y.; Fukuda, T.; Moad, G.; Rizzardo, E.; Thang, S. H. *Macromolecules*, in press.

(10) Matyjaszewski, K.; Shipp, D. A.; Wang, J.-L.; Grimaud, T.; Patten, T. E. *Macromolecules* **1998**, *31*, 6836.

(11) Shipp, D. A.; Wang, J.-L.; Matyjaszewski, K. *Macromolecules* **1998**, *31*, 8005.

(12) Haddleton, D. M.; Heming, A. M.; Kukulj, D.; Jackson, S. G. *Chem. Commun.* **1998**, 1719.

Appendix: Chain Length Distribution in Polymers Produced via Alternating Activation-Deactivation Processes – Derivation of Equation 1.5

Here we consider polymerization processes in which the propagating species experiences an activated and a deactivated state alternatingly. In the deactivated state, the active chain end is blocked in some way or another, and no propagation occurs. In the activated state, the chain can be added by a monomer unit with a probability p or deactivated with a probability $1-p$. The transition from the deactivated to activated state occurs with a probability density of y_n/t, so that y_n is the mean number of such transitions during time t. Here we assume that the time during which the chain is in the activated state is much shorter than the total time or $\tau y_n \ll t$, where τ is the "transient" lifetime, i.e., the mean time in the activated state per activation-deactivation cycle. We neglect all other reactions.

Clearly, the length distribution of the chain fragment produced in a cycle is a most probable one

$$f_1(x) = p^x(1-p) \tag{A-1}$$

where x is the degree of polymerization and it can take integers from 0 to ∞. If the chain experiences y such cycles, the number density distribution of the chain with length x is

$$f_y(x) = (1-p)^y p^x \binom{x+y-1}{x} \tag{A-2}$$

The last factor in the right-hand-side of equation A-2 denotes the number of ways to distribute x units over y groups, and it holds that

$$\sum_{x=0}^{\infty} p^x \binom{x+y-1}{x} = (1-p)^{-y} \tag{A-3}$$

That is, equation A-2 is normalized to unity. The probability that the chain has y cycles is given by a Poisson distribution:

$$g(y) = e^{-y_n} y_n{}^y / y! \tag{A-4}$$

where y_n is the mean value of y. Finally, the number density of the chain characterized by the two parameters x and y is given by

$$N(x,y) = g(y) f_y(x) \tag{A-5}$$

which is normalized to unity ($x, y = 0, 1, 2, \cdots$).

Moments of the distribution may be calculated by defining the function $N_s(x,y)$ of a dummy variable s

$$N_s(x,y) = (y_n{}^y / y!)(1-p)^y (ps)^x \binom{x+y-1}{x} \tag{A-6}$$

By referring to equations A-2 through A-5, the zeroth moment of N_s reads

$$\begin{aligned} Z_0(s) &= \sum_{y=0}^{\infty} \sum_{x=0}^{\infty} N_s(x,y) \\ &= \exp[y_n (1-p)/(1-ps)] \end{aligned} \tag{A-7}$$

Higher moments are obtainable by successively differentiating Z_0 according to

$$\begin{aligned} Z_k(s) &= \sum_{y=0}^{\infty} \sum_{x=0}^{\infty} x^k N_s(x,y) \\ &= s[\partial Z_{k-1}(s) / \partial s] \qquad (k = 1, 2, \cdots) \end{aligned} \tag{A-8}$$

The number- and weight-average degrees of polymerization are calculated as

$$x_n = Z_1(1) / Z_0(1) = p y_n / (1-p) \tag{A-9}$$

$$x_w = Z_2(1) / Z_1(1) = (1 + p + p y_n)/(1-p) \tag{A-10}$$

which give equation 1.5.

Summary

The main subject of this thesis is to determine the pseudo-first-order activation rate constants k_{act} in various living radical polymerization systems to establish the activation mechanism and evaluate the fundamental ability of each system. These results are summarized and compared in this section.

S-1. Activation Mechanisms

The author determined the k_{act} values as a function of the concentration of polymer radicals [P$^{\bullet}$] or the concentration of activators such as transition metal complexes [A] for four living radical polymerization systems in order to establish the activation mechanisms. The results showed that each examined system is driven virtually by a single mechanism, which is the thermal dissociation for the nitroxide system (Chapter 3), the degenerative chain transfer for both the iodide system (Chapter 6) and the dithiocompound system (Chapter 7), and the atom transfer mechanism for the bromide/CuBr system (Chapter 8), as illustrated in Scheme S-1.

S-2. Activation Rate Constants k_{act}

The author examined the activation processes in various systems. Table S-1 lists the values of k_{act}, C_{ex} (= k_{ex}/k_p), and k_A for polymer adducts, where the rate constants are defined in Scheme 1.1. The dormant adducts **27-37** presented in Table S-1 are illustrated in Figure 2.3. Since the k_{act} for systems 6 through 11 is proportional to the polymerization rate R_p, the listed values for those systems are referred to a standard value of $R_p = 4.8 \times 10^{-4}$ M s^{-1}, while the k_{act} for the other systems is independent of R_p. The results show that the magnitude of k_{act} significantly differs from system to system.

In comparison among the nitroxide systems 1 through 3, TEMPO, DBN, and DEPN attached to the same polymer (PS) give large differences in k_{act}. The open-chain nitroxides DBN and DEPN give larger k_{act} than the less bulky ring-chain nitroxide TEMPO, meaning that steric factors are important to determine k_{act}. It should also be noted that DBN gives a

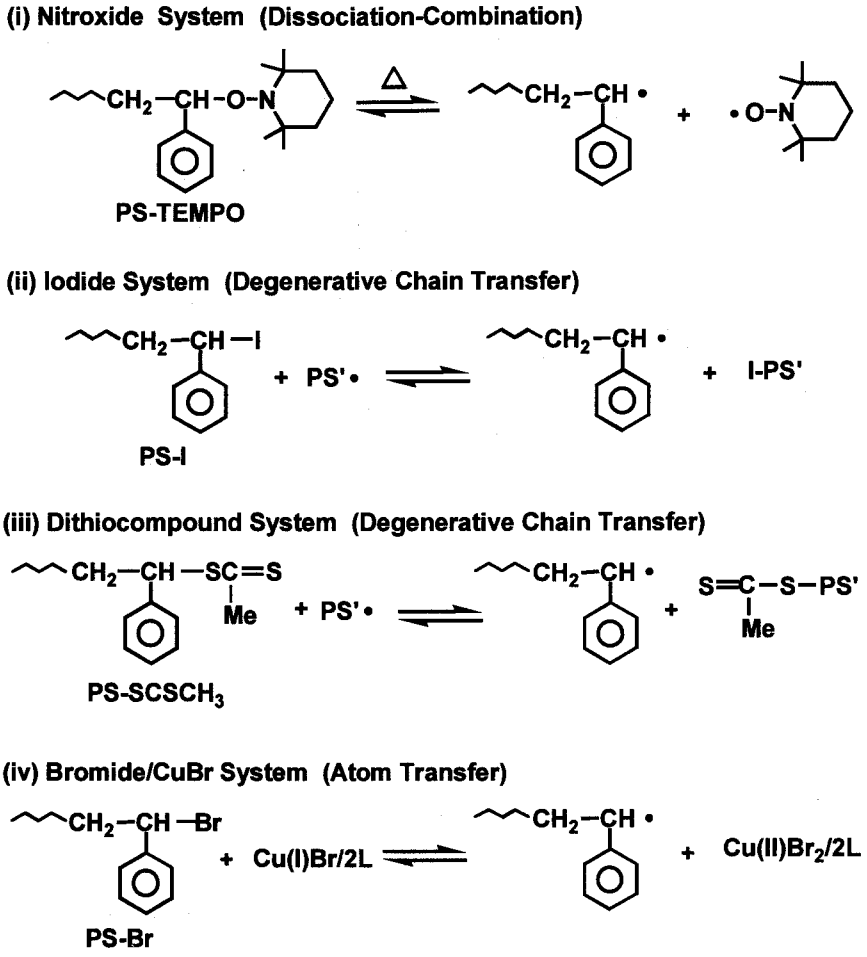

Scheme S-1. Activation mechanisms of (i) the nitroxide system, (ii) the iodide system, (iii) the dithiocompound system, and (ix) the bromide/CuBr system.

larger k_{act} than DEPN (at 120 °C) although the latter has a much bulkier side group than the former. This means that the electron-withdrawing phosphonate group in DEPN gives considerable electronic effect on k_{act}. Thus electronic factors also impart significant contribution on k_{act}. These kinetic knowledge would be highly useful in designing new high-performance nitroxides. The comparison of the absolute k_{act} values of the polymer adducts **27-29** and the corresponding low-mass analogues **6**, **11**, and **12** (Table 2.2) shows that the k_{act} of the former is larger than that of the latter by a factor of 2 to 3 in all the three cases,

Table S-1. Activation Rate Constants of Polymer Adducts

P-X	$10^3 k_{act}$ / s^{-1}	T / °C	Chapter
1. PS-TEMPO (**27**)	1.0	120	3
2. PS-DBN (**28**)	42	120	4
3. PS-DEPN (**29**)	11	120	4
4. PtBA-DBN (**30**)	1.0	120	5
5. PMA-Co/Porphyrin (**36**)	4.0 ± 2.0[a]	25	–
6. PS-I (**31**)	0.22[b]	80	6
	($C_{ex} = 3.6$)		
7. PS-SCSCH$_3$ (**32**)	9.6[b]	80	7
	($C_{ex} = 160$)		
8. PS-SCSPh (**33**)	360 ± 120[b]	80	7
	($C_{ex} = 6000 \pm 2000$)		
9. PMMA-SCSPh (**34**)	8.4[b]	60	7
	($C_{ex} = 140$)		
10. MMA-macromonomer (**37**)	0.013[b,c]	80	–
	($C_{ex} = 0.22$)		
11. PS-Br/CuBr (**35**)	23[b]	110	8
	($k_A = 0.45$ M^{-1} s^{-1})		

[a] Goto, A. et al., unpublished data. [b] Value approximately estimated for $R_p = 4.8 \times 10^{-4}$ M s^{-1}. (Systems 1-5 are independent of R_p.) [c] Moad, C. L.; Moad, G.; Rizzardo, E.; Thang, S. H. *Macromolecules* **1996**, *29*, 7717.

stressing the importance of the effects of chain length. On the other hand, for the CuBr-catalyzed ATRP (atom transfer radical polymerization) systems, the k_A of PS-Br (0.45 M^{-1} s^{-1}: system 11 in Table S-1) is close to that of the corresponding low-mass adduct PEBr **24** (0.42 M^{-1} s^{-1}: Chapter 9), meaning that k_A is nearly independent of the chain length. In this way, the importance of the chain length of alkyl moiety on k_{act} varies from system to system. According to Table S-1, the DBN-mediated polymerization of *t*-butyl acrylate (tBA) may be as well controlled as the TEMPO-mediated polymerization of styrene. Actually, however,

the thermal degradation of the active chain-end of PtBA-DBN occurs rather seriously at the high temperature, not allowing the polydispersity to be lowered as in the TEMPO/styrene system (Chapter 5). Clearly, a large k_{act} is a necessary but not a sufficient condition for a high performance living radical polymerization. The k_{act} value for PS-I system 6 is very small compared with other systems. According to equation 6.9, the smallest value of M_w/M_n possibly achievable at 80 °C is 1.28 in this system (in a batch system). The k_{act} value for the RAFT (reversible addition-fragmentation chain transfer) system 8 with PS-SCSPh is surprisingly large, about 40 times as large as those for the system 7 with PS-$SCSCH_3$ and the system 9 with PMMA-SCSPh, showing that the RAFT velocity is strongly dependent on the structures of the dithiocarbonate group and the alkyl (polymer) moiety. The k_{act} value for the ATRP system 11 is also large enough to account for the experimental observations that the system provides low-polydispersity polymers even *from an early stage of polymerization.* The table also includes a preliminary result obtained for the poly(methyl acrylate) PMA-Co/Porphyrin system 5, just for a comprehensive comparison.

List of Publications

Chapter 1.

1) Mechanisms and Kinetics of Living Radical Polymerizations
Fukuda, T.; **Goto, A.**; Ohno, K. *Macromol. Rapid Commun.* **2000**, *21*, 151.

Chapter 2.

2) Gel Permeation Chromatographic Determination of Activation Rate Constants in Nitroxide-Controlled Free Radical Polymerization, 1 Direct Analysis by Peak Resolution
Goto, A.; Terauchi, T.; Fukuda, T.; Miyamoto, T. *Macromol. Rapid Commun.* **1997**, *18*, 673.

3) Gel Permeation Chromatographic Determination of Activation Rate Constants in Nitroxide-Controlled Free Radical Polymerization, 2 Analysis of Evolution of Polydispersities
Fukuda, T.; **Goto, A.** *Macromol. Rapid Commun.* **1997**, *18*, 683.

Chapter 3.

4) Mechanism and Kinetics of Activation Processes in a Nitroxide-Mediated Polymerization of Styrene
Goto, A.; Fukuda, T. *Macromolecules* **1997**, *30*, 5183.

Chapter 4.

5) Comparative Study on Activation Rate Constants for Some Styrene/Nitroxide Systems
Goto, A.; Fukuda, T. *Macromol. Chem. Phys.* **2000**, *201*, 2138.

Chapter 5.

6) Kinetic Study on Nitroxide-Mediated Free Radical Polymerization of *tert*-Butyl Acrylate
Goto, A.; Fukuda, T. *Macromolecules* **1999**, *32*, 618.

Chapter 6.

7) Mechanism and Kinetics of Iodide-Mediated Polymerization of Styrene
Goto, A.; Ohno, K.; Fukuda, T. *Macromolecules* **1998**, *31*, 2809.

Chapter 7.

8) Mechanism and Kinetics of RAFT-Based Living Radical Polymerizations of Styrene and Methyl Methacrylate
Goto, A.; Sato, K.; Tsujii, Y.; Fukuda, T.; Moad, G.; Rizzardo, E.; Thang, S. H. *Macromolecules*, **2001**, *34(3)*, in press.

Chapter 8.

9) Kinetic Study on the Activation Process in an Atom Transfer Radical Polymerization
Ohno, K.; **Goto, A.**; Fukuda, T.; Xia, J.; Matyjaszewski, K. *Macromolecules* **1998**, *31*, 2699.

Chapter 9.

10) Determination of the Activation Rate Constants of Alkyl Halide Initiators for Atom Transfer Radical Polymerization
Goto, A.; Fukuda, T. *Macromol. Rapid Commun.* **1999**, *20*, 633.

Appendix.

11) Effects of Radical Initiator on Polymerization Rate and Polydispersity in Nitroxide-Controlled Free Radical Polymerization
Goto, A.; Fukuda, T. *Macromolecules* **1997**, *30*, 4272.

Other associated publications

12) Effects of Acetic Anhydride on the Activation and Polymerization Rates in Nitroxide-Mediated Polymerization of Styrene
Goto, A.; Tsujii, Y.; Fukuda, T. *Chem. Lett.* **2000**, 788.

13) Mechanism and Kinetics of Nitroxide-Controlled Free Radical Polymerization
Fukuda, T.; **Goto, A.**; Ohno, K.; Tsujii, Y. In "*Controlled Radical Polymerization*"; Matyjaszewski, K., Ed., *ACS Symp. Ser.* **685**: American Chemical Society: Washington, DC, 1998; Chapter 11.

14) Kinetics of Living Radical Polymerization
Fukuda, T.; **Goto, A.** In "*Controlled/Living Radical Polymerization*"; Matyjaszewski, K., Ed., *ACS Symp. Ser.* **768**: American Chemical Society: Washington, DC, 2000; Chapter 2.

15) Well-Defined Block Copolymers Comprising Styrene-Acrylonitrile Random Copolymer Sequences Synthesized by "Living" Radical Polymerization
Fukuda, T.; Terauchi, T.; **Goto, A.**; Tsujii, Y.; Miyamoto, T.; Shimizu, Y. *Macromolecules* **1996**, *29*, 6393.

16) Mechanisms and Kinetics of Nitroxide-Controlled Free Radical Polymerization
Fukuda, T.; Terauchi, T.; **Goto, A.**; Ohno, K.; Tsujii, Y.; Miyamoto, T.; Kobatake, S.; Yamada, B. *Macromolecules* **1996**, *29*, 3050.

Acknowledgements

The investigations described in this thesis were carried out at the Institute for Chemical Research, Kyoto University, during the period from 1995 to 2001.

The author wishes to express his sincere gratitude to Professor Takeshi Fukuda for his invaluable guidance, stimulating discussions, and encouragement throughout this work.

Grateful acknowledgement is due to Emeritus Professor Takeaki Miyamoto for his continuous comments and encouragement.

The author is sincerely grateful to Dr. Yoshinobu Tsujii, Associate Professor Masahiko Minoda (Kyoto Institute of Technology), and Professor Nobuo Donkai (Niigata Women's college) for their helpful suggestions.

Sincere appreciation is due to all of his colleagues for their kind helps, particularly, to Dr. Kohji Ohno and Mr. Koichi Sato for their active collaborations in a part of the study.

Finally, the author heartily wishes to express his thanks to his parents, Hiroshi Goto and Noriko Goto, and his sister, Rie Goto, for their devoted support, and to his wife, Yasuko Goto for her heartfelt encouragement.

This dissertation work was supported in part by a Research Fellowship of Japan Society for the Promotion of Science for Young Scientists (1998-2001), which is gratefully acknowledged.

January, 2001

Atsushi Goto